

PB94162823



U.S. Department  
of Transportation  
Federal Railroad  
Administration

## FIELD TESTING OF A WAYSIDE WHEEL CRACK DETECTION SYSTEM

---

Office of Research and  
Development  
Washington D.C. 20590

Robert K. Larson, Jr., Robert L. Florom, and  
Britto R. Rajkumar

Association of American Railroads  
Research and Test Department  
Transportation Test Center  
Pueblo, Colorado

---

DOT/FRA/ORD-92/07

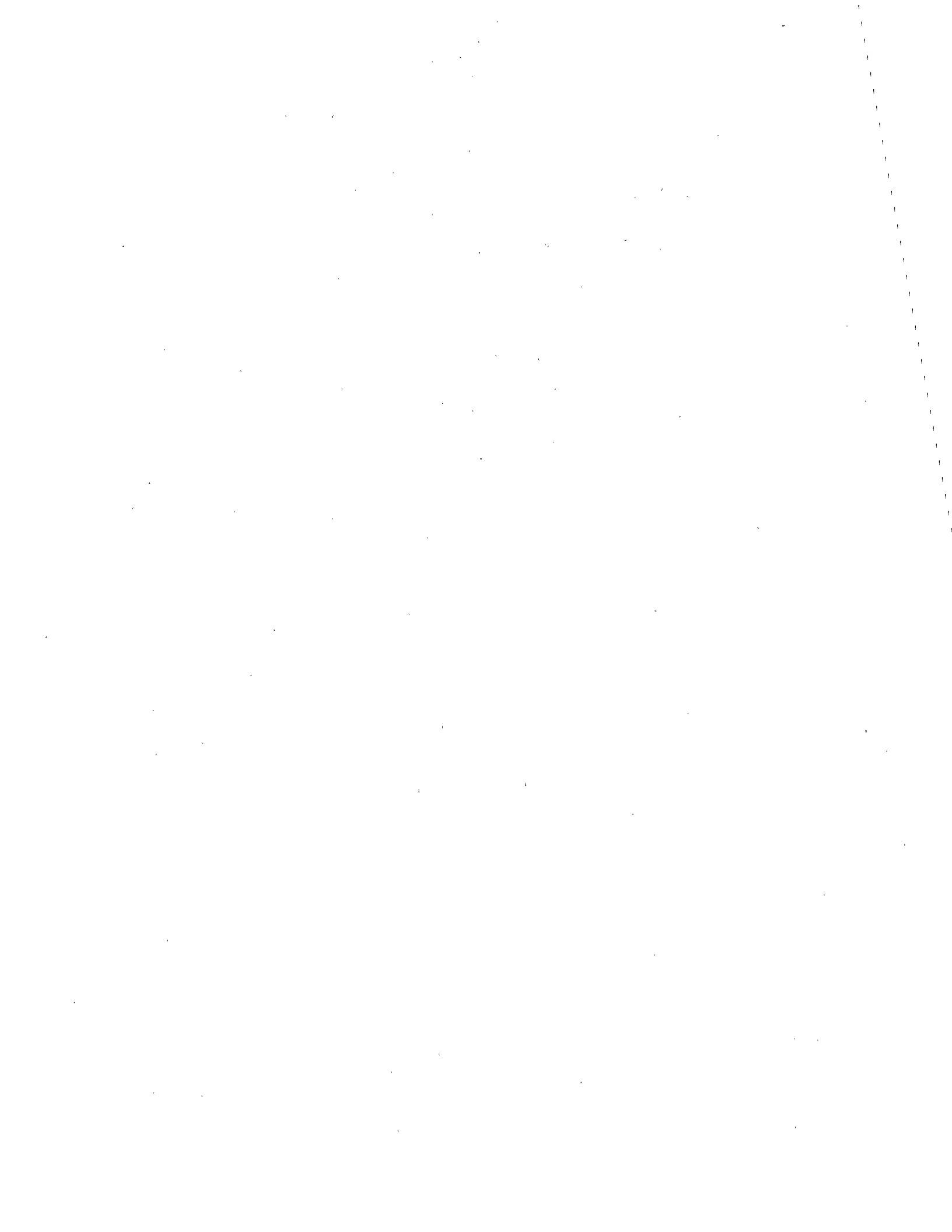
May 1992  
Final Report


This document is available to the  
U.S. public through the National  
Technical Information Service  
Springfield, Virginia 22161

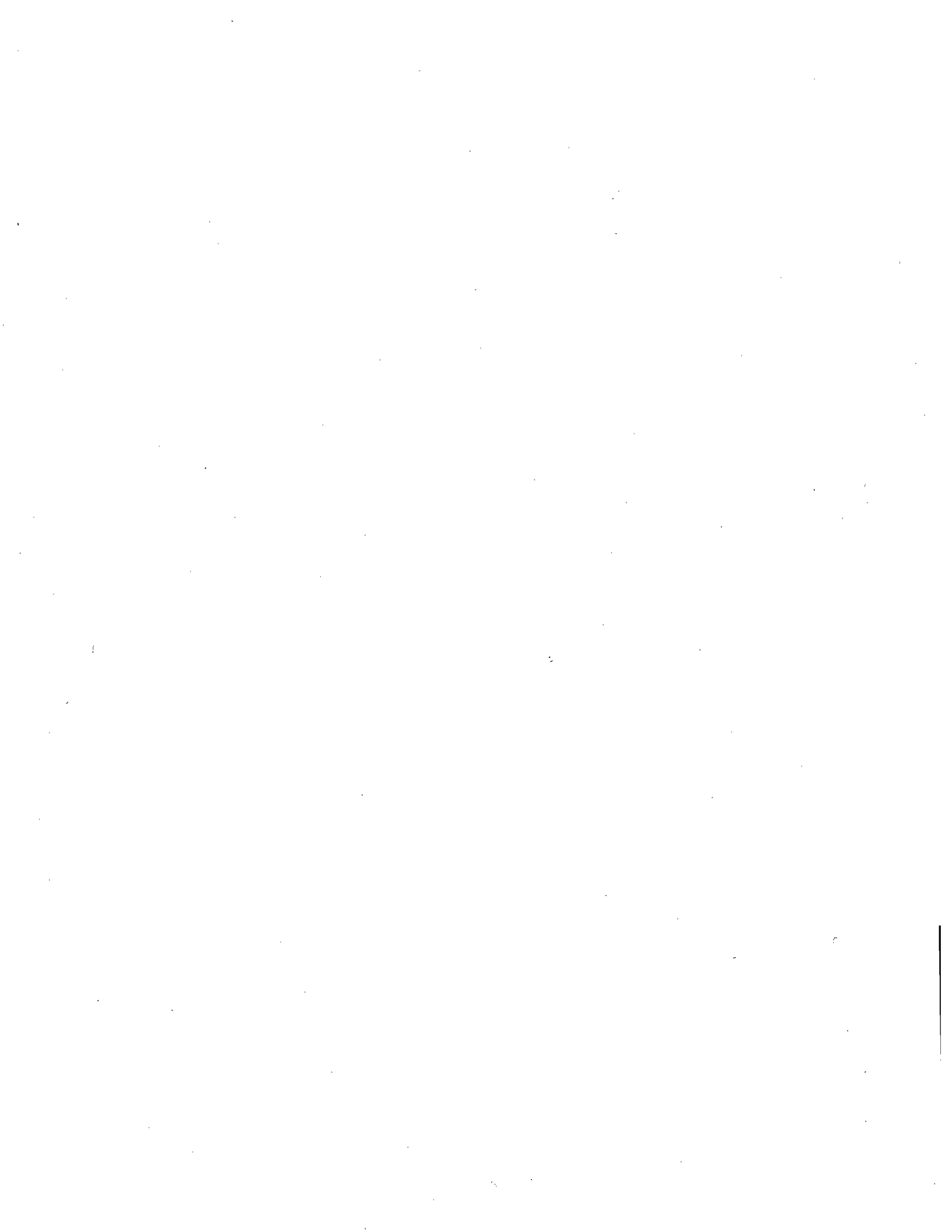


## **DISCLAIMER**

This document is disseminated under the sponsorship of the Department of Transportation in the interest of information exchange. The United States Government assumes no liability for the contents or use thereof. The United States Government does not endorse products or manufacturers. Trade or manufacturers' names appear herein solely because they are considered essential to the object of this report.



1. Report No. FRA/ORD-92/07		2. Government Accession No.		3. Report Number  PB94-162823	
4. Title and Subtitle FIELD TESTING OF WAYSIDE WHEEL CRACK DETECTION SYSTEM				5. Report Date May 1992	
7. Author(s) Robert K. Larson, Jr., Robert L. Florom and Britto R. Rajkumar				6. Performing Organization Code	
9. Performing Organization Name and Address Association of American Railroads Transportation Test Center P.O. Box 11130 Pueblo, CO 81001				8. Performing Organization Report No.	
12. Sponsoring Agency Name and Address U.S. Department of Transportation Federal Railroad Administration Office of Research and Development 400 Seventh Street SW Washington, D.C. 20590				10. Work Unit No. (TRAIS)	
				11. Contract or Grant No. DTFR53-82-C-00282 Task Order 30, Subtask C	
				13. Type of Report or Period Covered Final December 1989 - March 1992	
				14. Sponsoring Agency Code	
15. Supplementary Notes					
16. Abstract A prototype crack detection system for railroad wheels has been developed by the National Institute of Standards and Technology (NIST) for the Federal Railroad Administration (FRA). The system is designed to detect the presence of thermal cracks in railroad wheels as they pass by an inspection point.  The Association of American Railroads (AAR) has completed testing of the prototype wheel crack detector at the Transportation Test Center in Pueblo, CO. The response of the detector was measured for 20 wheel sets that were operated over the detector at speeds of 5, 10, and 20 mph.  Test results indicate that, with modifications, it may be possible to use the detector for the following types of wheel defects: - Tread Thermal Cracks - Tread Shelling  A slight difference was observed between the detector signature for thermal cracked wheels vs. shelled wheels. Future development and testing by NIST and AAR will focus on improving the ability of the detector to distinguish between different types of tread flaws and detector durability.					
17. Key Words Wayside wheel inspection system Wheel tread defects Thermal cracks, shelling			18. Distribution Statement This document is available through National Technical Information Service Springfield, VA 22161		
19. Security Classification (of the report)		20. Security Classification (of this page)		21. No. of Pages	22. Price



## EXECUTIVE SUMMARY

A program to evaluate the overall performance and reliability of a prototype railroad Wheel Crack Detector (WCD), developed by the National Institute of Standards and Technology (NIST) for the Federal Railroad Administration, was conducted by the Association of American Railroads, Transportation Test Center (TTC) Pueblo, Colorado. The system, designed to detect the presence of thermal cracks in railroad wheels as they pass by an inspection point, was tested to determine the overall reliability of the WCD system and document the response of the system for wheels with various tread defects operated over the detector at different speeds.

The results of the tests support the following conclusions:

- With appropriate signal processing, and successful development and incorporation of the modifications recommended in Section 8, the WCD system potentially could be used to identify wheels having the following tread defects:
  - Thermal Cracks
  - Non-condemnable Shelling
  - Condemnable Shelling
- The WCD system, appropriately augmented with acceleration or strain gage based wheel impact measurement instrumentation, may potentially have the capability to differentiate between wheels having thermal cracks and wheels having shelling.
- The system will need refining in order to eliminate the source of defect peaks observed on new wheels that were actually free of tread defects and to limit the number of false indications observed while testing used wheels.
- The current signal processing methods used to detect defects and estimate defect size need to be modified to obtain more reliable results.
- The system will need refining in order to achieve roll-by inspection speeds higher than 15 mph.

The following recommendations are based upon the results obtained in these tests:





- A new triggering circuit should be designed to ensure that a maximum input signal amplitude is achieved to allow higher roll-by inspection speeds. The design of the circuit should also address the durability and reliability improvements.
- A new electromagnetic-acoustic transducer (EMAT) package should be designed to ensure that a maximum input signal amplitude is achieved to allow higher roll-by inspection speeds, and obtain through peaks for thermal crack and shelled defects in the wheel tread.
- Consideration should be given to configuring the WCD system to provide a recognizable signal response for wheels having flange defects.
- Since defects can occur at any location around the circumference of the wheel, consideration should be given to the overall system design to compensate for the dead zones that occur adjacent to the detector contact point and at 180 degrees from the contact point.
- Additional wheels should be tested to statistically confirm whether shelled wheels can be consistently differentiated from thermal cracked wheels. The tests should include instrumentation for monitoring rail vibrations and acoustic emissions.
- Studies to investigate improved signal processing techniques including the use of the regions between through signals to detect defects and estimate defect size should be conducted.
- The source of noise at higher roll-by speeds should be investigated.

The tests performed in the program included evaluating the reliability of the trigger circuitry, durability of the EMAT package, and recording the response of the WCD system for a group of 20 wheels operated under loaded 70- and 100-ton capacity cars at test speeds of 5-, 10-, and 20-mph. Several static tests were also performed using individual wheel sets to investigate the effects of defect position relative to the detector.

The WCD system tested at the TTC uses two EMAT coils, a permanent magnet, and triggering circuitry to generate and detect Rayleigh or surface sound waves in the wheel tread of the test specimen.

The presence of defects in the wheel tread surface will partially reflect the surface waves, which are detected with the EMAT receiver coil. Analyzing the output signals from the receiver coil provides a means for detecting wheel tread defects.

## Table of Contents

1.0 INTRODUCTION .....	1
2.0 OBJECTIVE .....	1
3.0 WCD SYSTEM AND INSTRUMENTATION .....	1
3.1 SYSTEM DESCRIPTION/OPERATING THEORY .....	1
3.2 SYSTEM CONFIGURATION .....	5
3.3 ADDITIONAL INSTRUMENTATION .....	9
4.0 TEST PROCEDURES .....	9
4.1 PHASE I TESTS .....	9
4.1.1 Trigger Circuitry Evaluation .....	9
4.1.2 EMAT Package Durability Evaluation .....	9
4.2 PHASE II TESTS .....	9
4.2.1 Test Series 1 - Configuration I Static Tests .....	9
4.2.2 Test Series 2 - Roll-by Tests .....	10
4.2.3 Test Series 3 - Configuration II Static Tests .....	10
4.2.4 Test Series 4 - Configuration III Static Tests .....	10
4.2.5 Electromagnetic Interference Test .....	10
4.2.6 Phase II Test Matrix .....	11
5.0 RESULTS .....	12
5.1 PHASE I TEST RESULTS .....	12
5.1.1 Trigger Circuitry Evaluation .....	12
5.1.2 EMAT Package Durability Evaluation .....	12
5.2 PHASE II TEST RESULTS .....	12
5.2.1 WCD Signature Characteristics .....	12
5.2.2 WCD Signatures for Selected Defect Types .....	14
5.2.3 New Wheel WCD Signatures .....	29
5.2.4 Signature Variations with Speed .....	31
5.2.5 Wheel Position/Defect Orientation Tests .....	31
5.2.6 20-mph Roll-by Tests .....	32

6.0 DISCUSSION .....	32
6.1 DEFECT SIGNATURES .....	32
6.2 EFFECT OF ROLL-BY SPEED ON DETECTOR RESPONSE .....	32
6.3 EFFECT OF WHEEL POSITION AND DEFECT ORIENTATION ...	33
7.0 CONCLUSIONS .....	33
8.0 RECOMMENDATIONS .....	34
REFERENCES .....	35

## Table of Figures

Figure 1 - Wheel Set on WCD System .....	2
Figure 2 - WCD Signature for a Wheel with No Defects .....	3
Figure 3 - WCD Signature -- Single Tread Defect .....	4
Figure 4 - Typical EMAT Package .....	6
Figure 5 - Modification of Railhead to Accept EMAT Package .....	7
Figure 6 - EMAT Package Installed in a Rail Section .....	8
Figure 7 - View of Wheel No. 92345 Tread .....	14
Figure 8 - Detector Response for Wheel No. 92345, Stationary Test .....	15
Figure 9 - Detector Response for Wheel No. 92345, Roll-by Test -- 5 mph .....	15
Figure 10 - Detector Response Wheel No. 92345, Roll-by Test -- 10 mph .....	16
Figure 11 - View of Wheel No. 52897 Tread .....	17
Figure 12 -Detector Response for Wheel No. 52897, Stationary Test .....	18
Figure 13 -Detector Response for Wheel No. 52897 Roll-by Test -- 5 mph .....	18
Figure 14 -Detector Response for Wheel No. 52897 Roll-by -- 10 mph .....	19
Figure 15 - View of Wheel No. 24979 Tread .....	20
Figure 16 -Detector Response for Wheel No. 24979, Stationary Test .....	21
Figure 17 -Detector Response for Wheel No. 24979, Roll-by Test -- 5 mph .....	21
Figure 18 -Detector Response for Wheel No. 24979, Roll-by Test -- 10 mph .....	22
Figure 19 - View of Wheel No. 82253 Tread .....	23
Figure 20 -Detector Response for Wheel No. 82253, Stationary Test .....	24
Figure 21 -Detector Response for Wheel No. 82253, Roll-by Test -- 5 mph .....	24
Figure 22 -Detector Response for Wheel No. 82253, 10 mph .....	25
Figure 23 - View of Wheel No 275828 Tread .....	26
Figure 24 -Detector Response for Wheel No. 275828, Stationary Test .....	27
Figure 25 -Detector Response for Wheel No. 275828, Roll-by Test -- 5 mph .....	27
Figure 26 -Detector Response for Wheel No. 275828, Roll-by Test -- 10 mph .....	28
Figure 27 -Detector Response for Wheel No. N-1, Stationary Test, 5- mph and 10-mph Tests .....	29
Figure 28 -Detector Response for Wheel No. N-2, Stationary Test, 5-mph and 10 mph Tests .....	29

Figure 29 -Detector Response for Wheel No. N-3, Stationary Test, 5-mph and 10 mph Tests .....	30
Figure 30 -Detector Response for Wheel No. N-4, Stationary Test, 5-mph and 10 mph Tests .....	30

### Tables

Table 1 - Phase II Test Matrix .....	11
Table 2 - Summary of WCD Response Characteristics .....	13
Table 3 - Signal Amplitude Variation with Speed .....	31
Table 4 - Test Series 3 & 4 Results Summary .....	31



## **1.0 INTRODUCTION**

A prototype Wheel Crack Detector (WCD) system for railroad wheels has been developed by the National Institute of Standards and Technology (NIST) for the Federal Railroad Administration (FRA). The system is designed to detect the presence of thermal cracks in railroad wheels as they pass by an inspection point. The Association of American Railroads (AAR), Transportation Test Center (TTC), Pueblo, Colorado, entered into a contract with the FRA to conduct static and on-track tests to evaluate the performance of the WCD system. This report provides a summary of the test results and recommendations for areas of additional research that may lead to improved performance of the WCD system.

## **2.0 OBJECTIVE**

The objective of the testing program was to evaluate the overall performance and reliability of the WCD system. The response of the system was to be recorded for wheels with various tread defects operated over the detector at different speeds.

## **3.0 WCD SYSTEM AND INSTRUMENTATION**

The WCD system and data acquisition computer were provided by NIST. A brief description of the system is provided in the following subsections. A detailed description of the system is provided in references 1 and 2.

### **3.1 SYSTEM DESCRIPTION/OPERATING THEORY**

Figure 1 is a diagram showing a wheel with a tread defect located at an angle of 60 degrees relative to the WCD rail mounted instrumentation, along with the various signals that are generated during the inspection process.

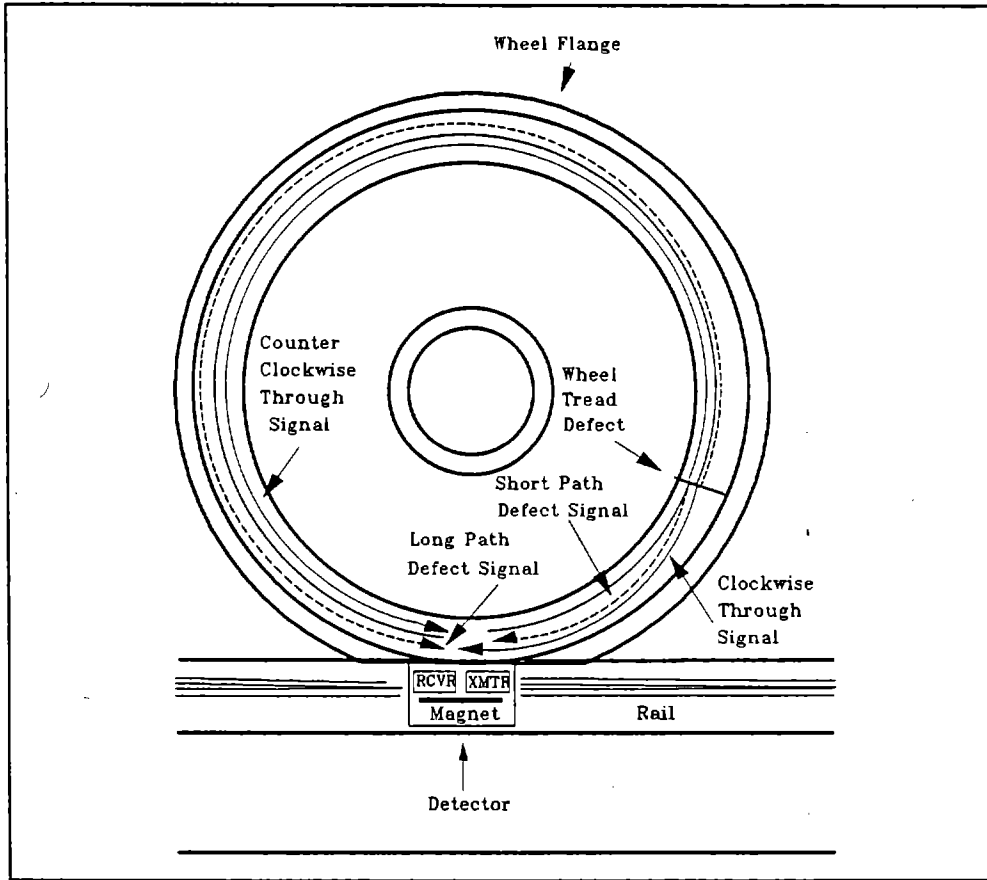


**Figure 1. Diagram of Wheel Set on WCD System**

As illustrated in Figure 1, the WCD system uses two electromagnetic-acoustic transducer (EMAT) coils, a permanent magnet, and triggering circuitry to generate and detect sound energy in the test specimen. Each EMAT package contains a transmitter coil, a receiver coil, and the triggering circuitry. The coils are laminated with a flexible type of plastic which allows the coils to conform to the profile of the wheel tread.

The EMAT transmitter coil is powered by a high current amplifier designed to produce 500 kHz current pulses. The design of the transmitter coil and the presence of a magnetic field, caused by the permanent magnet, produces bi-directional Rayleigh waves or surface waves that travel around the wheel tread but do not penetrate into the bulk of the wheel. These waves are shown in Figure 1.

The presence of defects in the wheel tread surface will partially reflect the surface waves. The reflected surface waves (as well as incident surface waves) can be detected with the EMAT receiver coil. The output signal from each of the EMAT receiver coils is conditioned using a low noise amplifier.



Analyzing the output signals from the receiver coil provides a means for detecting wheel tread defects.

A wheel with no tread defects should theoretically produce a WCD signature with the characteristics illustrated in Figure 2.

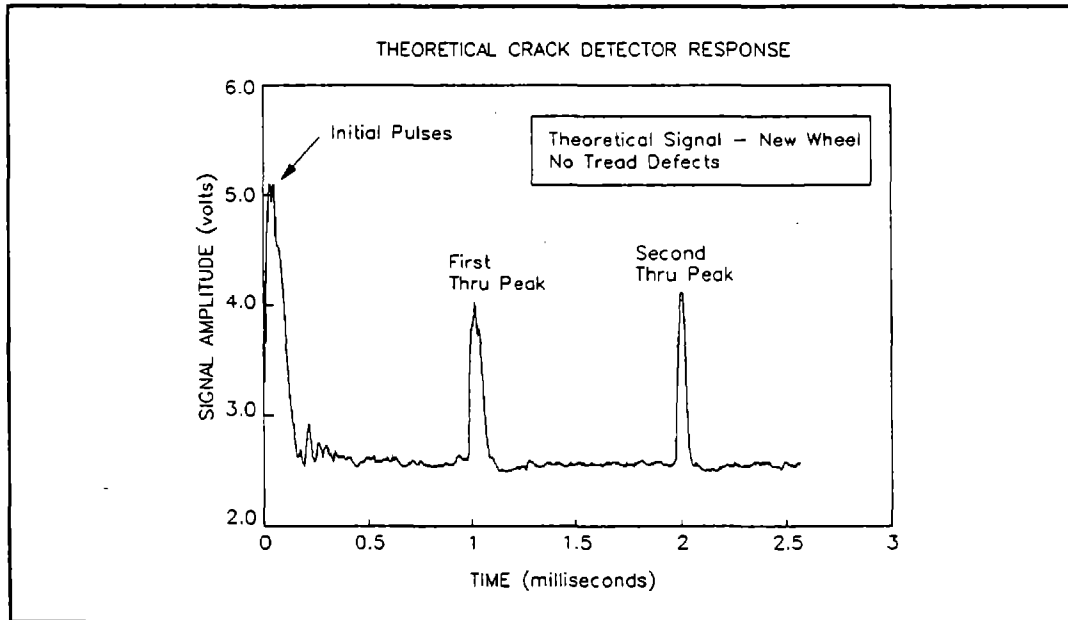


**Figure 2. WCD Signature for a Wheel with No Defects**

Referring to Figure 2, the first peak occurring at time zero is due to the initial output pulses from the transmitter coil inducing a series of pulses in the receiver coil and saturating the receiver coil amplifier. The initial transmitter input is commonly referred to as the main bang. During the time period that the receiver coil amplifier is saturated (recovery time), the system is not able to detect signals reflected from defects. The next peak, occurring at approximately 1 millisecond, is the first through peak from the initial pulses detected by the receiver coil. The detection of this peak indicates that the initial pulse has traveled around the entire circumference of the wheel (1<sup>st</sup> round trip). The next peak occurring at approximately 2 milliseconds is the second through peak. The detection of this peak indicates that the initial pulses has traveled around the circumference of the wheel twice (2<sup>nd</sup> round trip).

A wheel with a single tread defect, as illustrated in Figure 1, should theoretically produce a WCD signature with the characteristics illustrated in Figure 3.

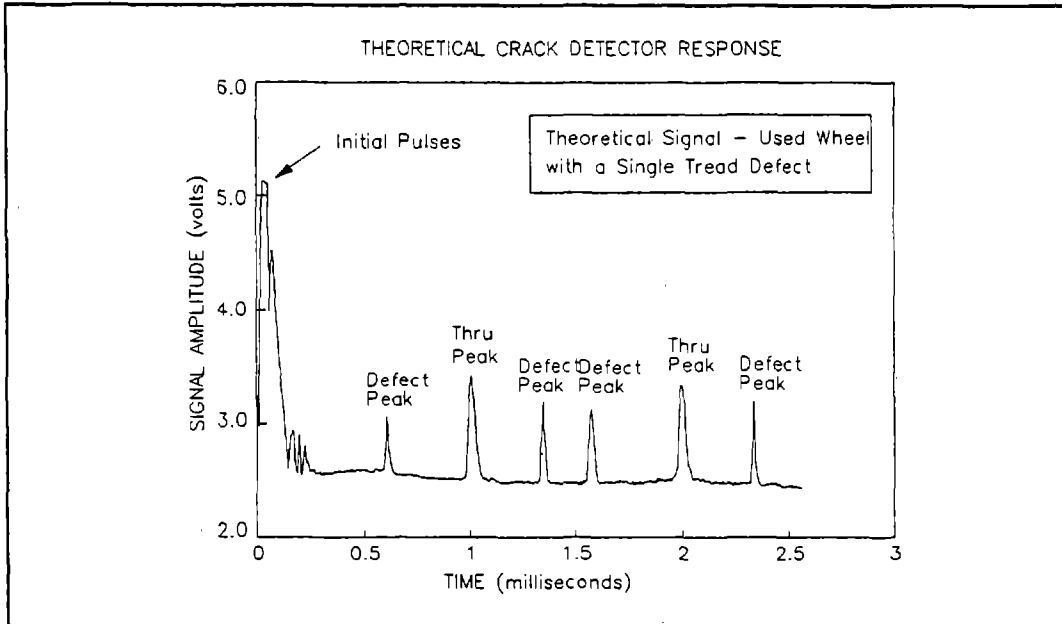


**Figure 3. WCD Signature - Single Tread Defect**

Referring to Figure 3, the first peak occurring at time zero and those occurring between time zero and 0.2 milliseconds are due to the main bang saturating the receiver coil amplifier. The first defect peak, caused by the short path defect signal, occurs at 0.66 millisecond. The first through peak detected by the receiver coil occurs at approximately 1 millisecond. The peak at 1.34 milliseconds is caused by the long path defect signal. The second through peak occurs at 2 milliseconds. The peak occurring at 1.66 milliseconds is caused by the short path defect signal from the first through signal, and the peak occurring at 2.34 milliseconds is caused by the long path defect signal from the first through signal (not shown in Figure 1).

The temporal relationships for the defect and through signals are governed by the following equations:

$$T_{C_n} = n(2\pi r / V_{RW}) \quad (\text{Equation 1})$$

Where:

$n$  = the number of round trip signals,  $n = \{0, 1, 2, 3, \dots\}$

$T_{C_n}$  = the time required for the initial signal to complete round trip  $n$

$r$  = the wheel radius

$V_{RW}$  = the velocity of sound in the material

$$T_{SP_n} = nT_c + (\theta/\pi)T_c \quad (\text{Equation 2})$$

Where:  $n$  = the number of round trip signals,  $n = \{0,1,2,3,\dots\}$   
 $T_c$  = the time required for the initial signal to complete one round trip  
 $T_{SP_n}$  = the short path defect signal time  
 $\theta$  = the angle between the detector and the defect, expressed in radians

$$T_{LP_n} = nT_c + [2 - (\theta/\pi)]T_c \quad (\text{Equation 3})$$

Where:  $n$  = the number of round trip signals,  $n = \{0,1,2,3,\dots\}$   
 $T_c$  = the time required for the initial signal to complete one round trip  
 $T_{LP_n}$  = the long path defect signal time for round trip signal  $n$   
 $\theta$  = the angle between the detector and the defect, expressed in radians

Inspection of equations 2, and 3 shows that when the defect is located at zero or 180 degrees, the defect peaks will coincide with the through peaks.

The WCD system evaluated at the TTC used the ratio of the amplitude of the defect peak occurring between the main bang and the first through peak, and the amplitude of the first through peak to estimate the size of the defect.

### **3.2 SYSTEM CONFIGURATION**

The following photographs show the components of the WCD system tested at the TTC. A typical EMAT package is shown in Figure 4, and the modification of the railhead necessary to install the EMAT package is shown in Figure 5. Figure 6 shows a typical EMAT package installed in a rail section.

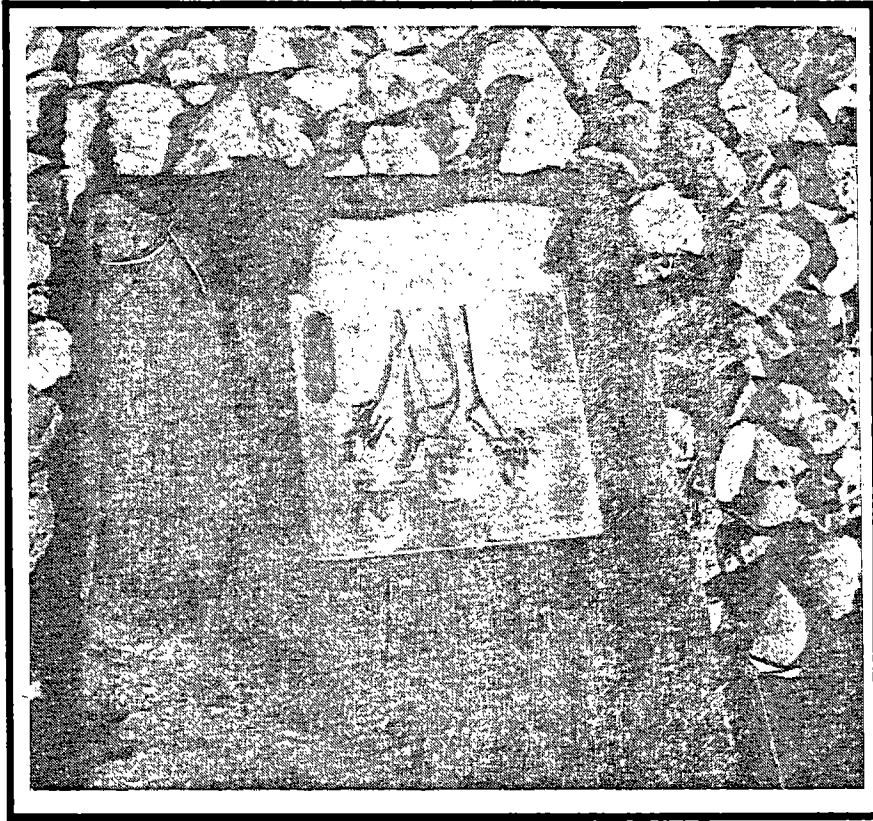


**Figure 4. Typical EMAT Package**

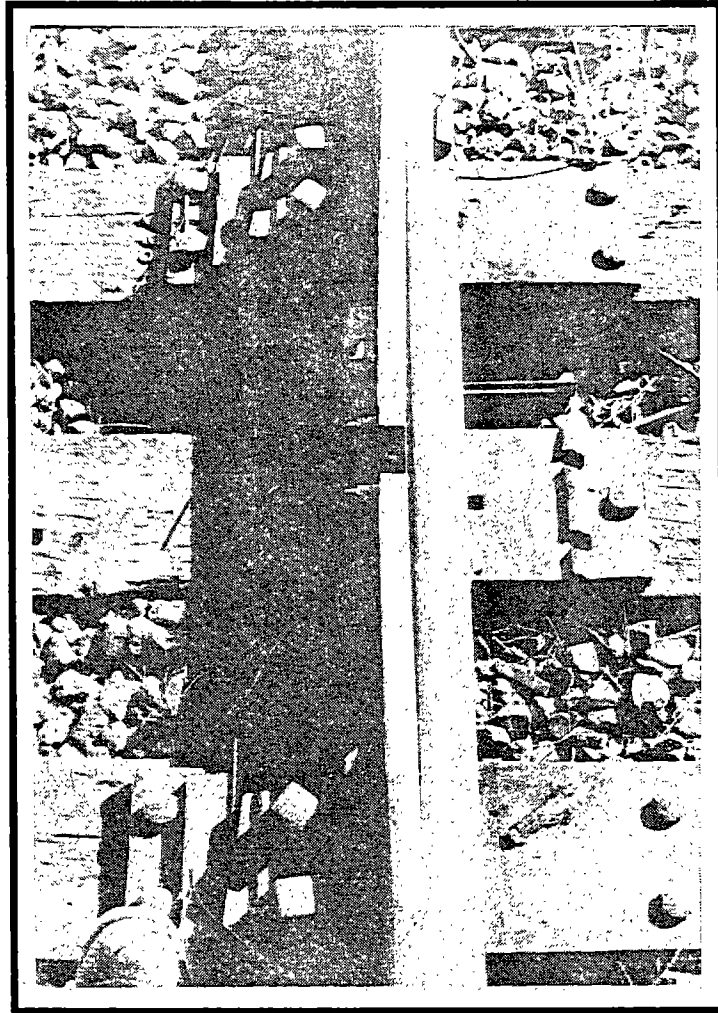


**Figure 5. Modification of Railhead to accept EMAT Package**

The EMAT packages were inserted in a cutout on the field side of the railhead that measured 4.25 inches long, 1.625 inches deep, and 1.375 wide. A transition section extended 12 inches on either side of the sensor. The section was machined with a 1:50 taper starting at a depth of 0.25 inch at the center of the sensor and extending up to the rail surface. The height of the sensor was adjusted as required to ensure proper contact with the tread surface of passing wheels.

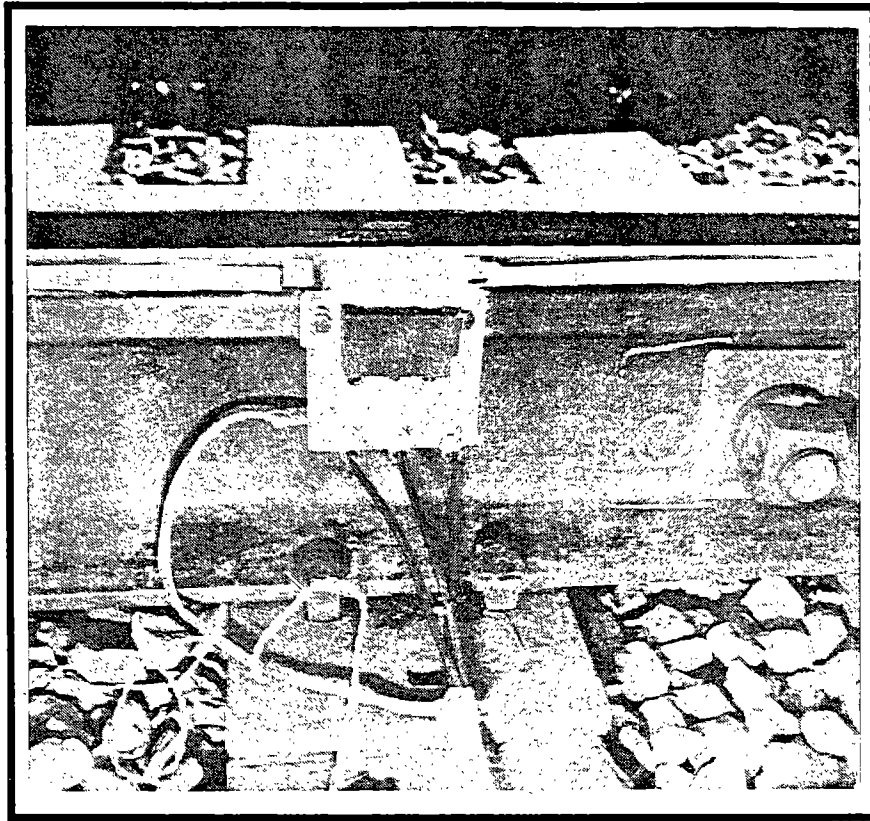


**Figure 6. EMAT Package Installed in a Rail Section**

During the tests, the WCD electronics, a data acquisition computer, and a digital oscilloscope were housed in a trailer located to the side of the test rail section where the WCD system was installed. The output signals from the EMAT receiver coil were recorded using the data acquisition computer and monitored during testing with the oscilloscope.

### **3.3 ADDITIONAL INSTRUMENTATION**

Additional instrumentation to measure rail vibration and displacement and air borne vibration was added before the start of the Phase II tests. The original plan was to reduce the number of test repetitions performed in Series 1, 2, 3 and 4, and use the funding to analyze the data collected with the additional instrumentation. However, upon performing these tests it was determined that the test repetitions could not be reduced. Therefore, the data collected with the additional instrumentation could not be analyzed.

## **4.0 TEST PROCEDURES**

### **4.1 PHASE I TESTS**

Initial tests of the WCD system were performed during November 1989 and again in May 1990. The tests described in the following subsections were performed.

#### **4.1.1 Trigger Circuitry Evaluation**

The purpose of this test was to evaluate the performance of the triggering circuitry used to activate the EMAT transmitter coil for each passing wheel.

#### **4.1.2 EMAT Package Durability Evaluation**

This test was added to the original planning when it was discovered that the EMAT packages as originally designed had significant durability limitations. The purpose of the test was to evaluate the durability of several designs of the EMAT package under simulated revenue service conditions to identify a design that would endure the Phase II tests.

### **4.2 PHASE II TESTS**

During Phase II testing, the response of the WCD system was recorded for a group of 20 wheels that were operated under loaded 70- and 100-ton capacity cars across the detector. The tests described in the following subsections were performed (See Table 1).

#### **4.2.1 Test Series 1 - Configuration I Static Tests**

Each wheel set in the test consist was positioned over the detector and the detector response was recorded for five consecutive EMAT pulses. A continuous trigger (provided with the detector system) was used to activate the EMAT transmitter. The objective of the tests was to evaluate the repeatability of the response of the detector to selected wheel defects. The original planning called for testing eight wheels with both AAR condemnable and non-condemnable defects. Twenty wheels were actually tested including four new wheels (See Table 1).

#### **4.2.2 Test Series 2 - Roll-by Tests**

The test consist was operated over the detector at 5, 10, and 20 mph. The test was repeated five times at each test speed. The purpose of these tests was to evaluate the effects of operating speed on the detector response for selected wheel defects. The original planning called for testing two wheels with flange and rim thermal cracks. Twenty wheels were actually tested including four new wheels (See Table 1).

#### **4.2.3 Test Series 3 - Configuration II Static Tests**

Selected test wheel sets were placed over the detector and rotated through 12 angular positions (30-degree increments). The response of the detector was recorded for each position for five consecutive EMAT pulses. Hydraulic jacks and bearing adaptors were used to lift the wheel sets during the rotating operation, and the wheel sets were rotated by hand to the desired position then lowered onto the detector test rail section. The objective of the tests was to determine the sensitivity of the detector response to variations in defect location from the detector. The original planning called for testing only two wheel sets having flange and rim cracks. A total of eight wheels were actually tested (See Table 1).

#### **4.2.4 Test Series 4 - Configuration III Static Tests**

Selected test wheel sets were positioned in the two lateral extremes on the test rails (with the flange throat of one wheel against the gage side of the railhead), and Test Series 3 was repeated. The purpose of the tests was to determine the effects of lateral wheel set position on the detector response. The original planning called for testing only two wheels having flange and rim cracks. A total of four wheels were actually tested (See Table 1).

#### **4.2.5 Electromagnetic Interference Test**

The Electromagnetic Interference Test was not performed because the WCD system was returned to NIST for repairs and additional development work.



#### 4.2.6 Phase II Test Matrix

Table 1 lists the test wheels that were used during Phase II testing and the type of tests that were performed on each wheel.

**Table 1. Phase II Test Matrix**

WHEEL	TREAD DEFECT TYPE	TEST SERIES PERFORMED			
		1	2	3	4
52897	Thermal Cracks	X	X	X	X
91342	Thermal Cracks	X	X		
51265	Thermal Cracks	X	X	X	
00669	Thermal Cracks/Shelling	X	X		
94472	Thermal Cracks/Shelling	X	X		
16037	Thermal Cracks/Shelling	X	X		
92345	Slot in Outer Tread	X	X	X	X
64796	Slot in Inner Tread	X	X	X	X
82253	Gouge	X	X	X	
8757	Cracked Rim	X	X	X	
8341	Gouge	X	X		
54844	Shelled Tread (Two 3" shells)	X	X	X	
24979	Shelled Tread (11% of circumference)	X	X	X	X
514114	Shelled Tread (Non-condemnable)	X	X		
275828	Grooved Tread	X	X		
2269	Grooved Tread (Non-condemnable)	X	X		
N-1	New Wheel/No Defects	X	X		
N-2	New Wheel/No Defects	X	X		
N-3	New Wheel/No Defects	X	X		
N-4	New Wheel/No Defects	X	X		

## **5.0 RESULTS**

### **5.1 PHASE I TEST RESULTS**

The results obtained in the Phase I tests are summarized in the following subsections.

#### **5.1.1 Trigger Circuitry Evaluation**

Initial tests of the trigger circuitry showed that the trigger did not produce reliable results for all of the wheels operated over the detector. NIST provided several EMAT packages with various design modifications which addressed the problem, and a system was obtained which reliably triggered the detector for all wheels tested.

#### **5.1.2 EMAT Package Durability Evaluation**

Initial tests of the EMAT package showed that the solder connections to the EMAT coils were prone to failure from vibration induced by passing wheel sets. NIST provided several EMAT packages incorporating various design modifications which addressed the problem, and a package was attained with sufficient durability to complete the Phase II tests. All of the EMAT packages provided by NIST had failed by the completion of the Phase II tests. The primary cause of failure for the EMAT packages was broken solder joint connections within the EMAT packages.

### **5.2 PHASE II TEST RESULTS**

The results obtained in the Phase II Tests are summarized in the following subsections.

#### **5.2.1 WCD Signature Characteristics**

Table 2 summarizes basic characteristics of the WCD signatures for each of the wheels evaluated in the program.

**Table 2. Summary of WCD Response Characteristics**

WHEEL ID	TREAD DEFECT TYPE	+DISTINCT DEFECT PEAK			*ATTENUATED WITH SPEED
		STATIC	5 MPH	10 MPH	
52897	Thermal Cracks	**	**	**	Yes
91342	Thermal Cracks	**	**	**	Yes
51265	Thermal Cracks	**	**	**	Yes
00669	Thermal Cracks/Shelling	**	**	**	Yes
94472	Thermal Cracks/Shelling	**	**	**	Yes
16037	Thermal Cracks/Shelling	**	**	**	Yes
92345	Slot in Outer Tread	Yes	Yes	Yes	No
64796	Slot in Inner Tread	No	Yes	Yes	No
82253	Gouge	No	Yes	No	Yes
8341	Gouge	No	Yes	No	No
8757	Cracked Rim	Yes	Yes	Yes	No
54844	Shelled Tread (Two 3" shells)	No	Yes	Yes	Yes
24979	Shelled Tread (11% of circumference)	No	Yes	No	No
514114	Shelled Tread (Non-condemnable)	No	Yes	Yes	Yes
275828	Grooved Tread	No	Yes	Yes	No
2269	Grooved Tread (Non-condemnable)	Yes	No	Yes	No
N-1	New Wheel/No Defects	No	No	No	No
N-2	New Wheel/No Defects	No	Yes	Yes	Yes
N-3	New Wheel/No Defects	No	No	No	No
N-4	New Wheel/No Defects	No	No	Yes	Yes

\* Greater than 1/3 reduction in maximum signal peaks

+ Defect signal peak(s) greater than 1/3 of 1st through signal peak and above noise level

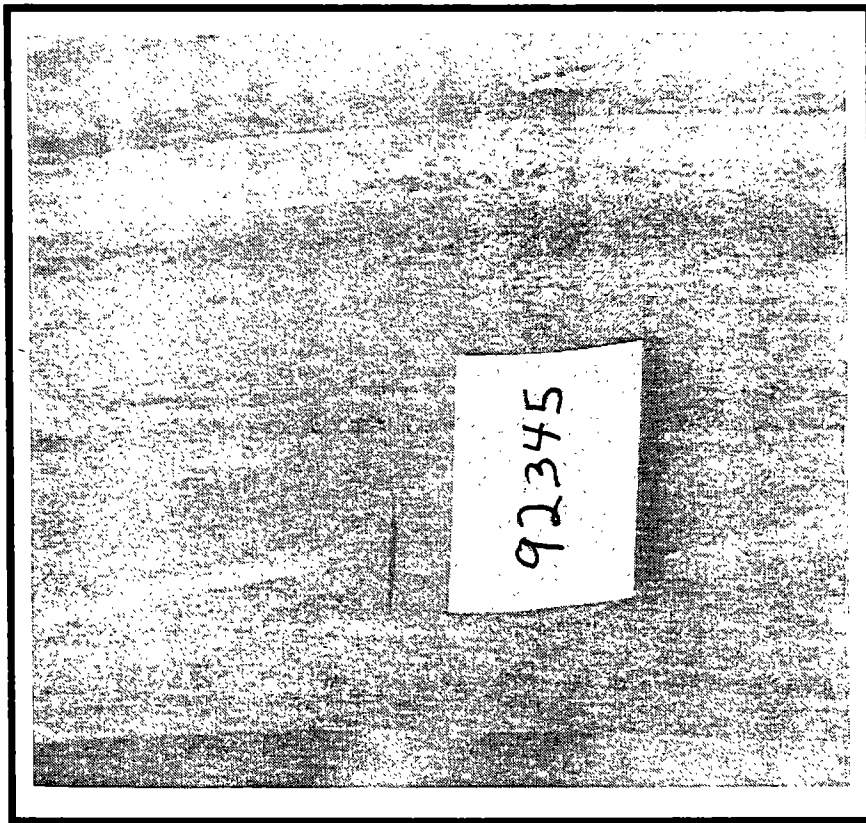
\*\* No through signal peak detected

### **5.2.2 WCD Signatures for Selected Defect Types**

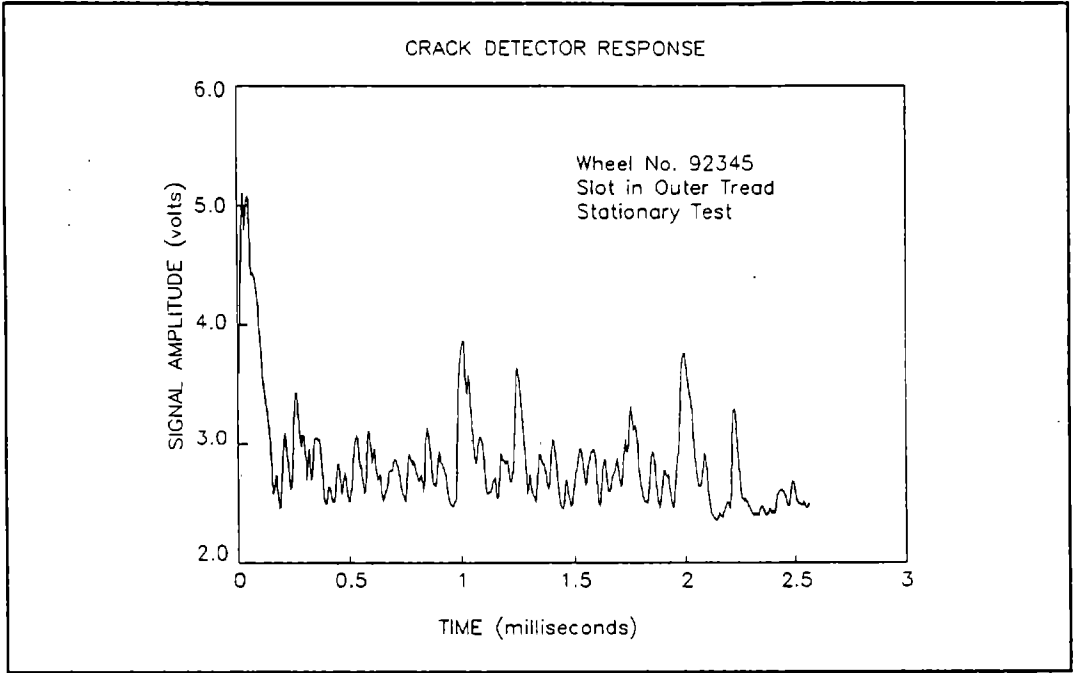
#### **SLOTTED TREAD DEFECT SIGNATURE**

Figure 7 shows a view of the slot machined into the tread of the test wheel. The slot measured 0.5 inch long and 0.08 inch deep.

Figures 8 through 10 show the detector response signals for the 0-, 5- and 10-mph tests.



**Figure 7. View of Wheel No. 92345 Tread**



**Figure 8. Detector Response for Wheel No. 92345  
Stationary Test**

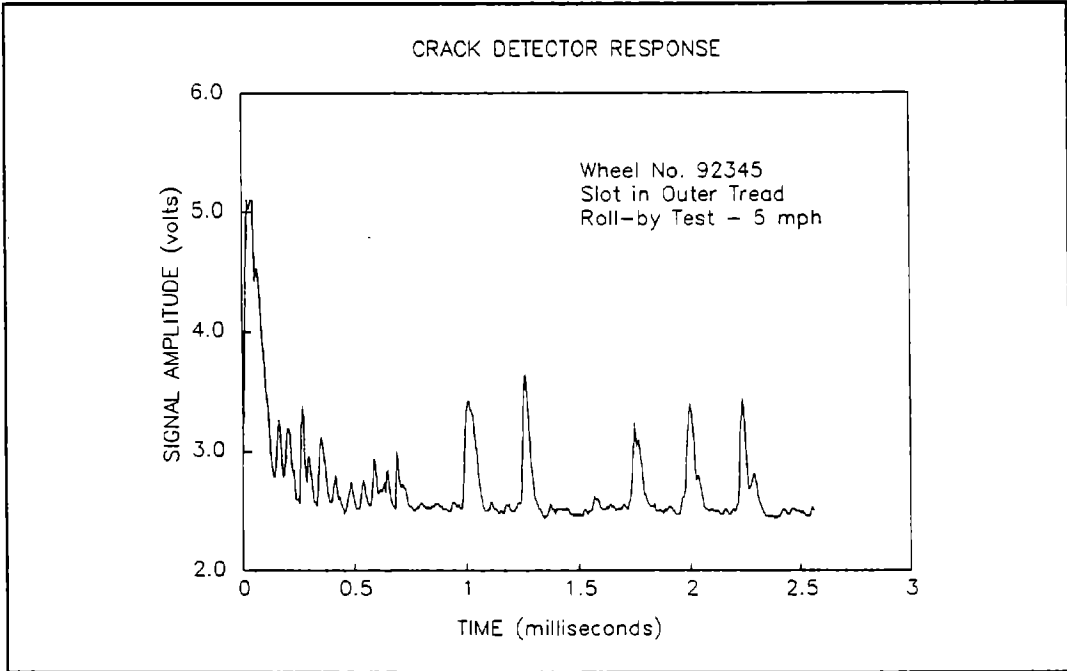


**Figure 9. Detector Response for Wheel No. 92345  
Roll-by Test -- 5 mph**

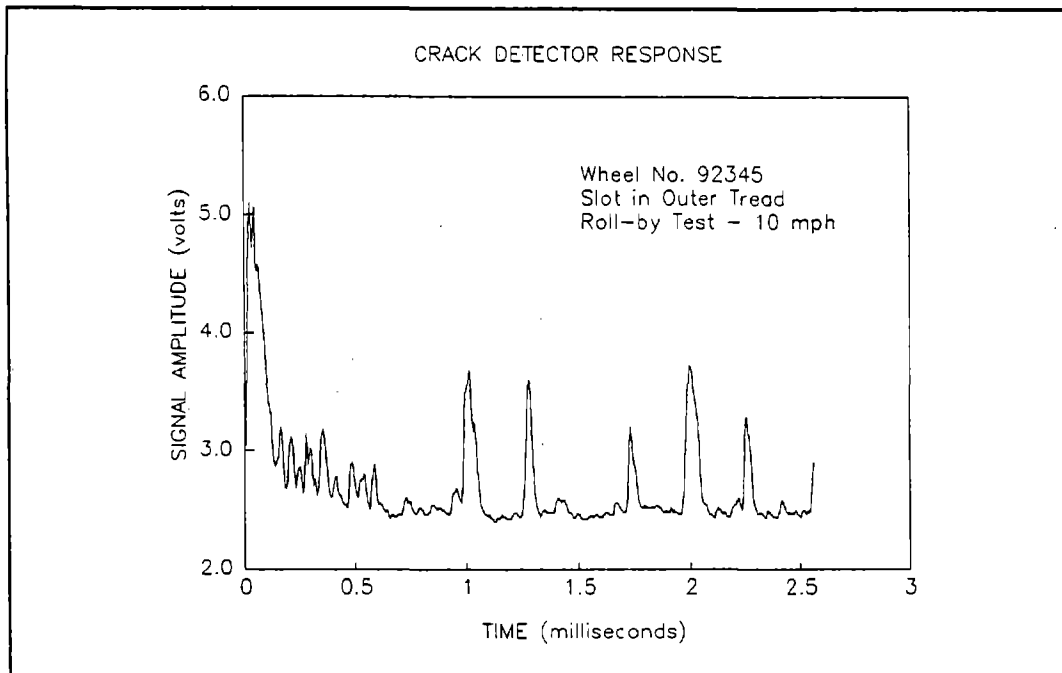


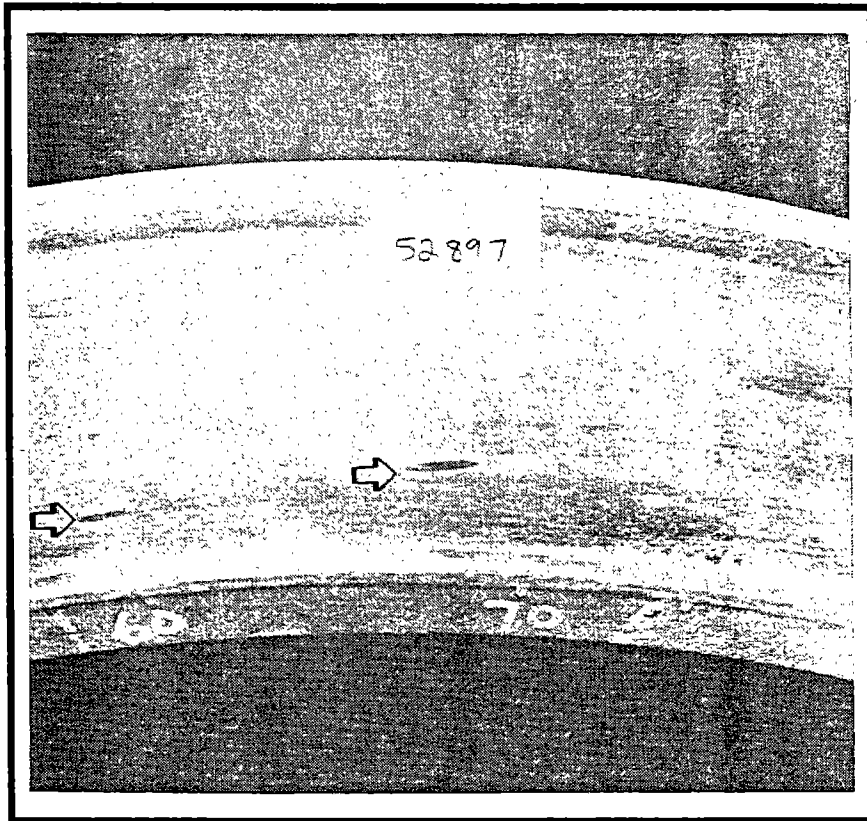
**Figure 10. Detector Response for Wheel No. 92345  
Roll-by Test -- 10 mph**

Inspection of Figures 8 through 10 shows that the detector response signals for the slot defect exhibits distinct defect and through peaks at each of the test speeds. The peaks occurring at approximately 1 and 2 milliseconds are the through peaks, and those occurring at approximately 1.3, 1.7, and 2.3 milliseconds are the defect peaks. When comparing these results to the theoretical results illustrated in Figure 3, it should be noted that the initial defect peak that was expected to occur between the main bang and the first through peak is not clearly discernable in the actual signature. As stated previously, the WCD system tested at the TTC was designed to use the amplitude of the defect peak occurring between the main bang and the first through signal as an indicator of the defect size. The absence of a distinct defect peak in this region suggests that an alternate scheme for estimating defect size will be required.

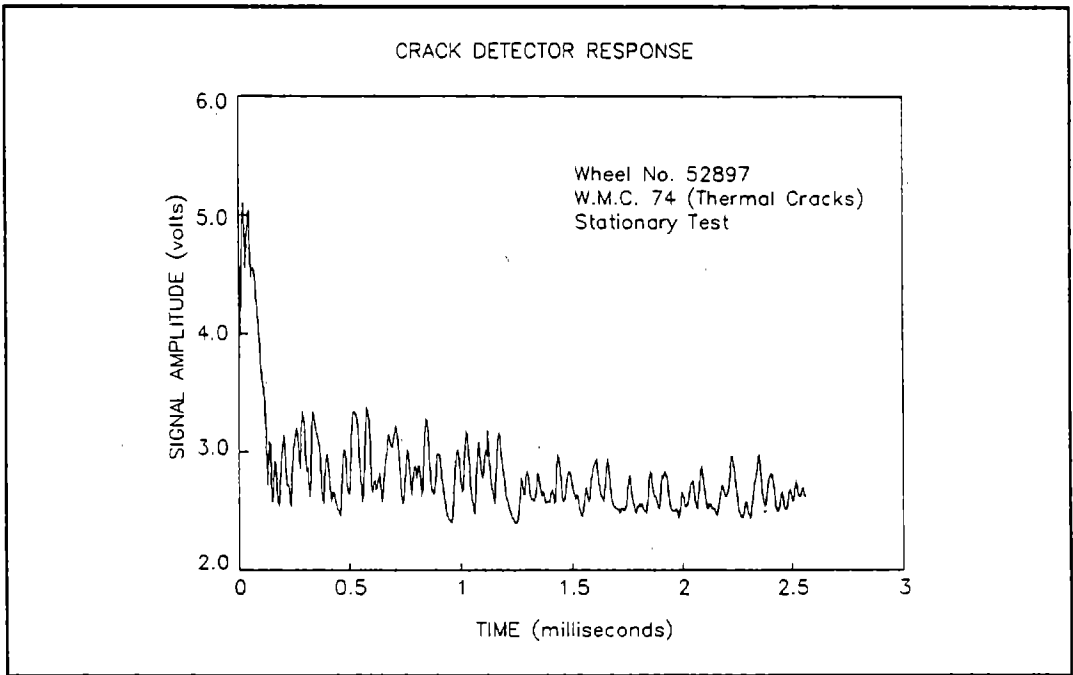
**TREAD THERMAL CRACK DEFECT SIGNATURE**

Figure 11 shows a view of the thermal crack defects in the tread of the test wheel.

Figures 12 through 14 show the detector response signals for the 0-, 5-, and 10-mph tests.



**Figure 11. View of Wheel No. 52897 Tread**



**Figure 12. Detector Response for Wheel No. 52897  
Stationary Test**

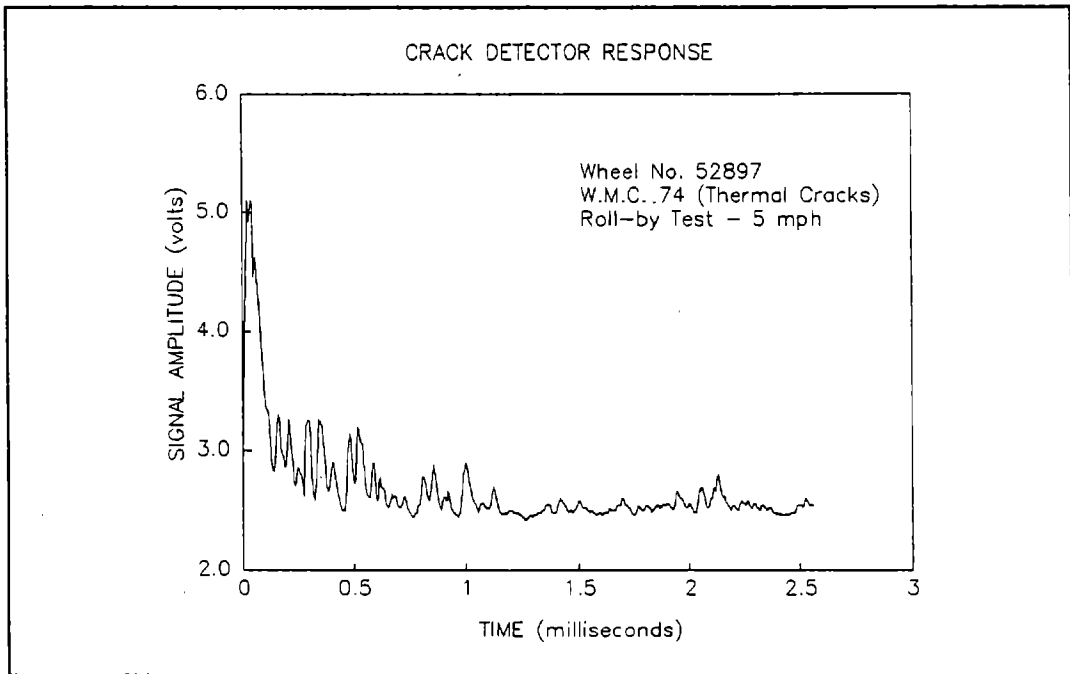


**Figure 13. Detector Response for Wheel No. 52897  
Roll-by Test -- 5 mph**



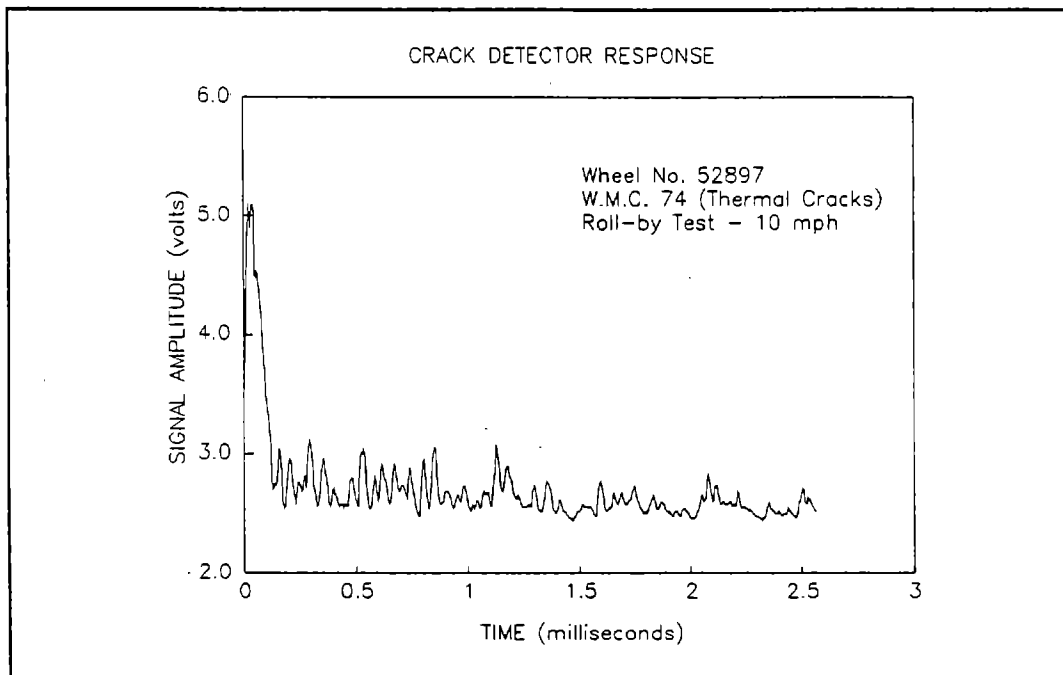


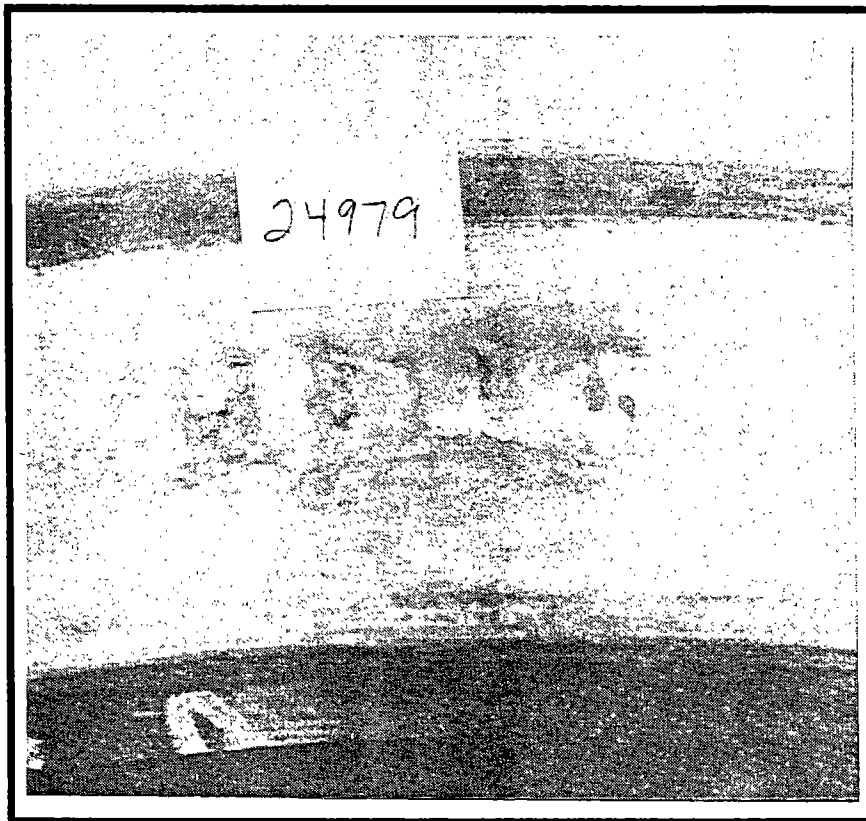
**Figure 14. Detector Response for Wheel No. 52897  
Roll-by Test -- 10 mph**

Inspection of Figures 12 through 14 shows that the detector response signals for the thermal crack defects exhibits multiple defect peaks, but no distinct through peaks for any of the test speeds including the stationary test.

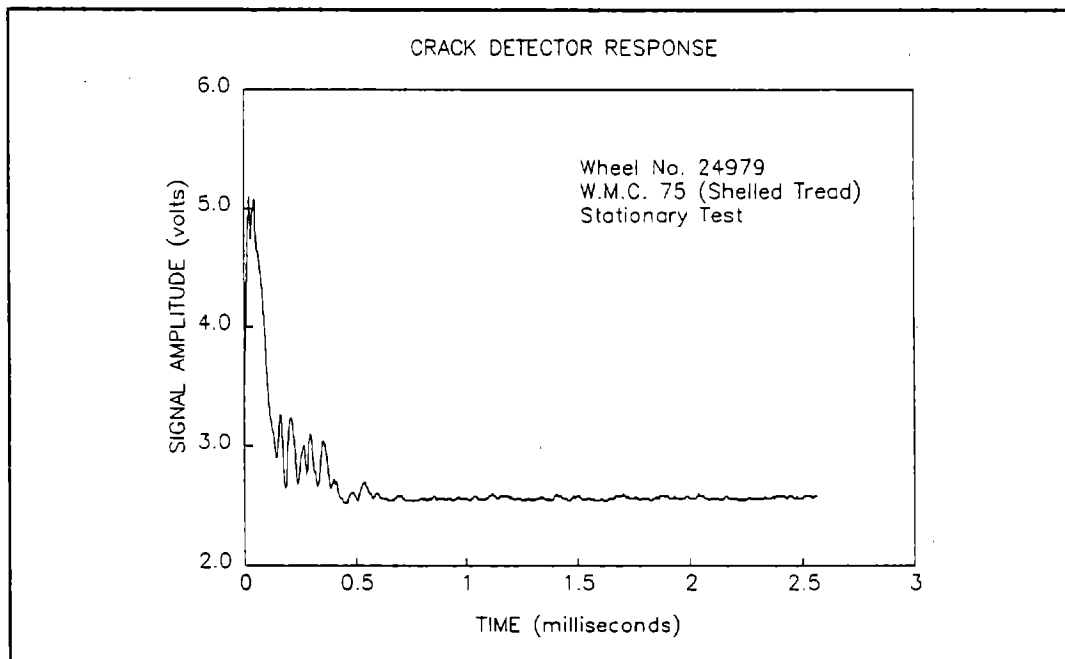
**SHELLED TREAD DEFECT SIGNATURE**

Figure 15 shows a view of the shell defect in the tread of the wheel.

Figures 16 through 18 show the detector response signals for the 0-, 5-, and 10-mph tests.



**Figure 15. View of Wheel No. 24979 Tread**



**Figure 16. Detector Response for Wheel No. 24979  
Stationary Test**

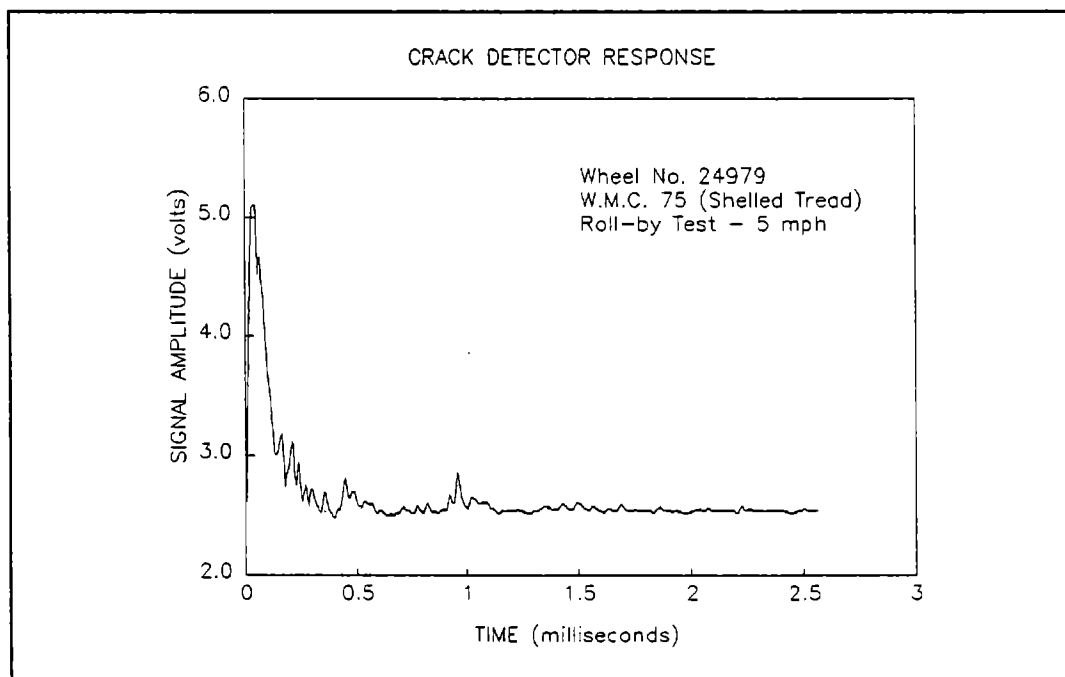


**Figure 17. Detector Response for Wheel No. 24979  
Roll-by Test -- 5 mph**

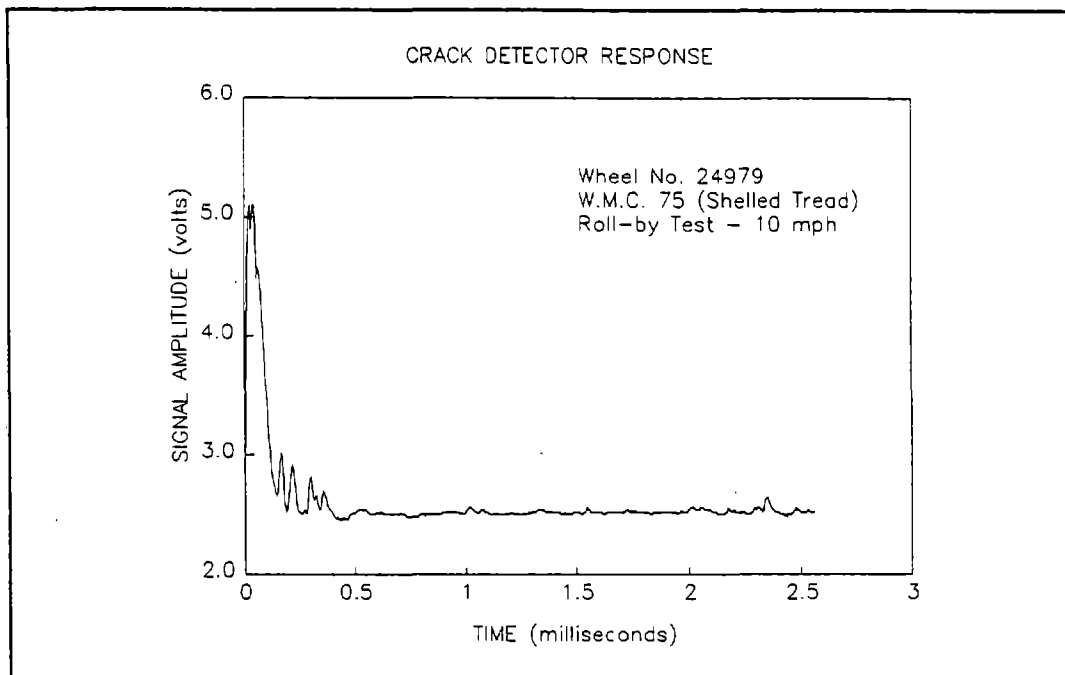


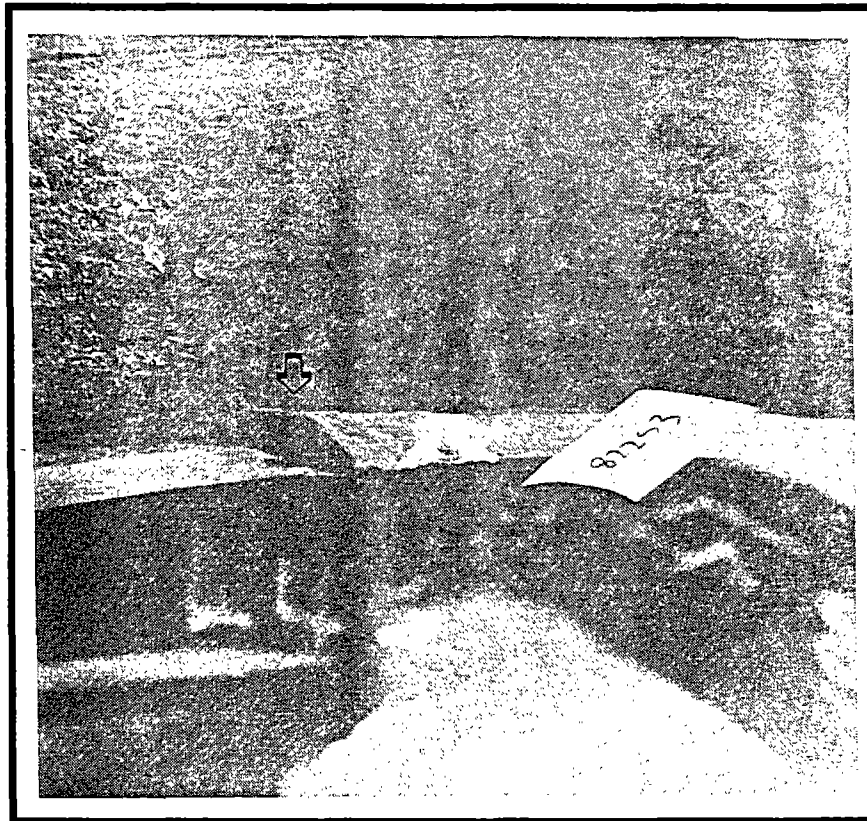
**Figure 18. Detector Response for Wheel No. 24979  
Roll-by Test -- 10 mph**

Inspection of Figures 16 through 18 shows that the energy from the initial pulses is almost completely scattered by the shelled tread defect resulting in little or no detector response signal for any of the speeds tested including the stationary test. This characteristic may be useful in distinguishing wheels with tread shelling defects from those with tread thermal crack defects.

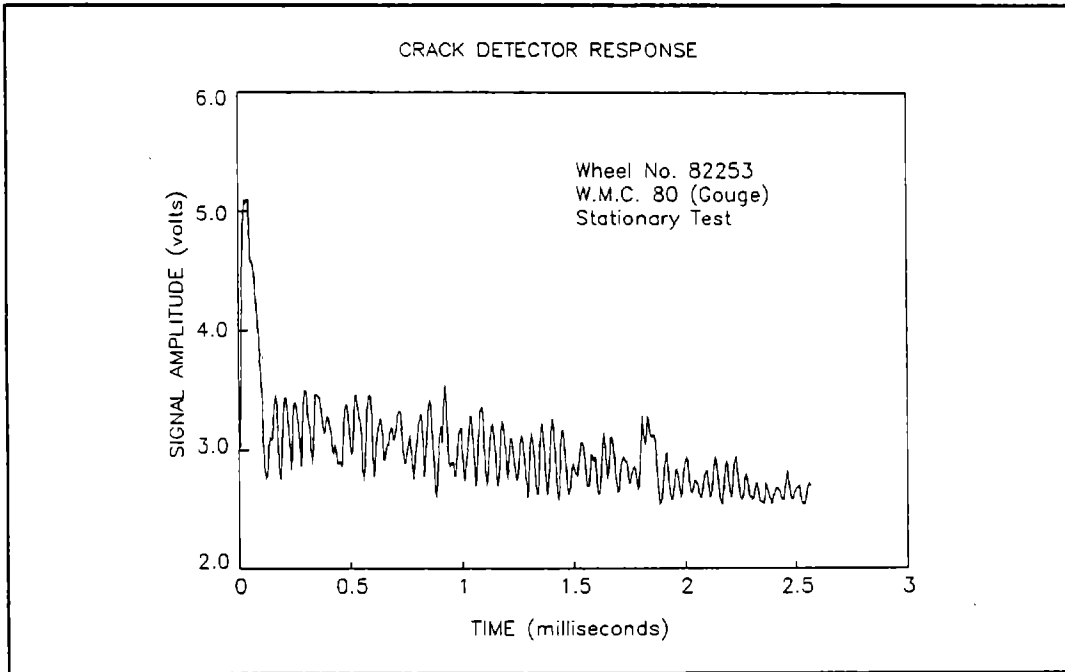
**GOUGED RIM DEFECT SIGNATURE**

Figure 19 shows a view of the gouge in the rim of the test wheel.

Figures 20 through 22 show the detector response signals for the 0-, 5-, and 10-mph tests.



**Figure 19. View of Wheel No. 82253 Tread**



**Figure 20. Detector Response for Wheel No. 82253  
Stationary Test**

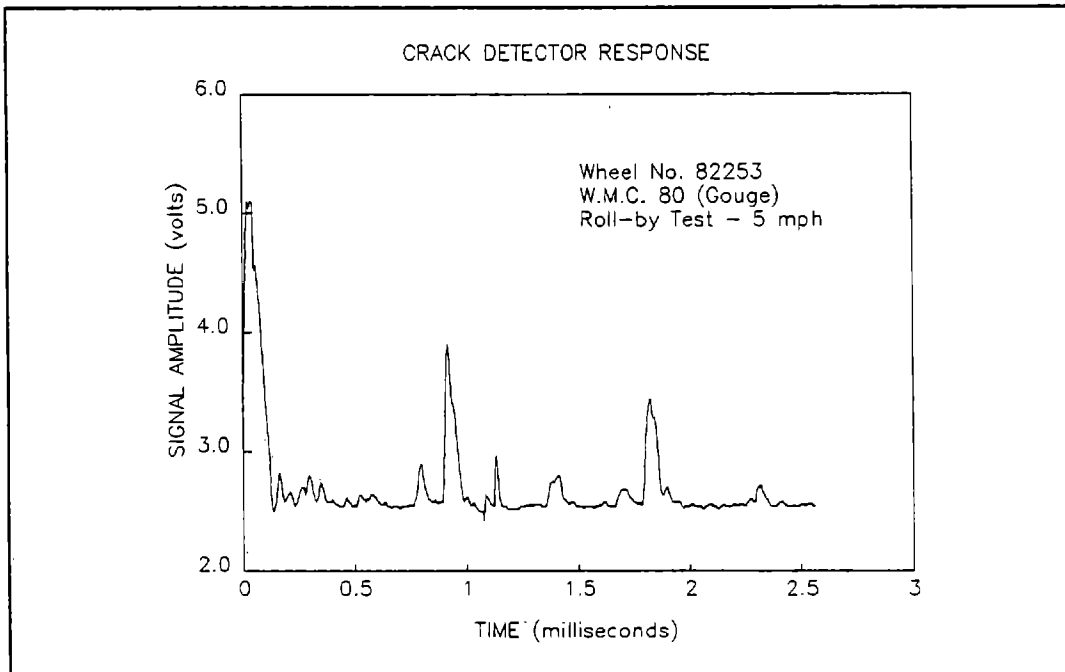


**Figure 21. Detector Response for Wheel No. 82253  
Roll-by Test -- 5 mph**

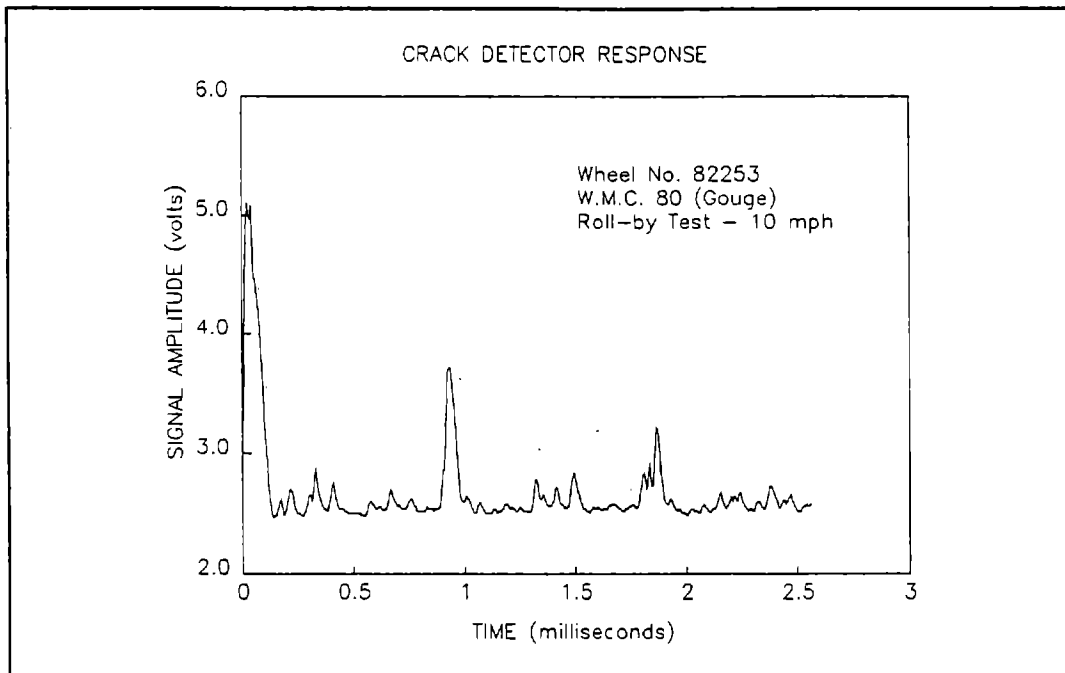


**Figure 22. Detector Response for Wheel No. 82253  
Roll-by Test -- 10 mph**

Inspection of Figures 20 through 22 shows that the detector response signals for the gouge defect in the rim exhibits distinct defect and through peaks for each test speed. For this wheel, the through peaks occurred at 0.9 and 1.8 milliseconds.

### 5.2.3 New Wheel WCD Signatures

The following figures show the WCD results obtained for four new wheels.

Inspection of Figure 27 shows that two distinct defect peaks were detected at approximately 0.7 and 0.8 milliseconds in the 5-mph roll-by test. Similar results were obtained for the 10-mph test. These defect peaks were not actually associated with any wheel defects and would result in the generation of a false alarm by the WCD system.

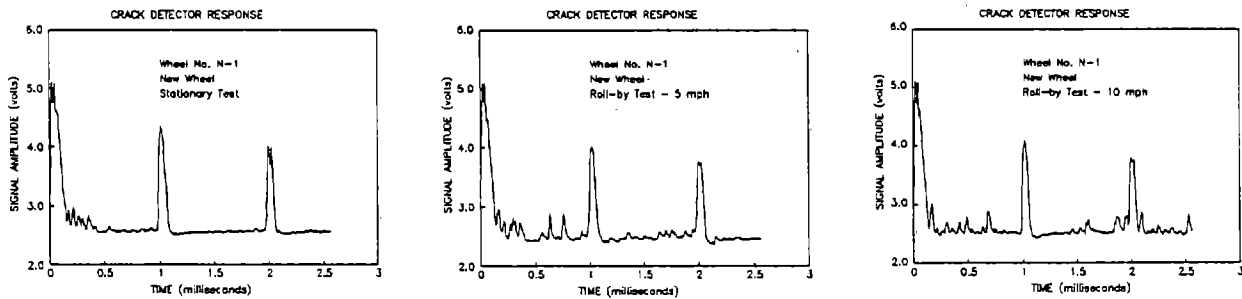


**Figure 27. Detector Response for Wheel No. N-1  
Stationary Test, 5-mph and 10-mph Tests**

Inspection of Figure 28 shows that a distinct defect peak was detected at approximately 0.3 milliseconds in the 5-mph roll-by test. Similar results were obtained for the 10-mph test. The defect peak was not actually associated with any wheel defect and would result in the generation of a false alarm by the WCD system.

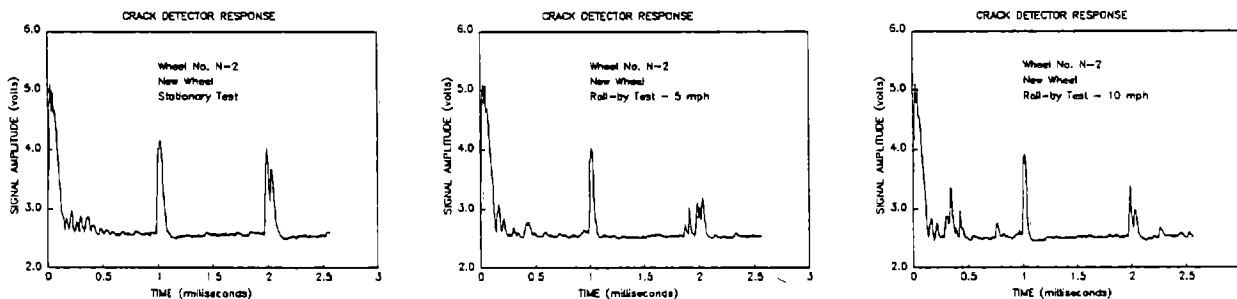


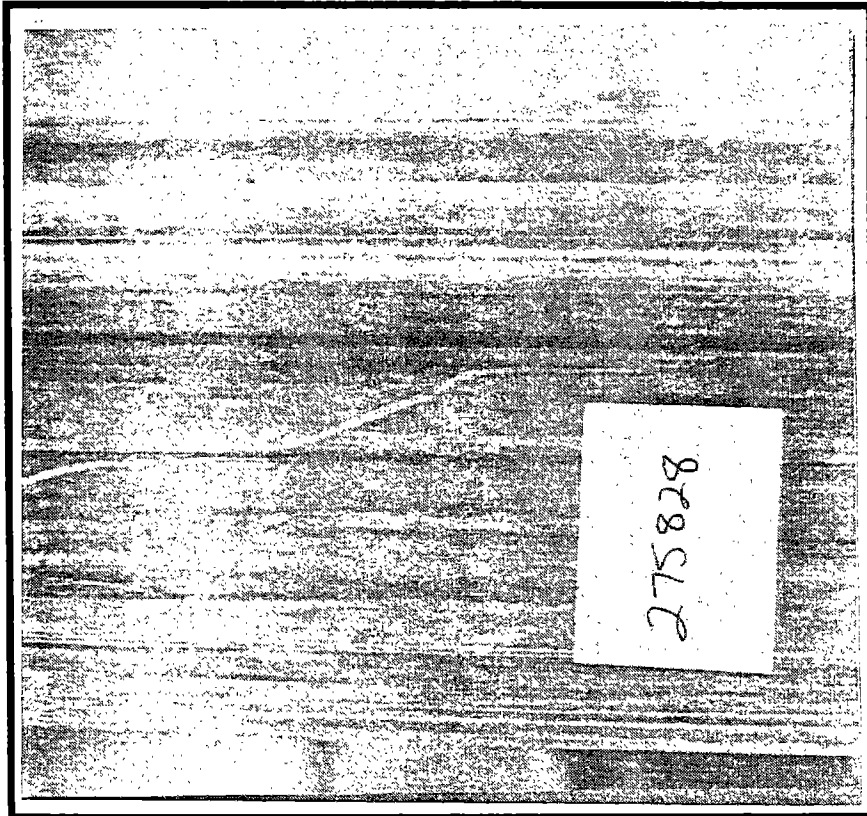
**Figure 28. Detector Response for Wheel No. N-2  
Stationary Test, 5-mph and 10-mph Tests**



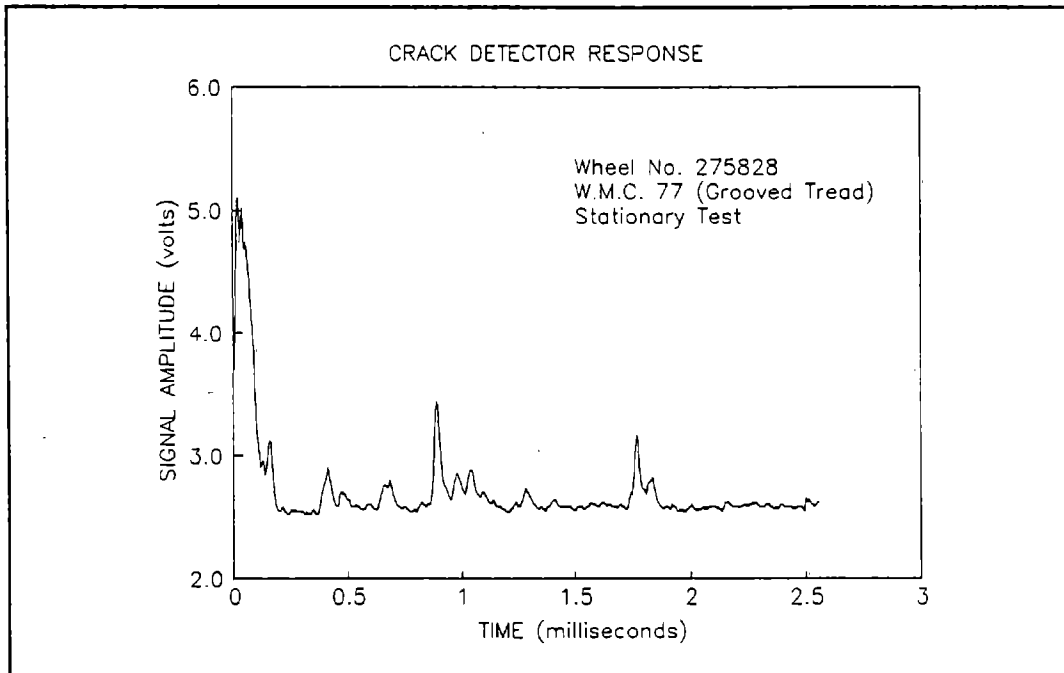
**GROOVE TREAD DEFECT SIGNATURE**

Figure 23 shows a view of the grooves in the tread of the test wheel.

Figures 24 through 26 show the detector response signals for the 0-, 5-, and 10-mph tests.



**Figure 23. View of Wheel No. 275828 Tread**



**Figure 24. Detector Response for Wheel No. 275828  
Stationary Test**

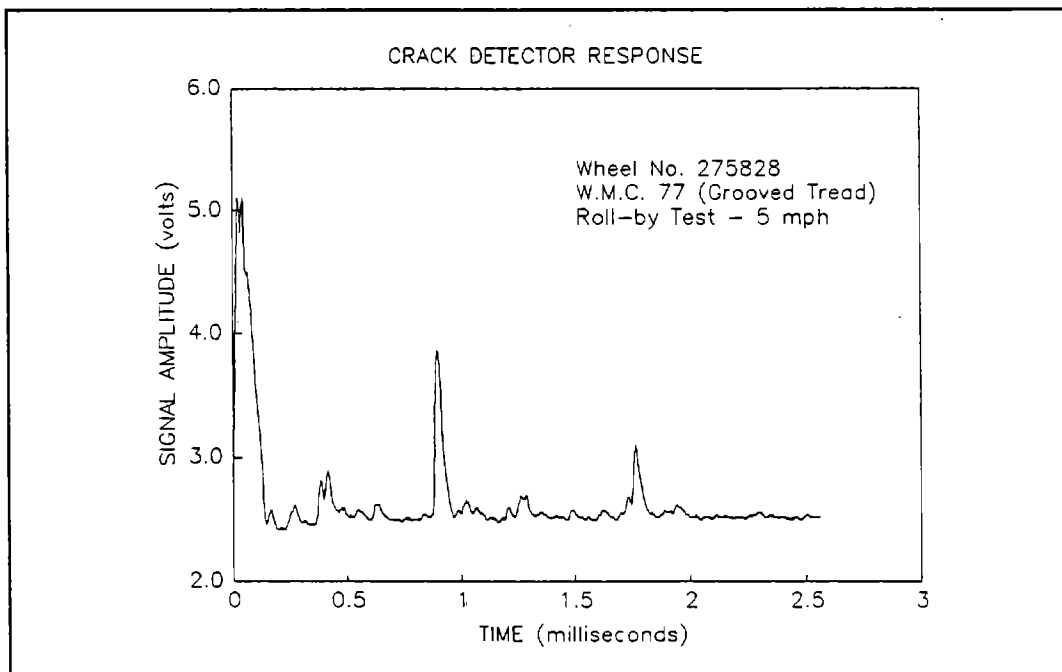


**Figure 25. Detector Response for Wheel No. 275828  
Roll-by Test -- 5 mph**

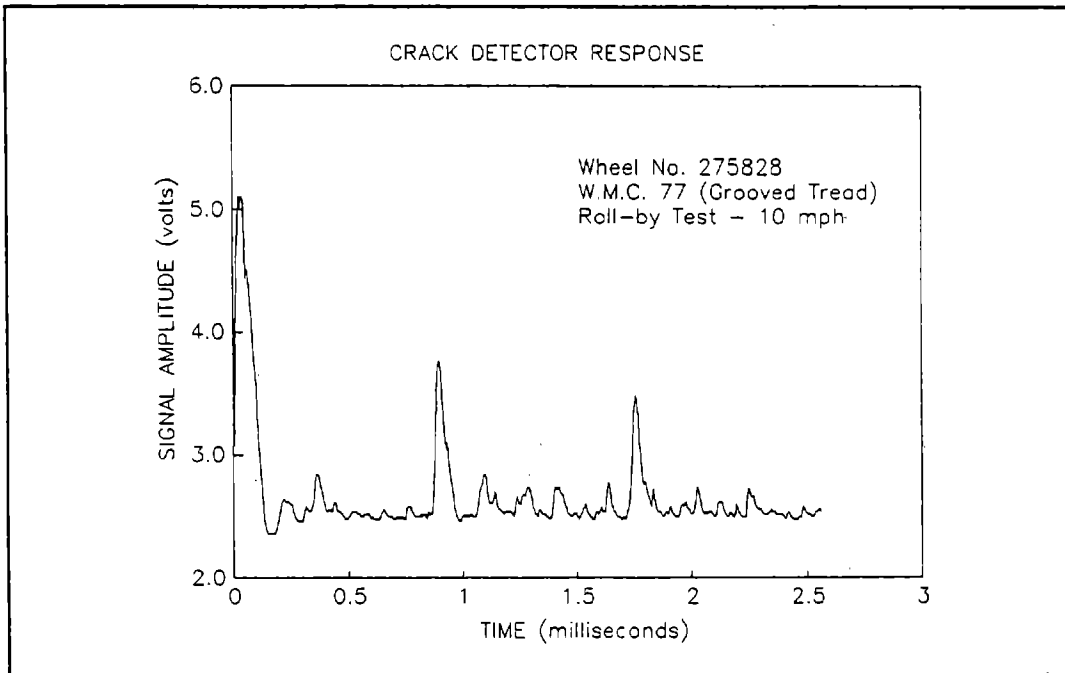


**Figure 26. Detector Response for Wheel No. 275828  
Roll-by Test -- 10 mph**

Inspection of Figures 24 through 26 shows that the detector response signals for the grooved rim defect exhibits defect and through peaks for each test speed. For this wheel, the through peaks occurred at 0.8 and 1.6 milliseconds.

Inspection of Figure 29 shows that a distinct defect peak was detected at approximately 0.4 milliseconds in the 5-mph roll-by test and three-defect peaks were detected in the 10-mph test. The defect peaks were not actually associated with any wheel defects and would result in the generation of a false alarm by the WCD system.

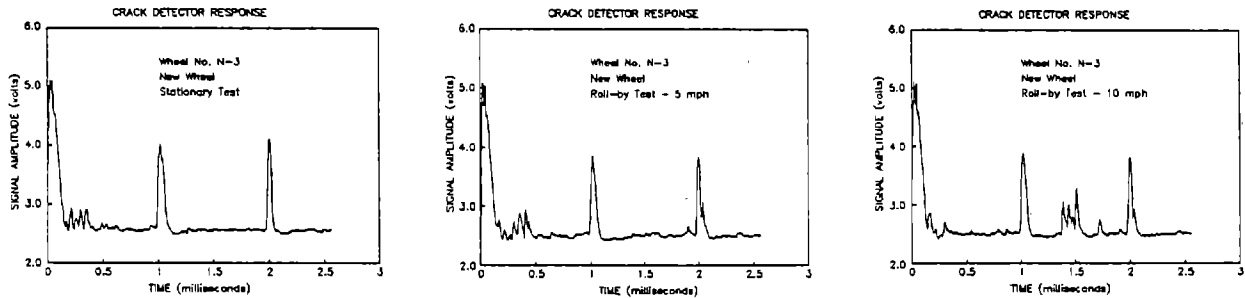


**Figure 29. Detector Response for Wheel No. N-3  
Stationary Test, 5-mph and 10-mph Tests**

Inspection of Figure 30 shows that a distinct defect peak was detected at approximately 0.3 milliseconds in the 5-mph test. Similar results were obtained in the 10-mph test. The defect peak was not actually associated with any wheel defect and would result in the generation of a false alarm by the WCD system.

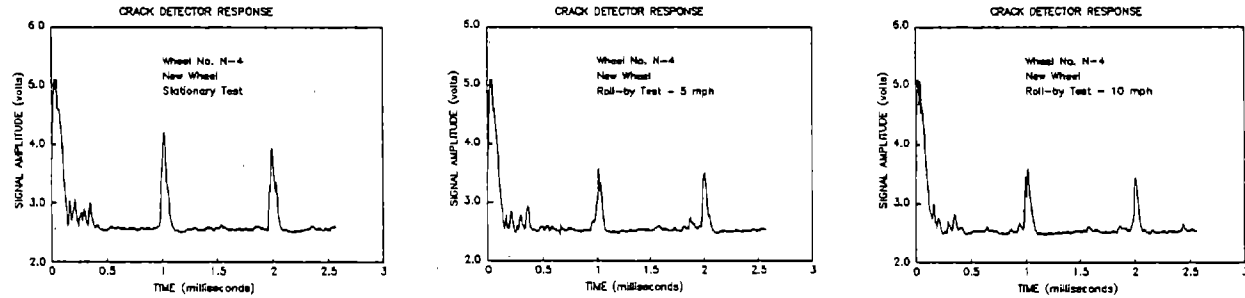


**Figure 30. Detector Response for Wheel No. N-4  
Stationary Test, 5-mph and 10-mph Tests**

### 5.2.4 Signature Variations with Speed

The WCD signatures were generally attenuated at 5-mph and 10-mph roll-by test speeds as compared to stationary tests. The percent reduction in the amplitude of the first through signal, as compared to the stationary test, measured for each of the new wheels at each speed is shown in Table 3.

**Table 3. Signal Amplitude Variation with Speed**

WHEEL	THROUGH SIGNAL AMPLITUDE STATIONARY TEST (millivolts)	PERCENT REDUCTION IN THROUGH SIGNAL AMPLITUDE RELATIVE TO STATIONARY TEST	
		5-MPH ROLL-BY TEST	10-MPH ROLL-BY TEST
N-1	89	-15	-11
N-2	79	-9	-13
N-3	70	-7	-6
N-4	82	-35	-43

### 5.2.5 Wheel Position/Defect Orientation Tests

A summary of the results obtained for Test Series 3 and 4 is given in Table 4.

**Table 4. Test Series 3 & 4 Results Summary**

WHEEL ID	TREAD DEFECT TYPE	NUMBER OF ANGULAR POSITIONS DEFECT SIGNAL PEAK WAS DETECTED		
		WHEEL SET CENTERED	TEST WHEEL FLANGED	MATE WHEEL FLANGED
52897	Thermal Cracks	*	**	**
51265	Thermal Cracks	*	-	-
92345	Slot in Outer Tread	12	8	12
64796	Slot in Inner Tread	11	6	7
82253	Gouge	2	-	-
8757	Cracked Rim	12	-	-
54844	Shelled Tread (two 3" shells)	10	-	-
24979	Shelled Tread (11% of circumference)	*	**	**

\* No through signal

\*\* Some through signals

- Wheel not tested

### **5.2.6 20-mph Roll-By Tests**

The detector trigger did not work consistently during the 20-mph roll-by tests. The trigger did activate all of the test wheels in five of the ten 20-mph runs. For all of the runs, a high noise level was evident in the signal response.

## **6.0 DISCUSSION**

### **6.1 DEFECT SIGNATURES**

The following characteristics were observed in the detector response measured for the various wheel defects:

- The detector signal exhibited distinct defect peaks and through signal peaks for wheels containing slots (simulated defects) in the tread.
- The detector signal was strongly attenuated (decreased) for wheels having thermal cracks or shelling. For these defect types no through signals were detected.
- There was a difference in the signal level for wheels having thermal cracks as compared to wheels having tread shells. The signal level obtained from wheels with tread thermal cracks was significantly higher than the signal level obtained for shelled wheels. The signal level obtained for two of the wheels with shelled tread defects was reduced to zero within 1.5 milliseconds of introducing the initial pulses into the wheels.
- For wheels having both thermal cracks and minor pitting or shelling, the detector response was similar to that for wheels having only thermal cracks.
- The detector signal measured for a wheel with condemnable shelling (wheel 24979) appeared to be indistinguishable from the signal measured for a wheel with non-condemnable shelling (wheel 514114).
- The detector signal measured for a wheel with gouged rim defects produced distinct through peaks but the defect peaks measured were only of minimal amplitude.

### **6.2 EFFECT OF ROLL-BY SPEED ON DETECTOR RESPONSE**

For a given test wheel, the detector signal peaks were generally somewhat higher for the stationary tests as compared to the roll-by tests. The detector response measured for the 5-mph roll-by tests were virtually the same as the response measured for the 10-mph tests. For the 20-mph roll-by tests, a high noise level was observed in the detector signal; for that test speed the signals did not produce distinct signatures for the different types of wheel defects.

### **6.3 EFFECT OF WHEEL POSITION AND DEFECT ORIENTATION**

The results of Test Series 3 indicate that, as expected, the WCD system will not detect defects located near the EMAT/wheel contact point nor at 180 degrees from the contact point. The results for Test Series 4 indicate that when an inspected wheel is shifted laterally with zero flange-way clearance the detector signal can be reduced in strength. However, for most of the 5-mph and 10-mph roll-by tests, the measured detector signal had similar characteristics to those measured for the centered stationary tests performed in Test Series 3. Shifting the wheel set laterally to maximize the flange-way clearance had no detrimental effects on the system performance.

### **7.0 CONCLUSIONS**

The test data supports the following conclusions:

- With appropriate signal processing and incorporation of the modifications recommended in Section 8, the WCD system could likely be used to identify wheels having the following tread defects:
  - Thermal Cracks
  - Non-condemnable Shelling
  - Condemnable Shelling
- The WCD system, appropriately augmented with acceleration or strain gage based wheel impact measurement instrumentation, may potentially have the capability to differentiate between wheels having thermal cracks and wheels having shells.
- The system will need refining in order to eliminate the source of defect peaks observed on new wheels that were actually free of tread defects, and to limit the number of false indications observed when testing used wheels.
- The system will need refining in order to improve the durability and reliability of the EMAT package and the trigger circuitry.
- The current methods used to detect defects and estimate defect size need to be modified to obtain more reliable results.
- The system will need refining in order to achieve roll-by inspection speeds higher than 15-mph.

## 8.0 RECOMMENDATIONS

The following recommendations are based upon the results obtained in these tests:

- A new triggering circuit should be designed to ensure that a maximum input signal amplitude is achieved to allow higher roll-by inspection speeds. The design of the circuit should also address the durability and reliability improvements.
- A new EMAT package should be designed to ensure that a maximum input signal amplitude is achieved to allow higher roll-by inspection speeds, and obtain through peaks for thermal crack and shelled defects in the wheel tread.
- Consideration should be given to configuring the WCD system to provide a recognizable signal response for wheels having flange defects.
- Since defects can occur at any location around the circumference of the wheel, consideration should be given to the overall system design to compensate for the dead zones that occur adjacent to the detector contact point and at 180 degrees from the contact point.
- Additional wheels should be tested to statistically confirm whether shelled wheels can be consistently differentiated from thermal cracked wheels. The tests should include instrumentation for monitoring rail vibrations and acoustic emissions.
- Studies to investigate improved signal processing techniques including the use of the regions between through signals to detect defects and estimate defect size should be conducted.
- The source of noise at higher roll-by speeds should be investigated.



## REFERENCES

1. Schramm, R. E., P. J. Shull, A. V. Clark, Jr. and D. V. Mitrakovic. *EMAT Examination for Cracks in Railroad Wheel Treads*, National Institute of Standards and Technology, Boulder CO, 1988.
2. Schramm, R. E., et al. *Tread Crack in Railroad Wheels: An Ultrasonic System Using EMATS*, National Institute of Standards and Technology, Boulder, CO, May 1991.

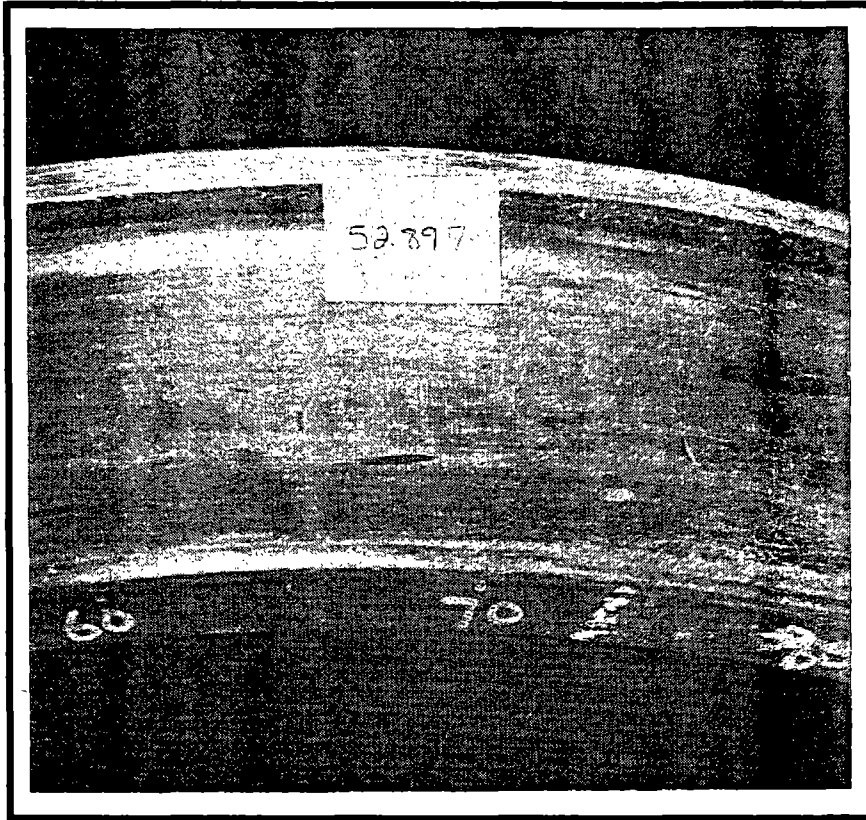
## **APPENDIX**

### **TEST WHEEL PHOTOGRAPHS**

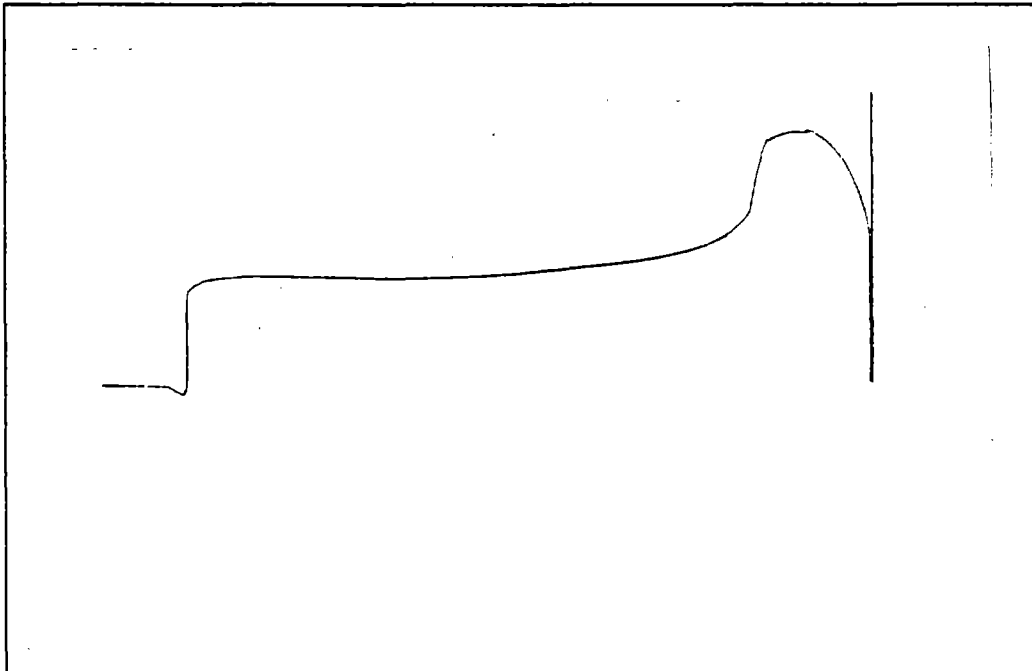
### **TEST WHEEL PROFILE GRAPHS**

### **WCD SIGNATURE GRAPHS**

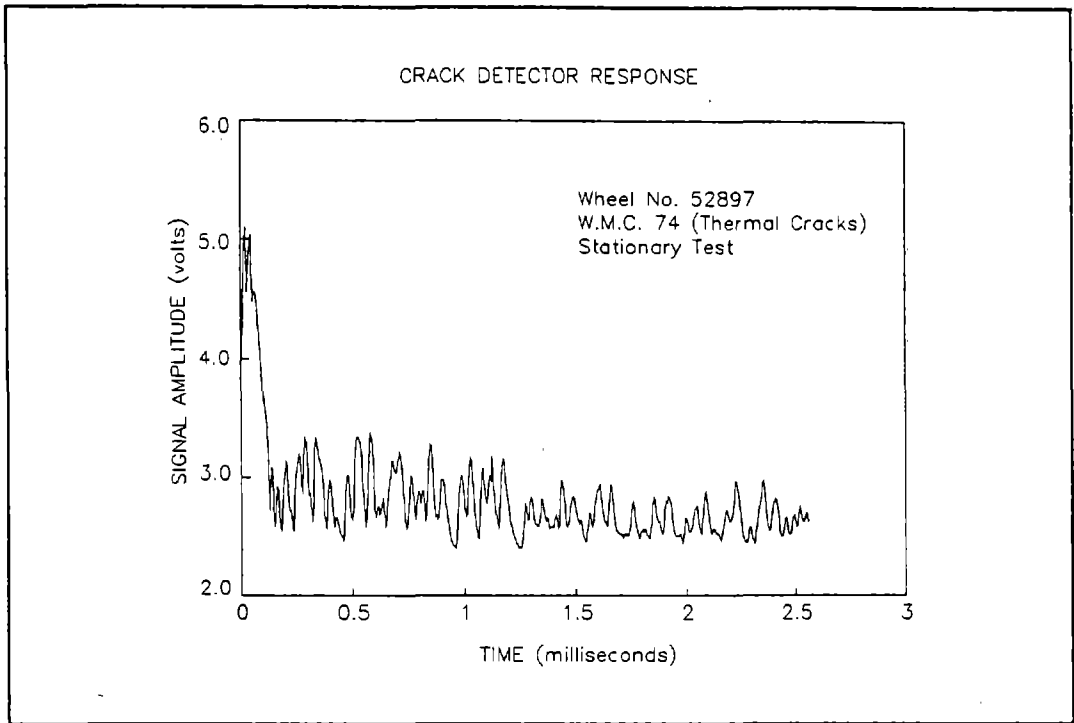
*For each of the wheels used in the test program, the characteristic tread defect was photographed and a profile of the tread contour was obtained using a Yoshida Profilometer. The wheel defect photographs, tread profiles, typical WCD Signature time histories for each test wheel, and signal amplitude distributions are provided in this appendix. The data shown correspond to one of five test runs that were performed for each test condition (stationary, 5-mph roll-by, and 10-mph roll-by). The complete test data is on file at the Association of American Railroads, Transportation Test Center, Pueblo, Colorado.*



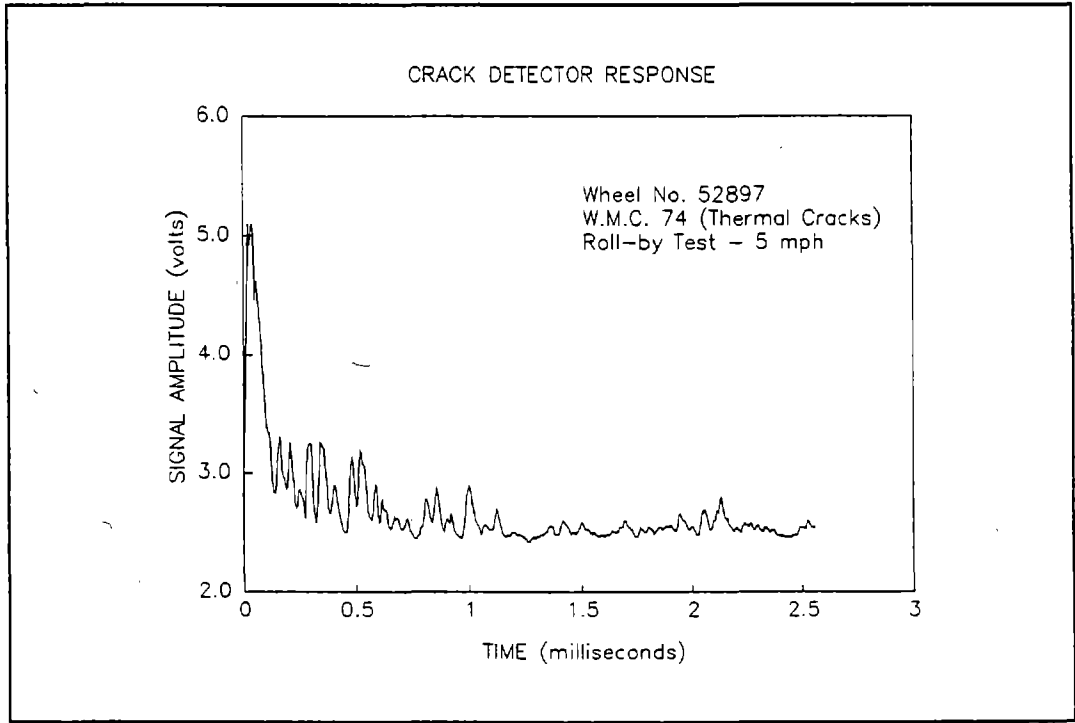
**View of Wheel No. 52897 Tread**



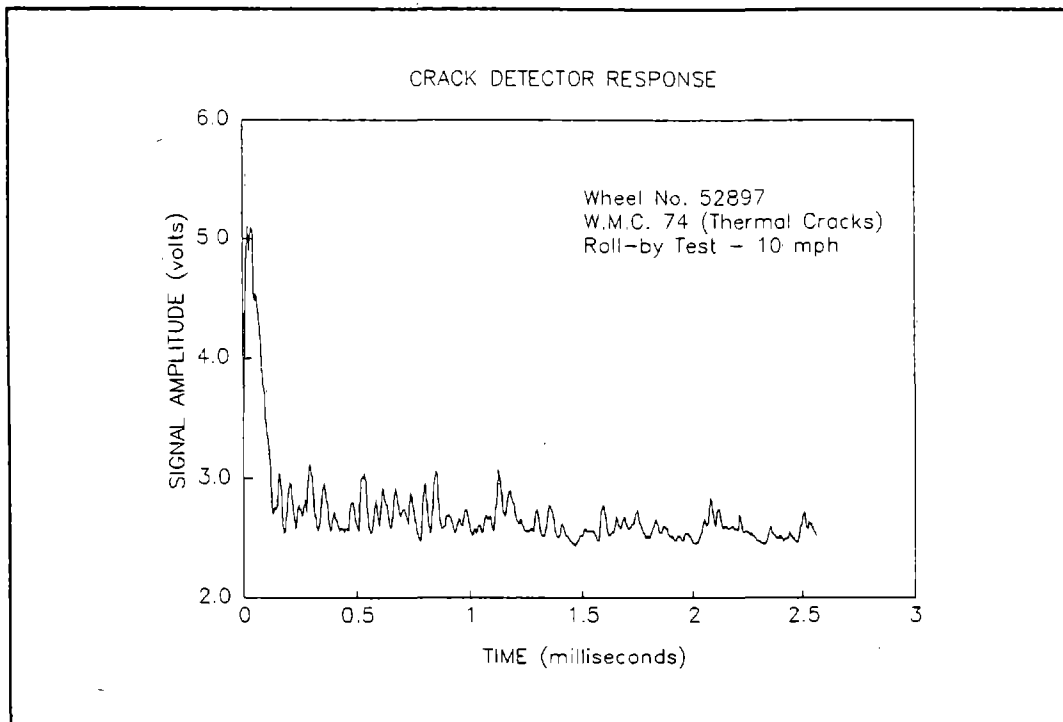
**Wheel No. 52897 Tread Profile**



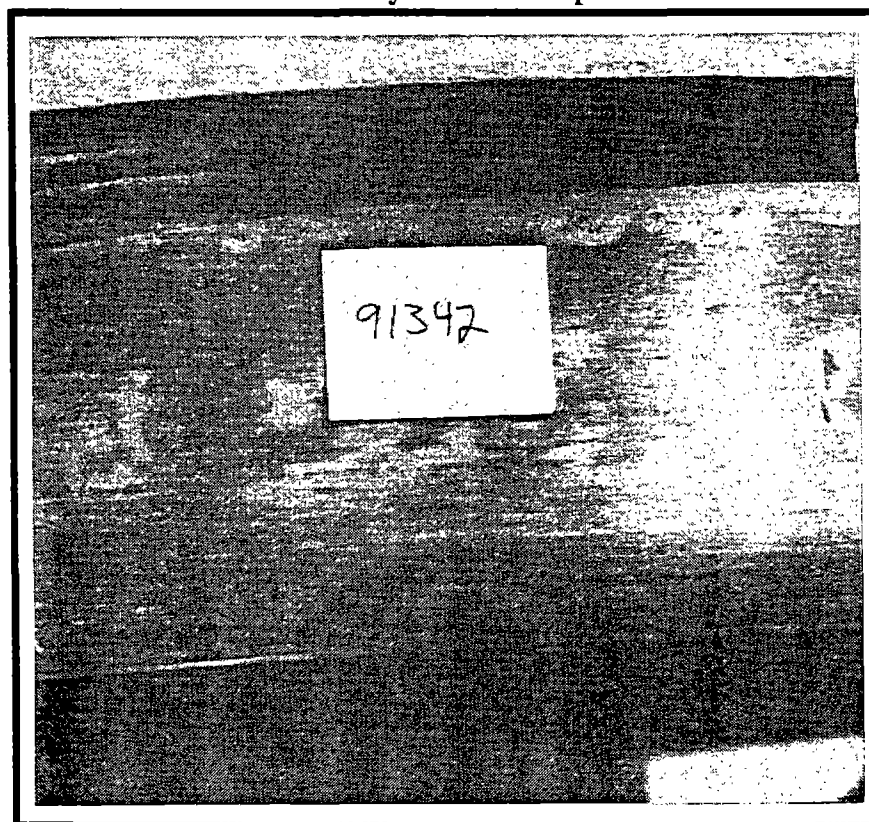
**Detector Response for Wheel No. 52897  
Stationary Test**



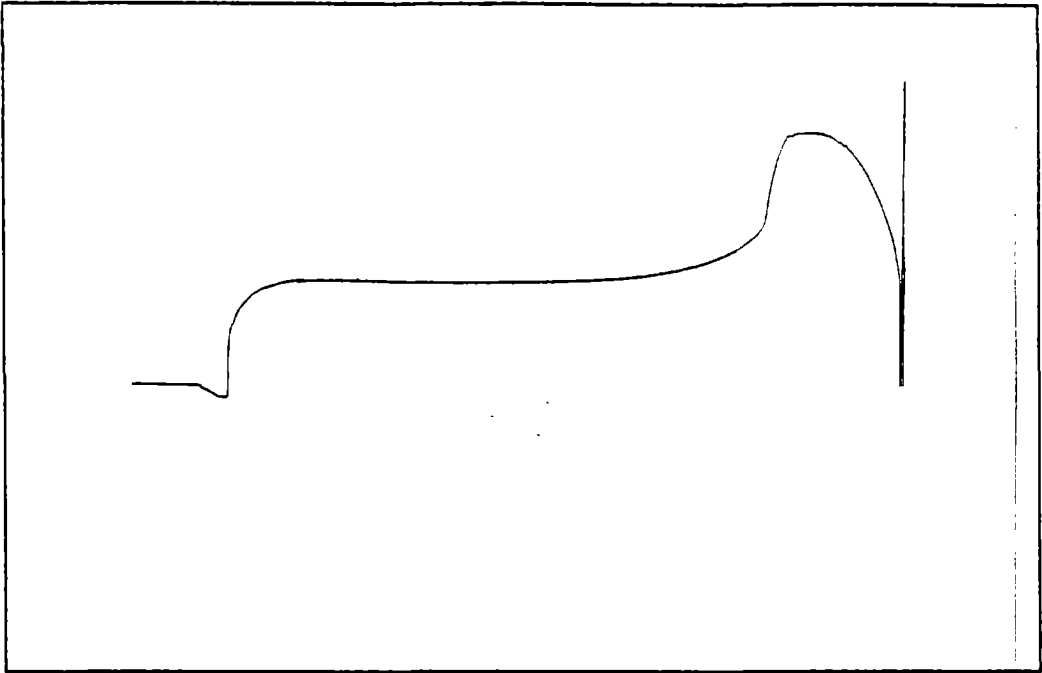
**Detector Response for Wheel No. 52897  
Roll-by Test -- 5 mph**



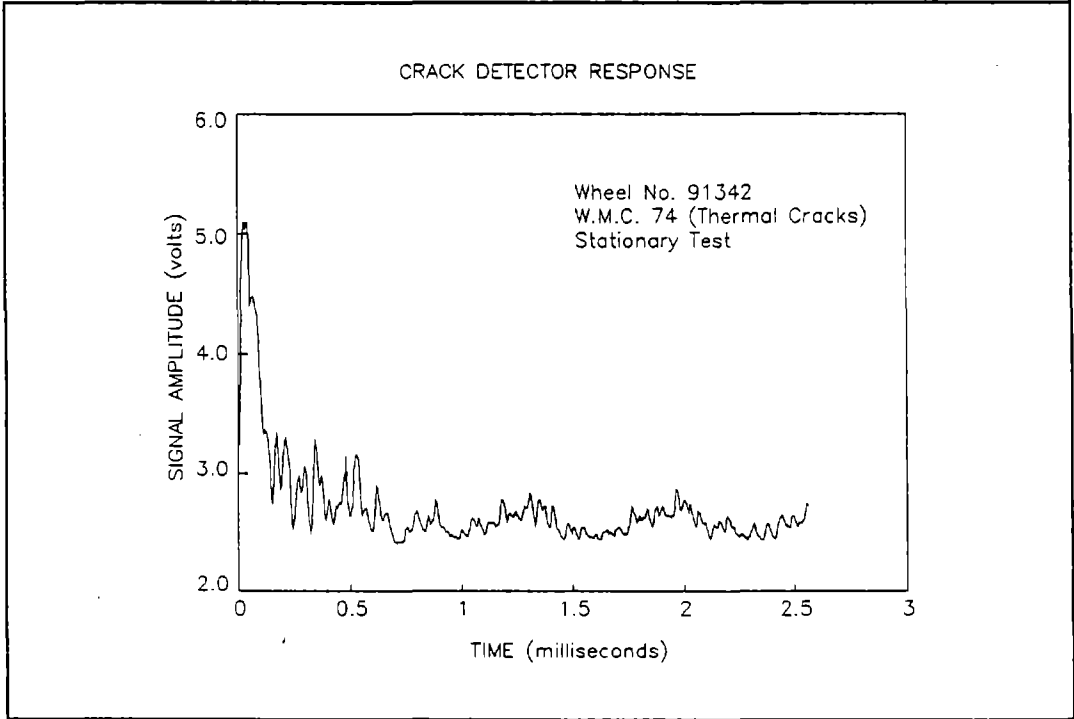
**Detector Response for Wheel No. 52897  
Roll-by Test -- 10 mph**



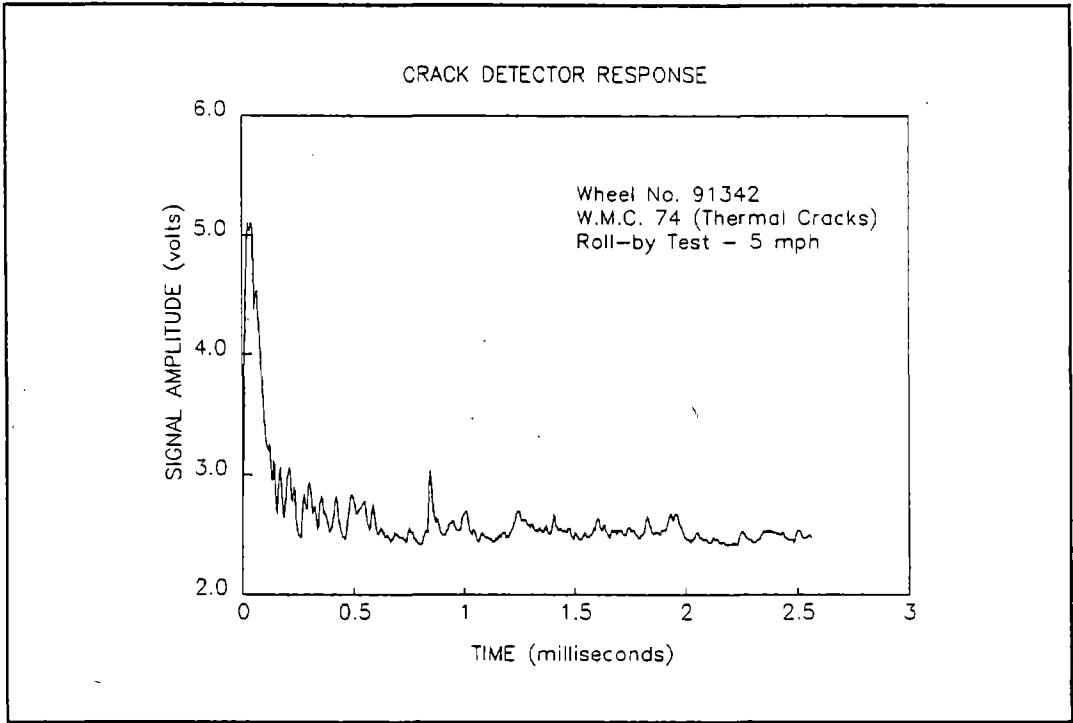
**View of Wheel No. 91342 Tread**



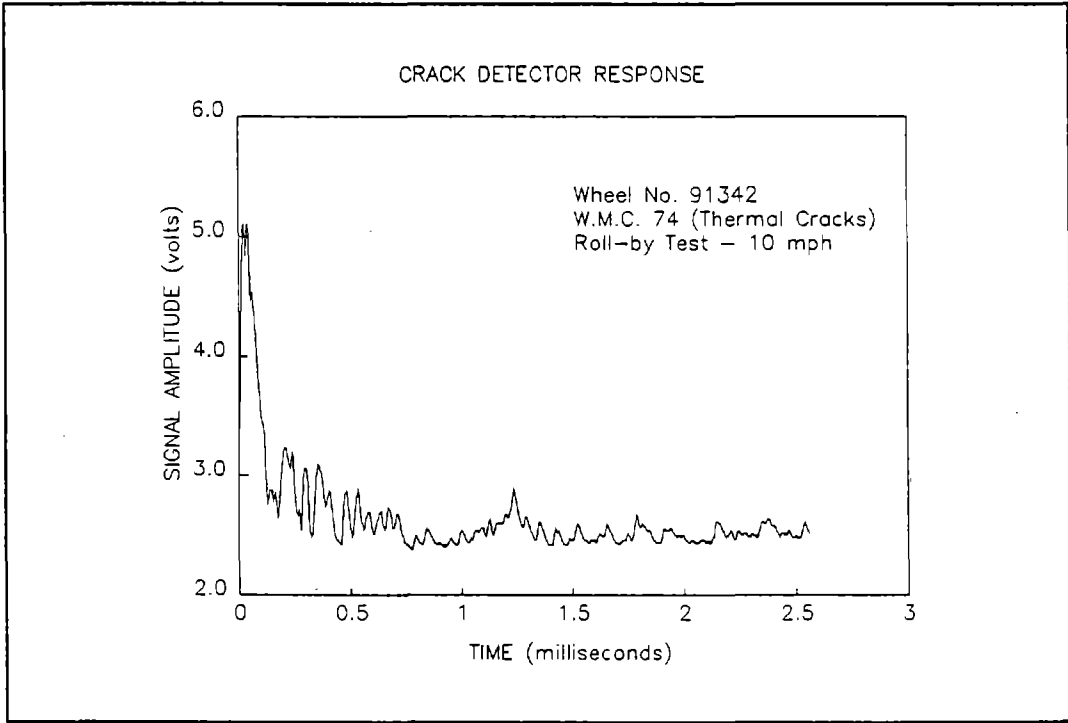
**Wheel No. 91342 Tread Profile**



**Detector Response for Wheel No. 91342  
Stationary Test**



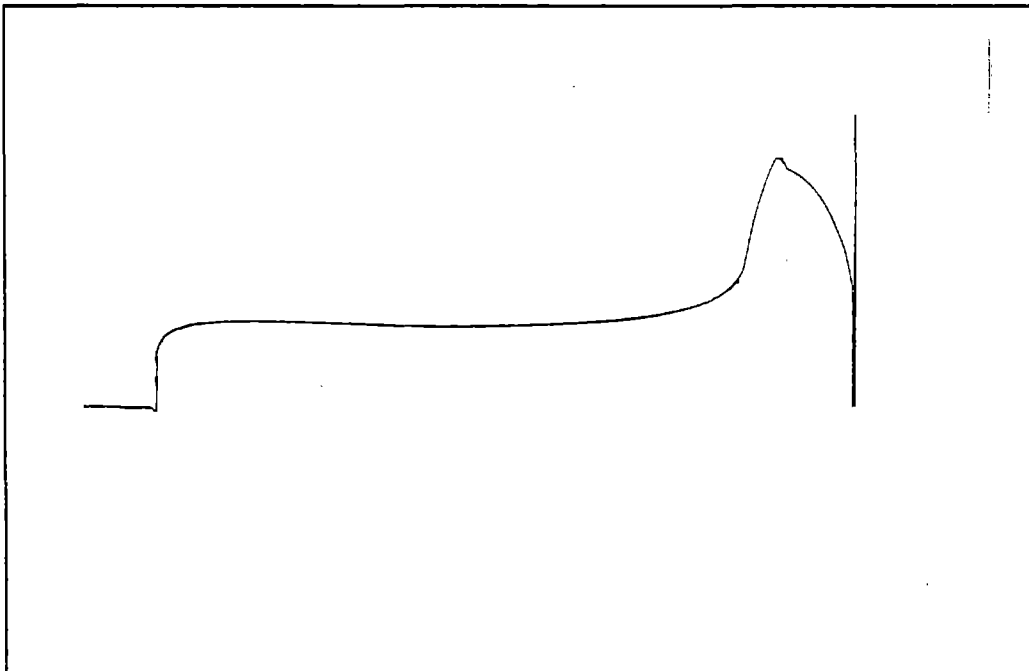
**Detector Response for Wheel No. 91342  
Roll-by Test -- 5 mph**



**Detector Response for Wheel No. 91342  
Roll-by Test -- 10 mph**

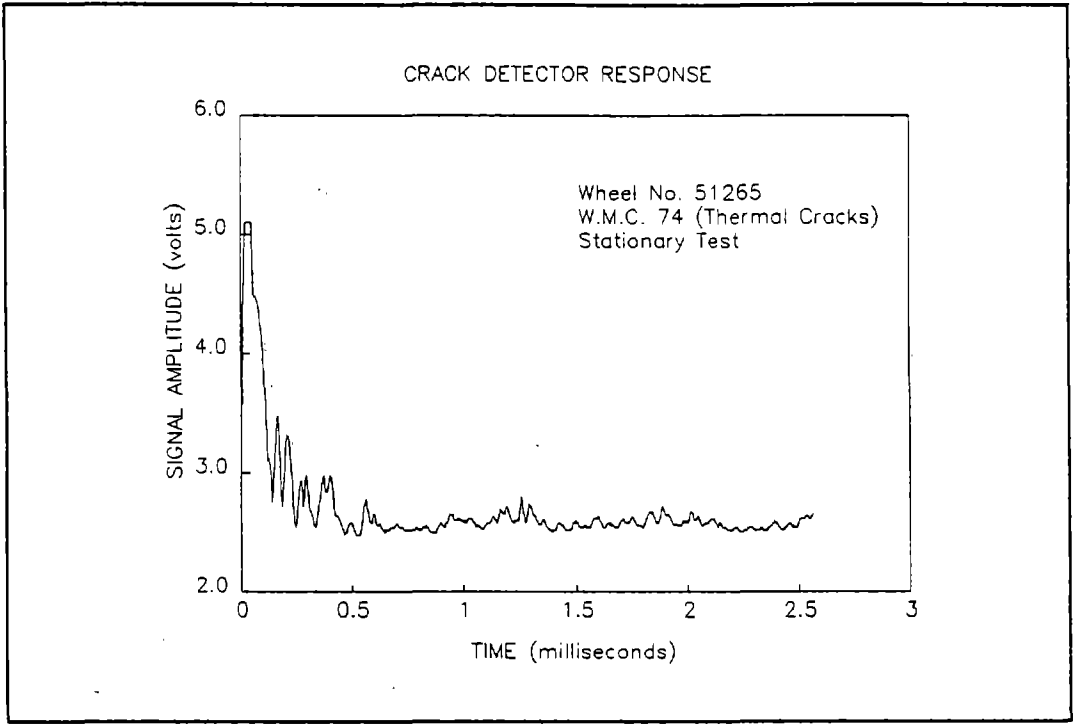


**View of Wheel No. 51265 Tread**

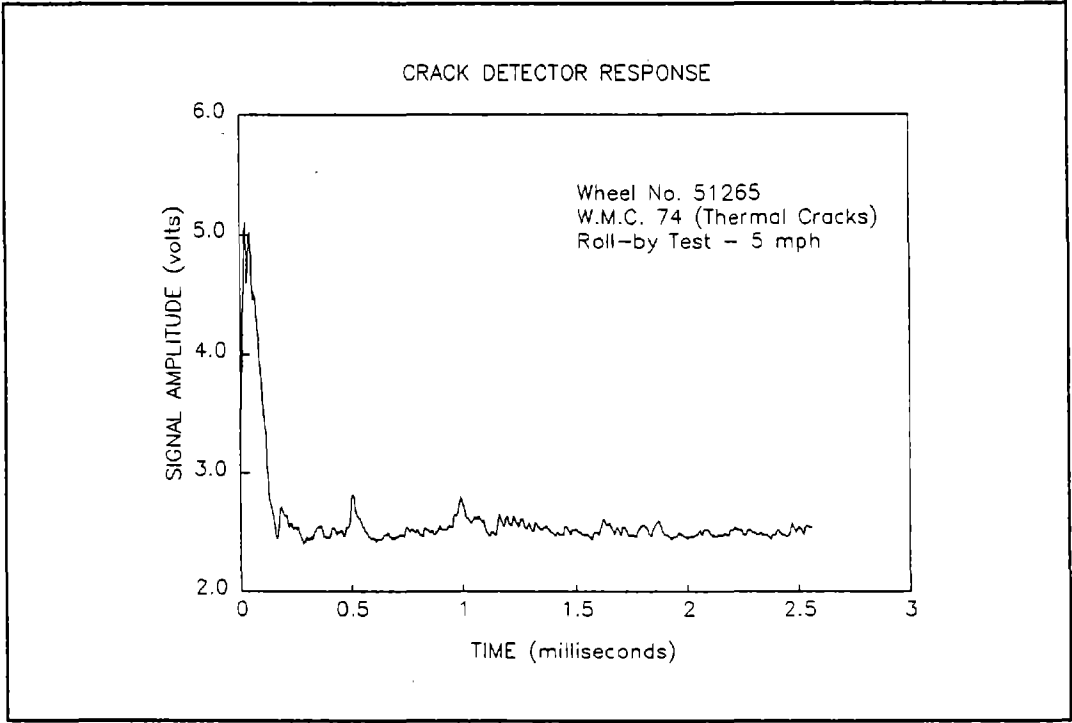


**Wheel No. 51265 Tread Profile**

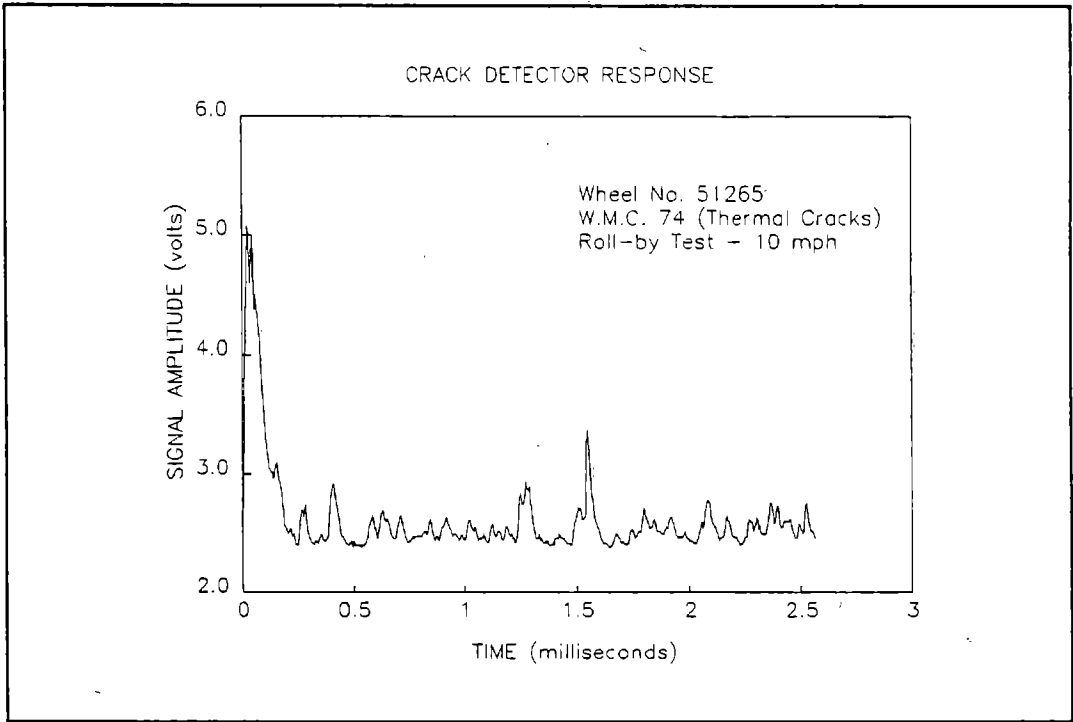




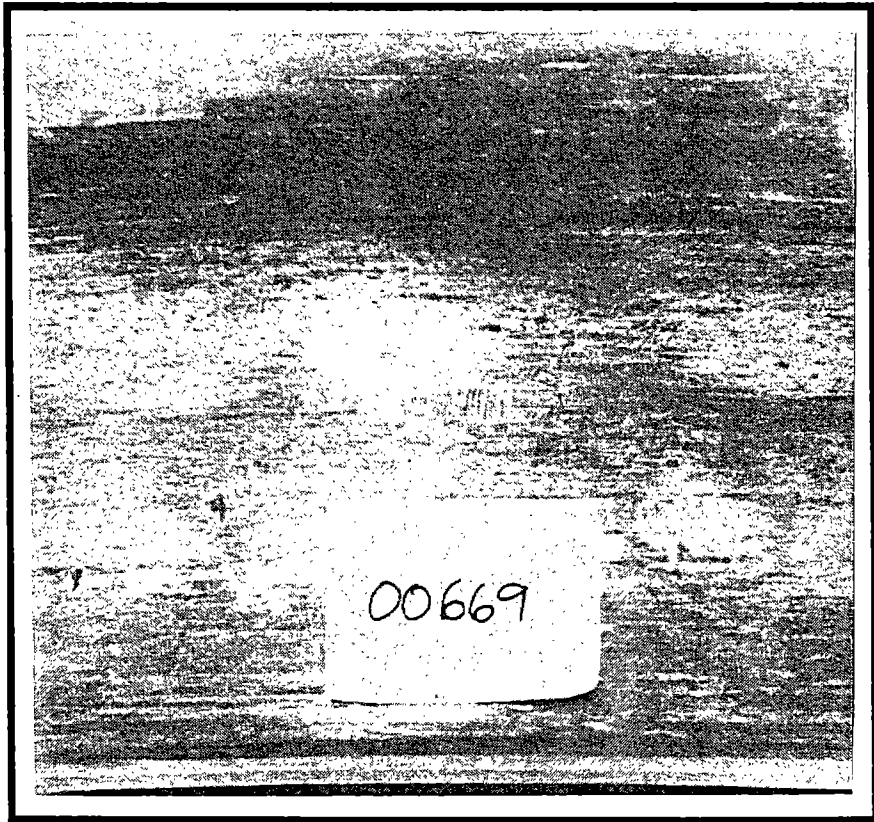
**Detector Response for Wheel No. 51265  
Stationary Test**



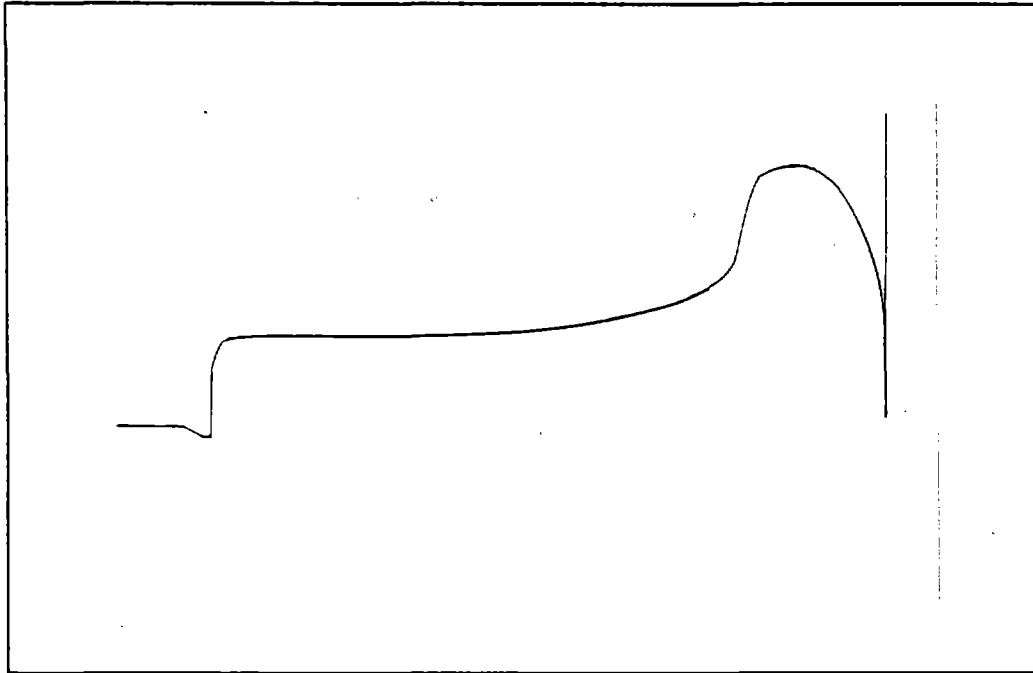
**Detector Response for Wheel No. 51265  
Roll-by Test -- 5 mph**



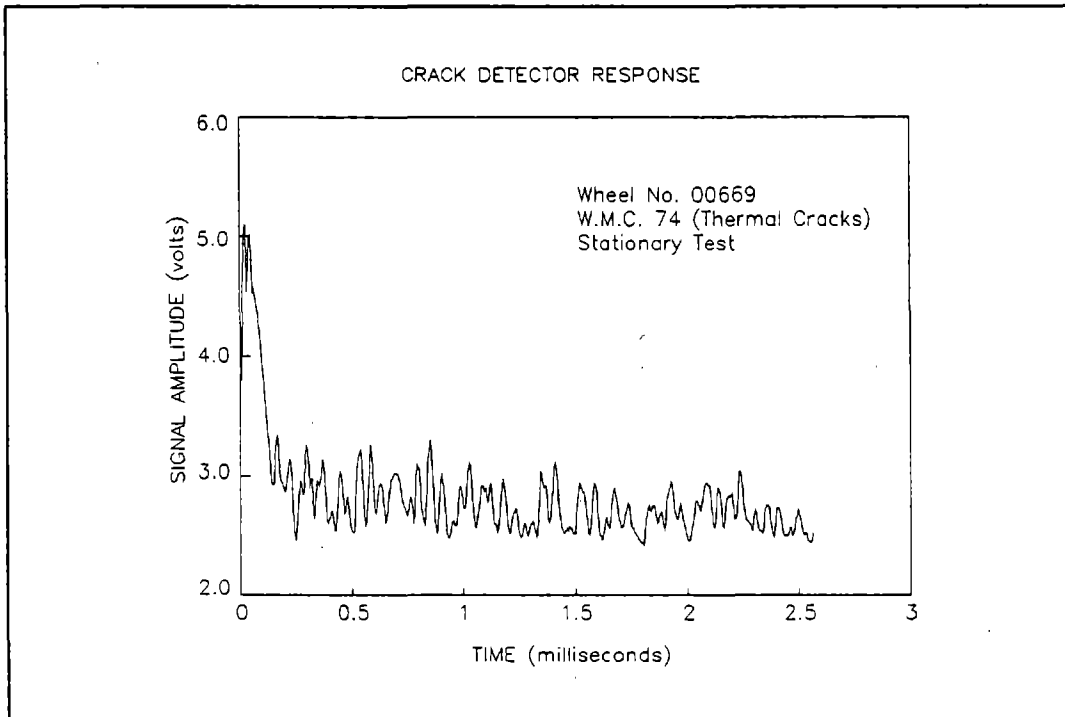
**Detector Response for Wheel No. 51265  
Roll-by Test -- 10 mph**



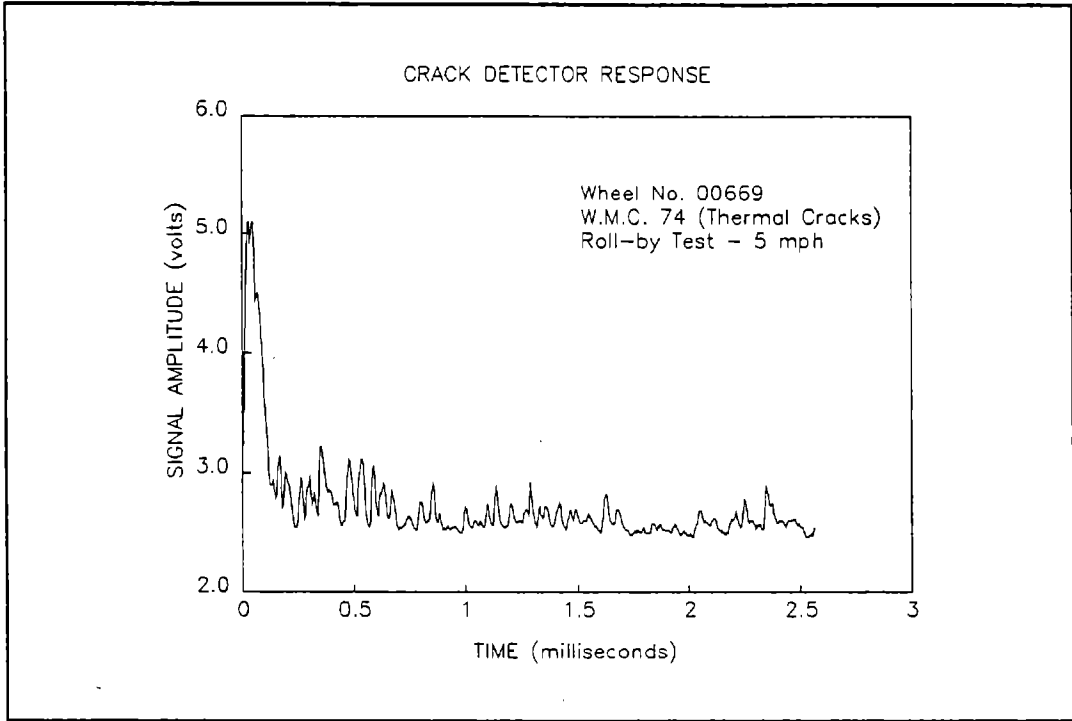
**View of Wheel No. 00669 Tread**



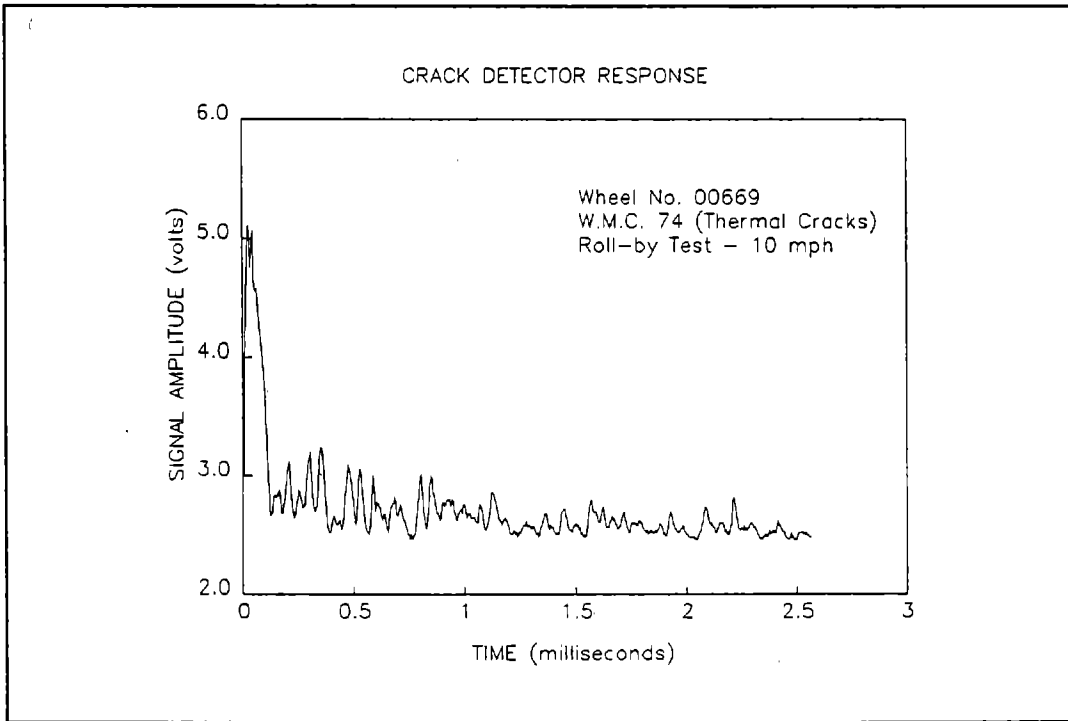
**Wheel No. 00669 Tread Profile**



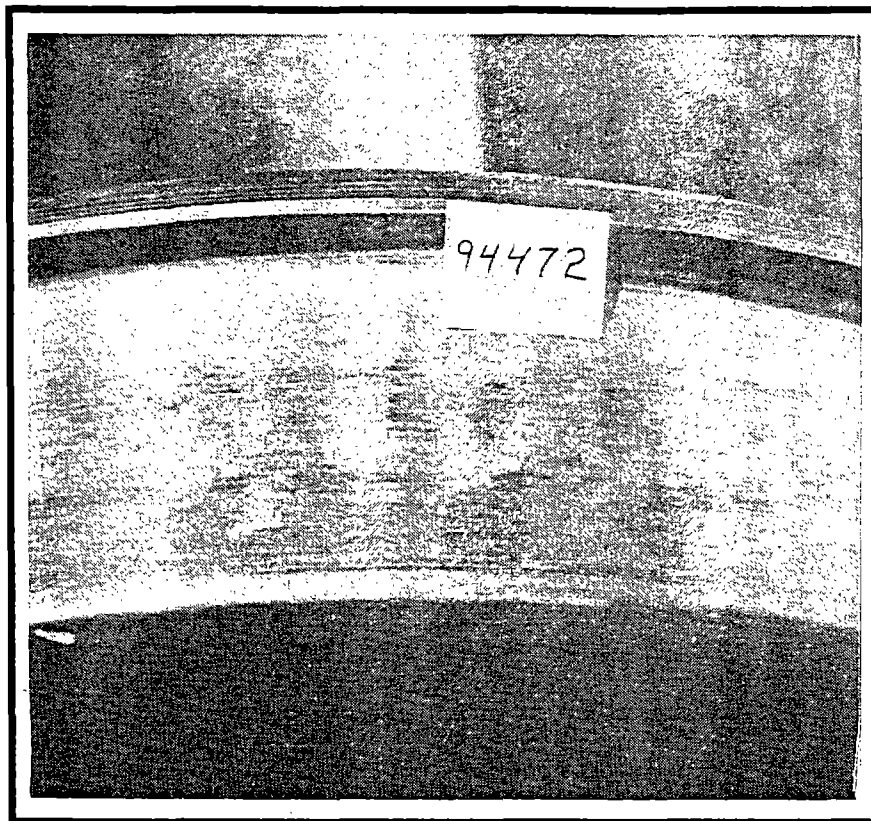
**Detector Response for Wheel No. 00669  
Stationary Test**



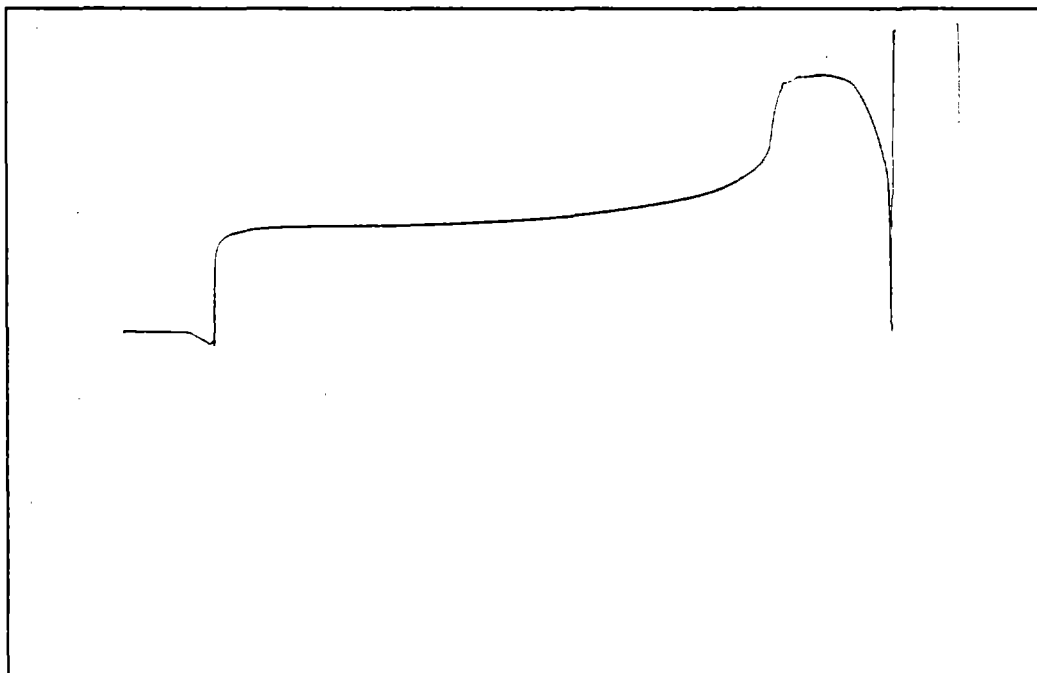
**Detector Response for Wheel No. 00669  
Roll-by Test -- 5 mph**



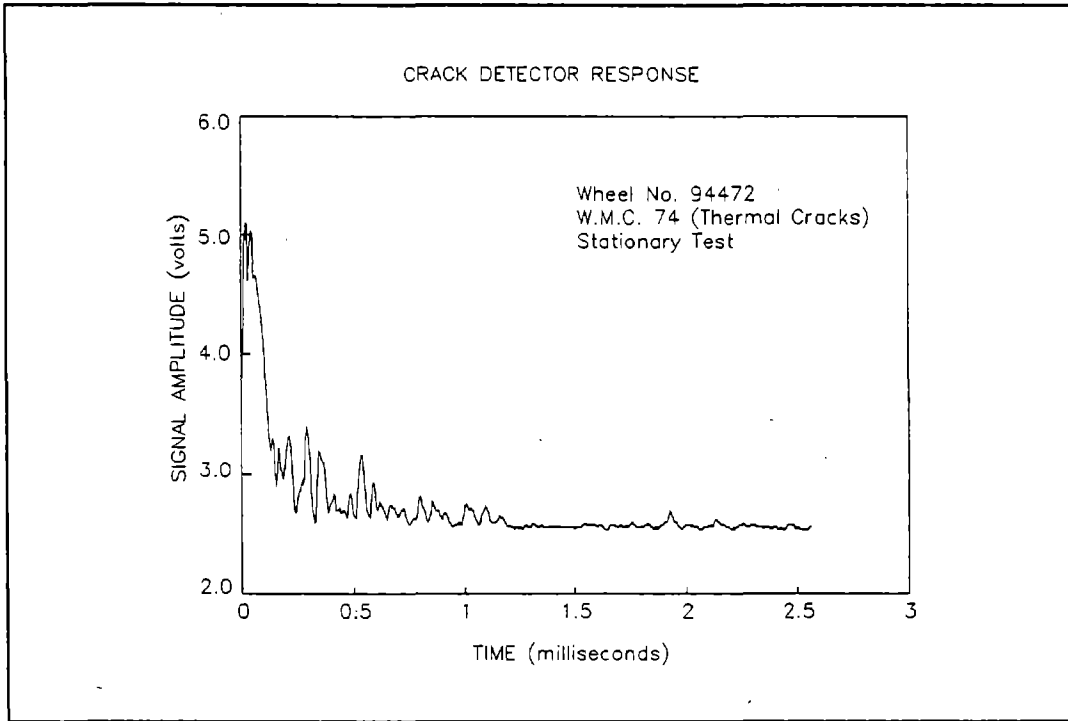
**Detector Response for Wheel No. 00669  
Roll-by Test -- 10 mph**



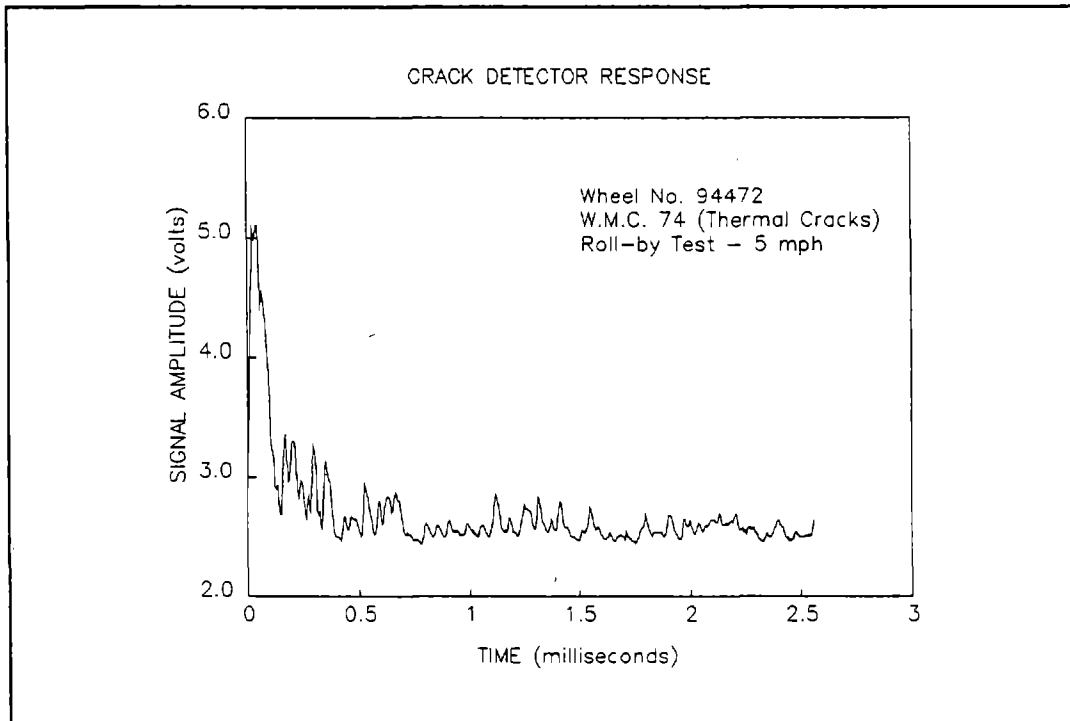
**View of Wheel No. 94472 Tread**



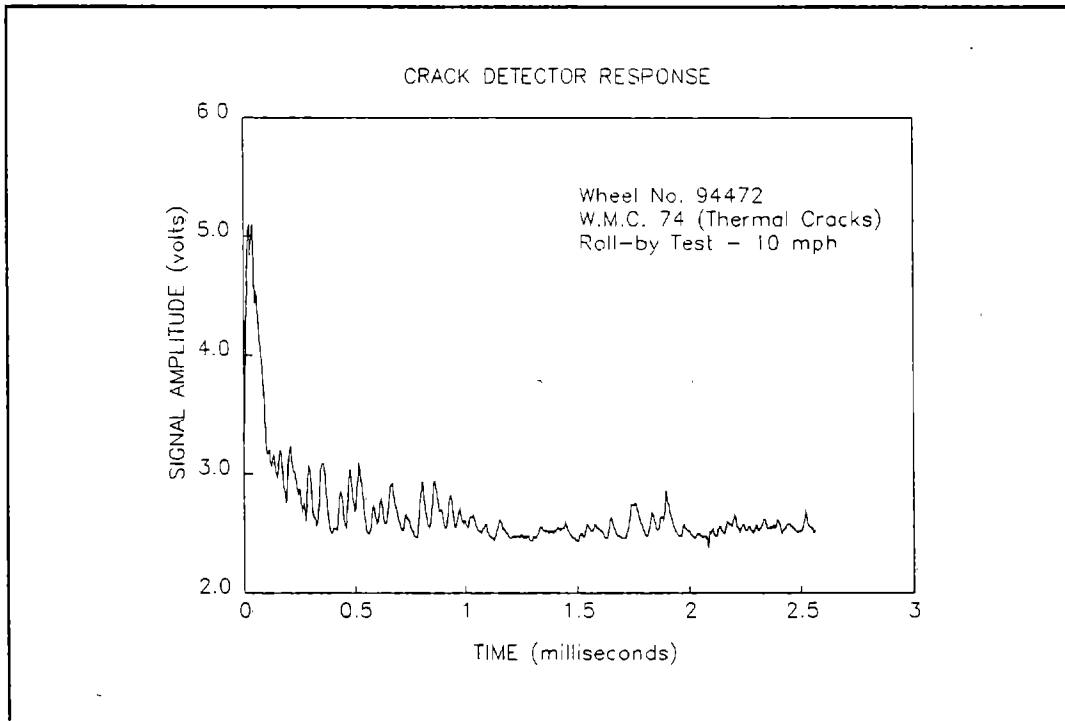
**Wheel No. 94472 Tread Profile**



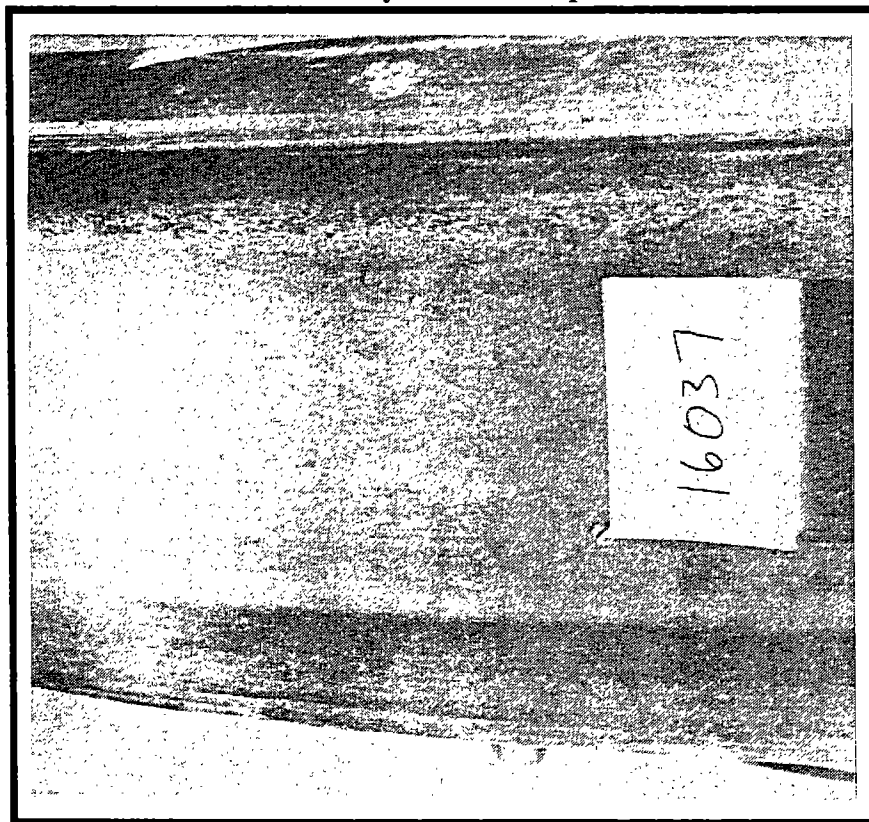
**Detector Response for Wheel No. 94472  
Stationary Test**



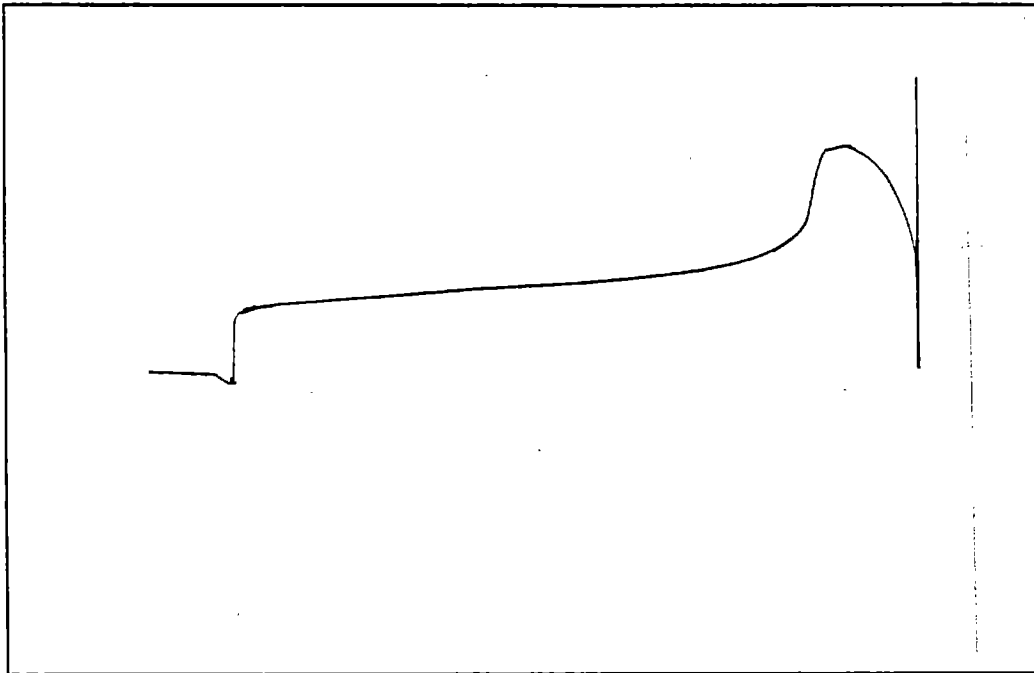
**Detector Response for Wheel No. 94472  
Roll-by Test -- 5 mph**



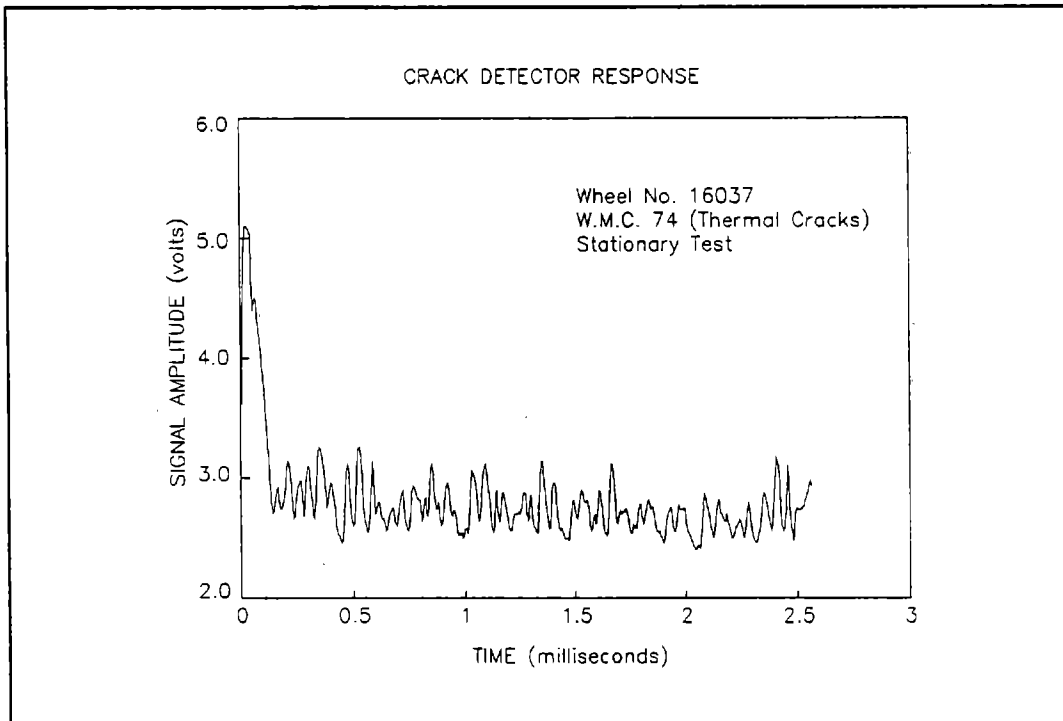
**Detector Response for Wheel No. 94472  
Roll-by Test -- 10 mph**



**View of Wheel No. 16037 Tread**

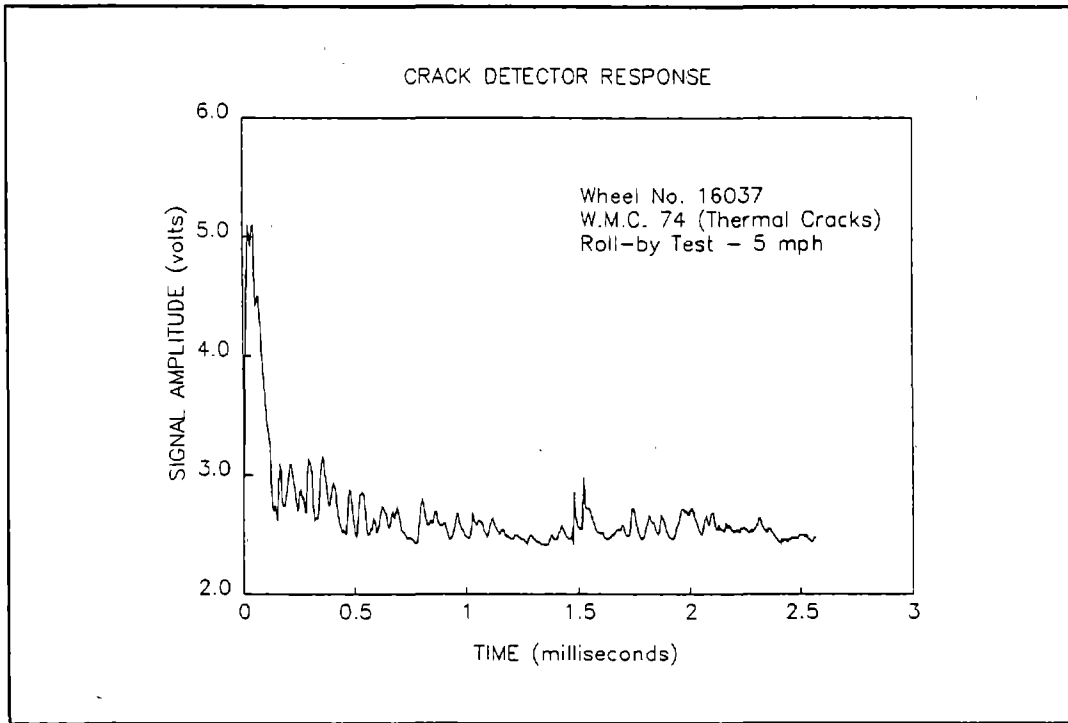


**Wheel No. 16037 Tread Profile**

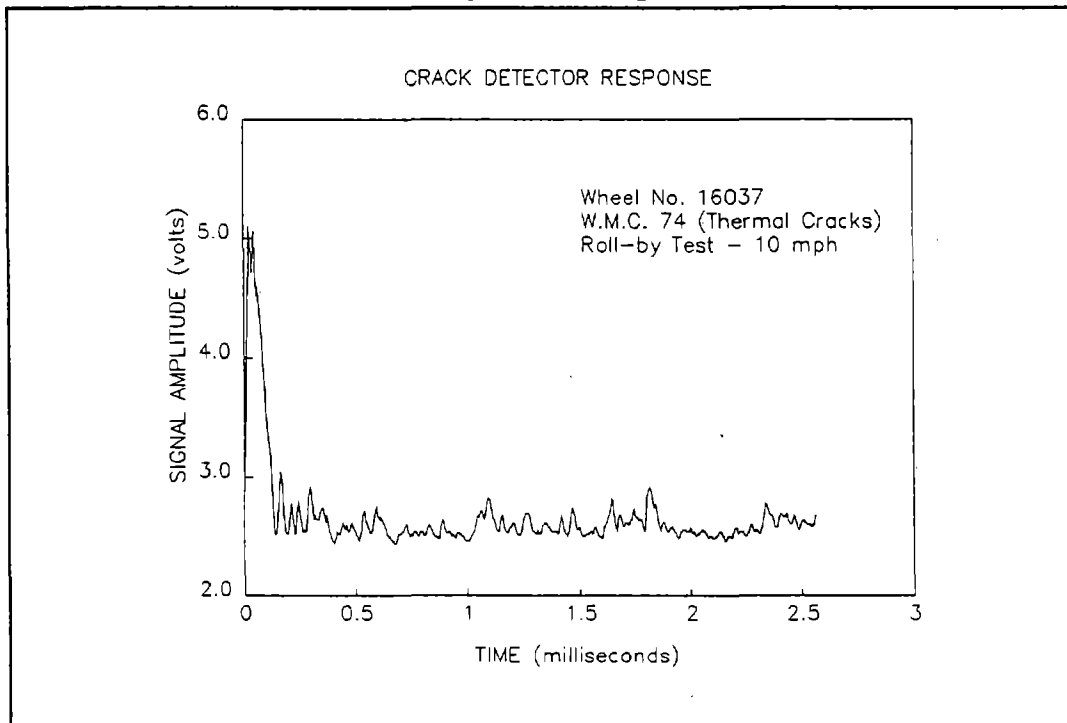


**Detector Response for Wheel No. 16037  
Stationary Test**





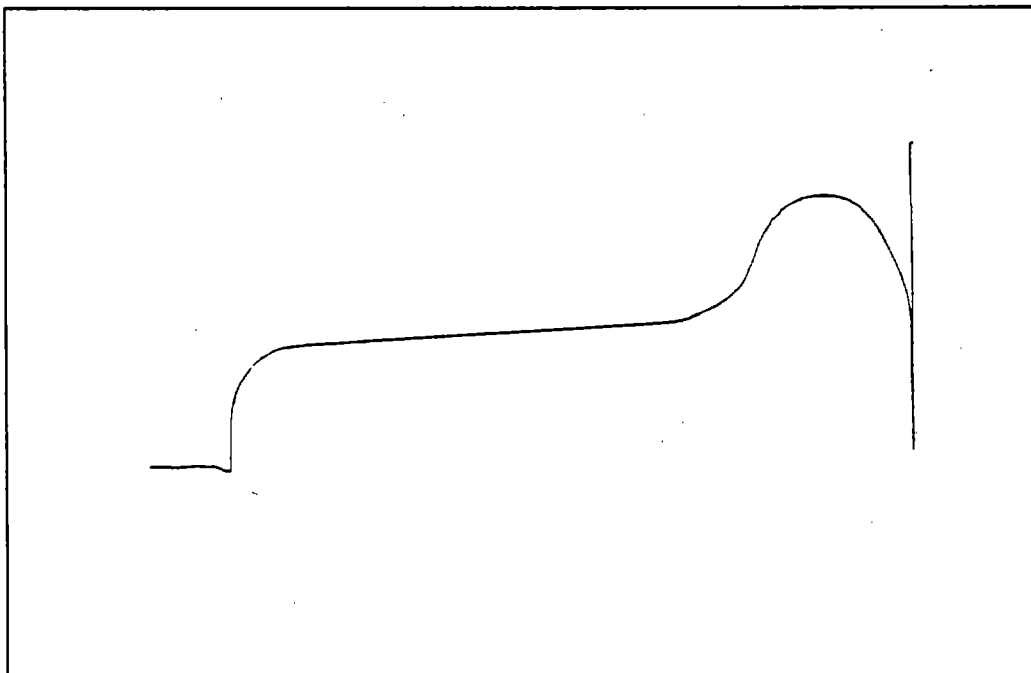
**Detector Response for Wheel No. 16037  
Roll-by Test -- 5 mph**



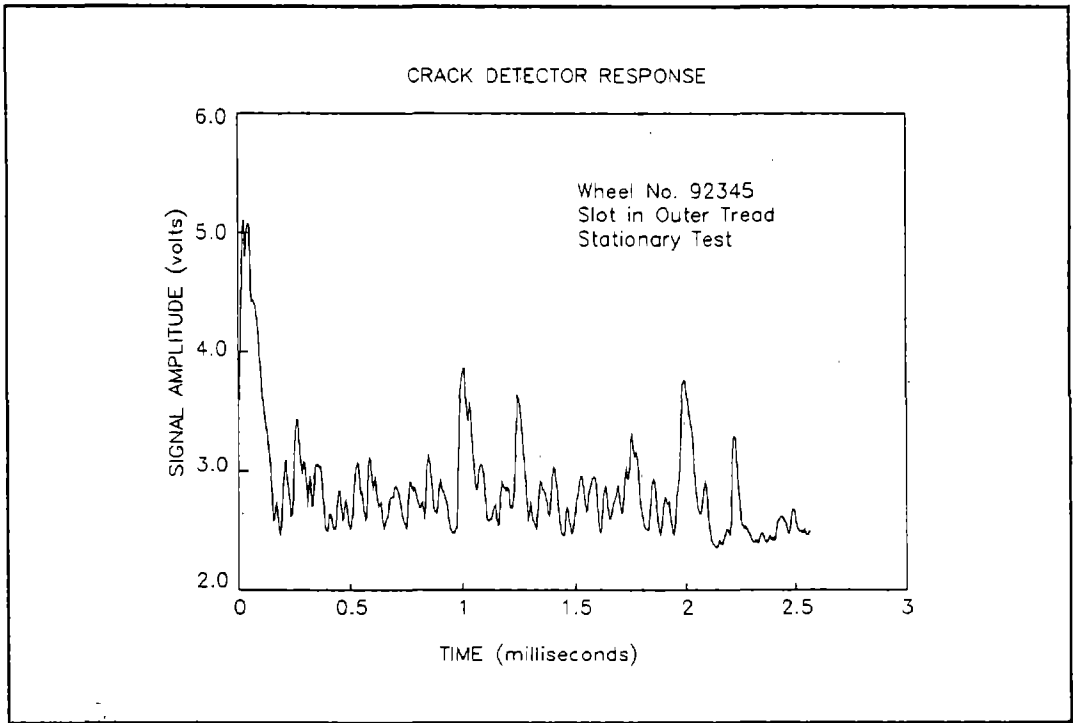
**Detector Response for Wheel No. 16037  
Roll-by Test -- 10 mph**



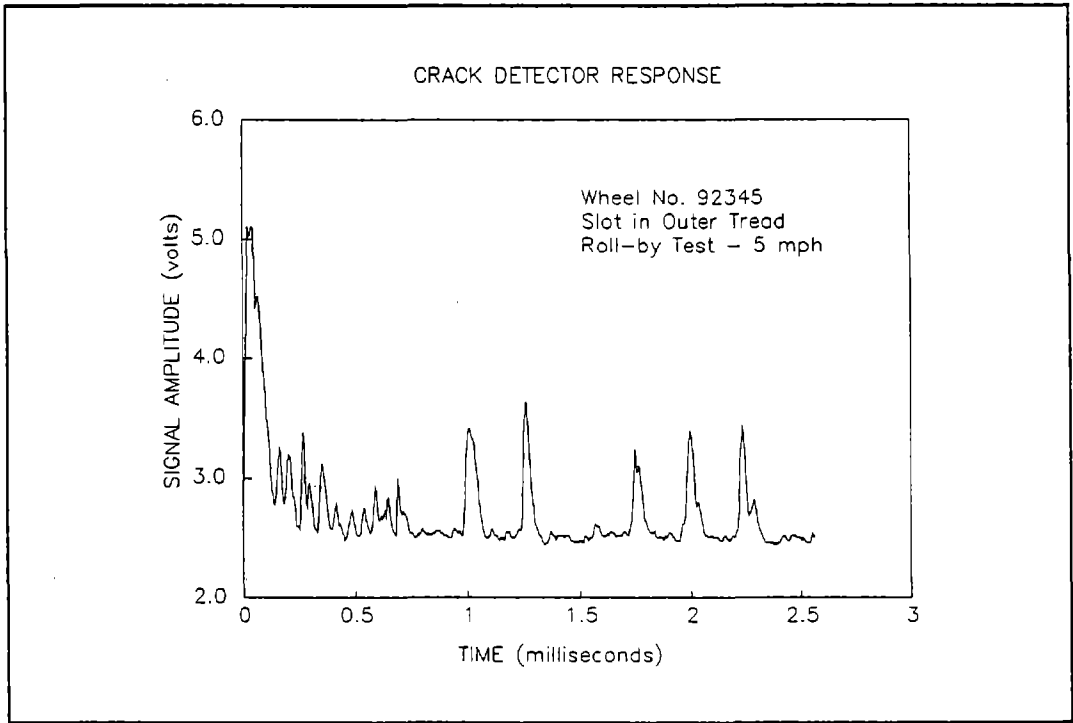
**View of Wheel No. 92345 Tread**



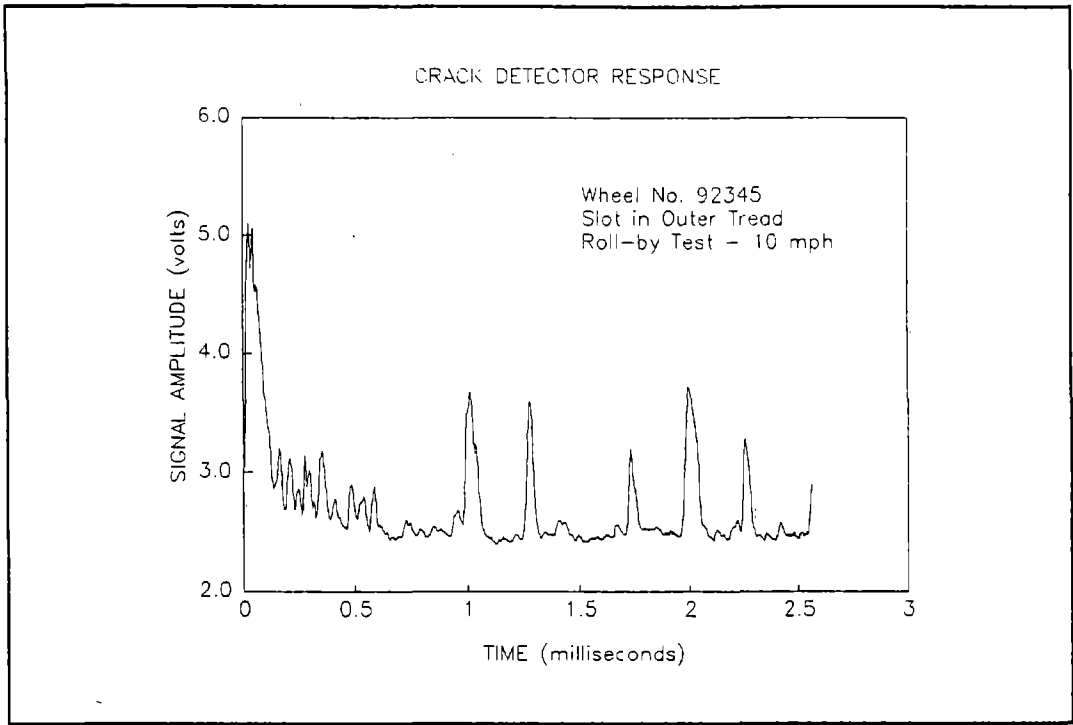
**Wheel No. 92345 Tread Profile**



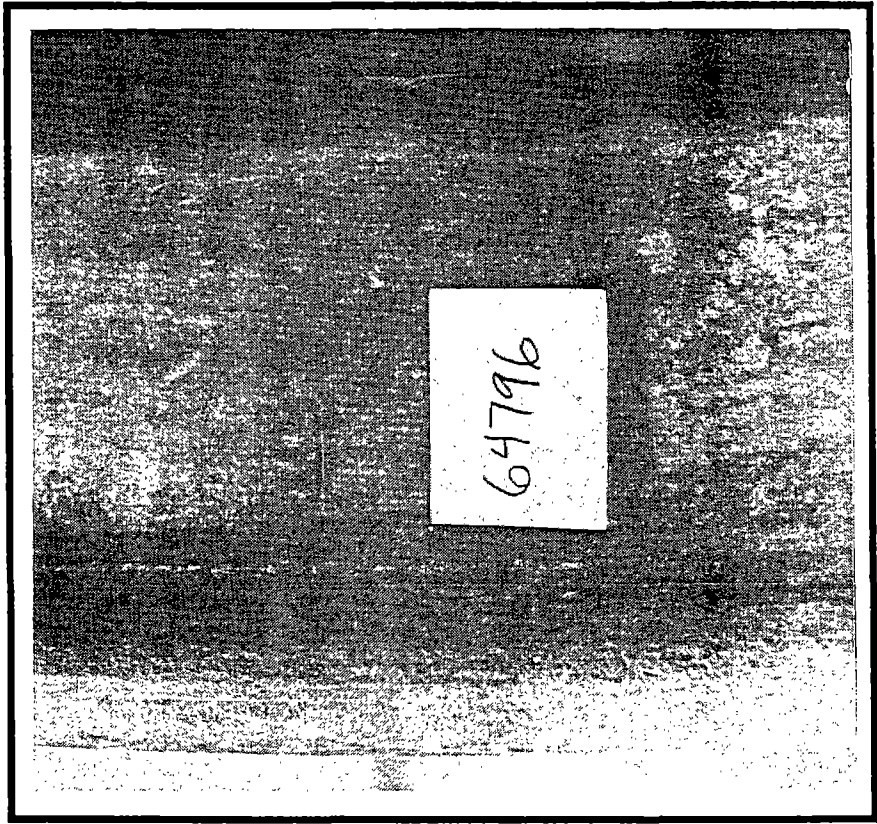
**Detector Response for Wheel No. 92345  
Stationary Test**



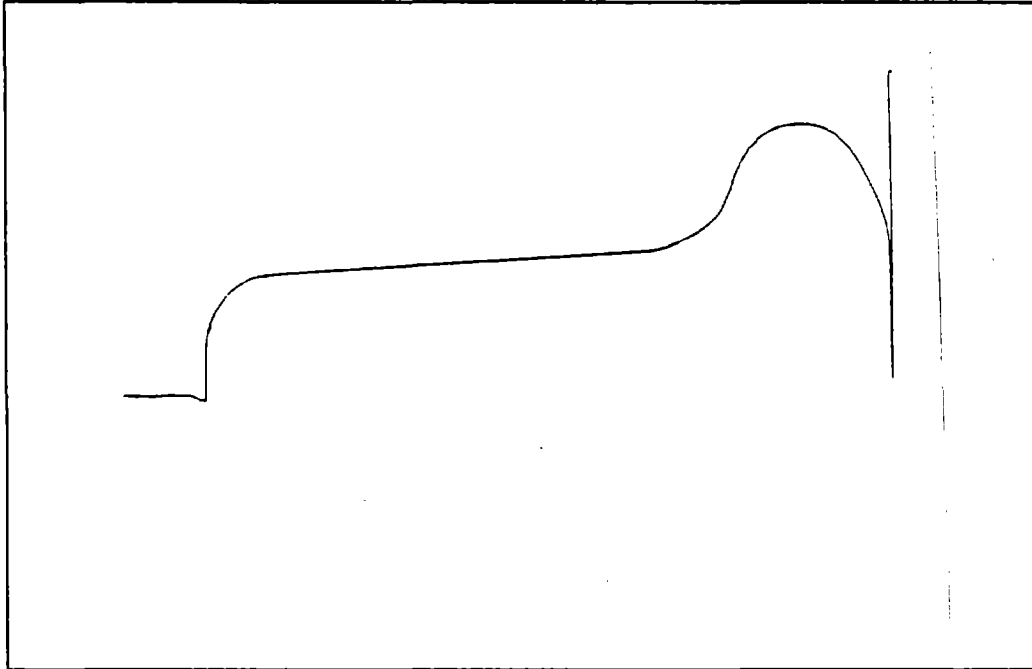
**Detector Response for Wheel No. 92345  
Roll-by Test -- 5 mph**



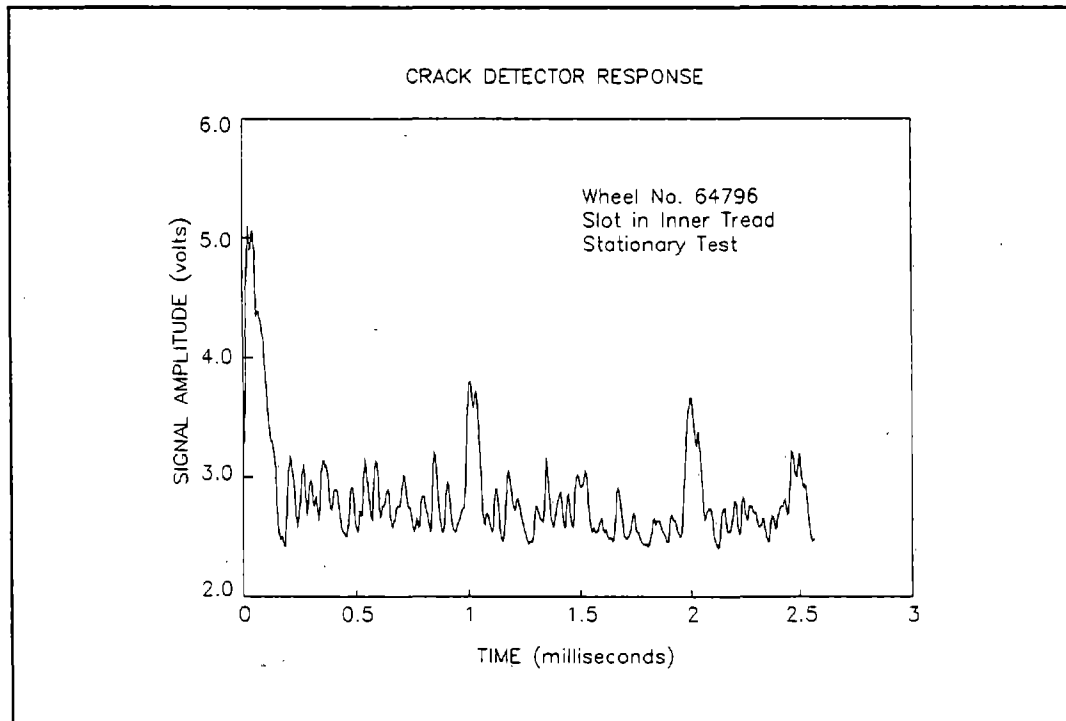
**Detector Response for Wheel No. 92345  
Roll-by Test -- 10 mph**



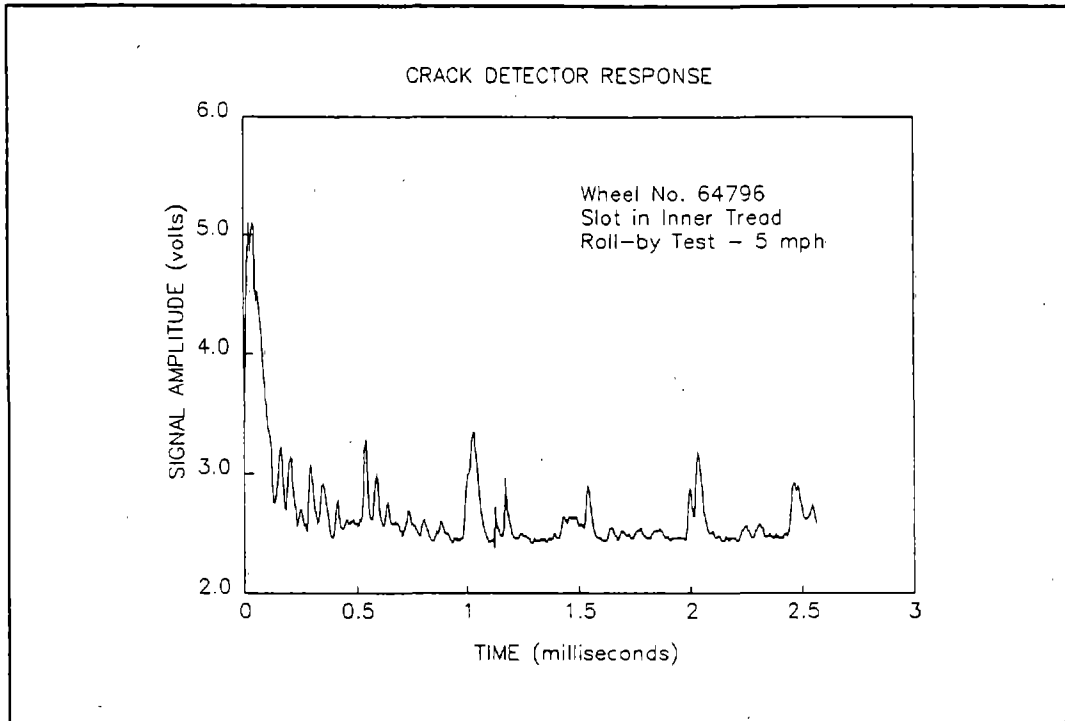
**View of Wheel No. 64796 Tread**



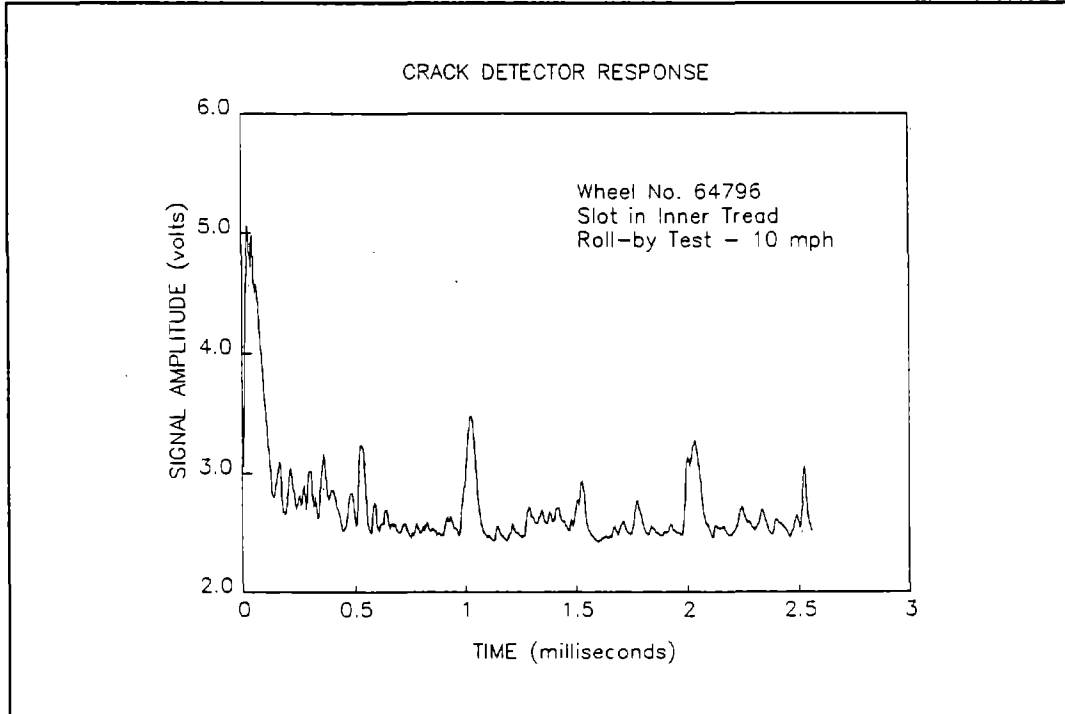
**Wheel No. 64796 Tread Profile**



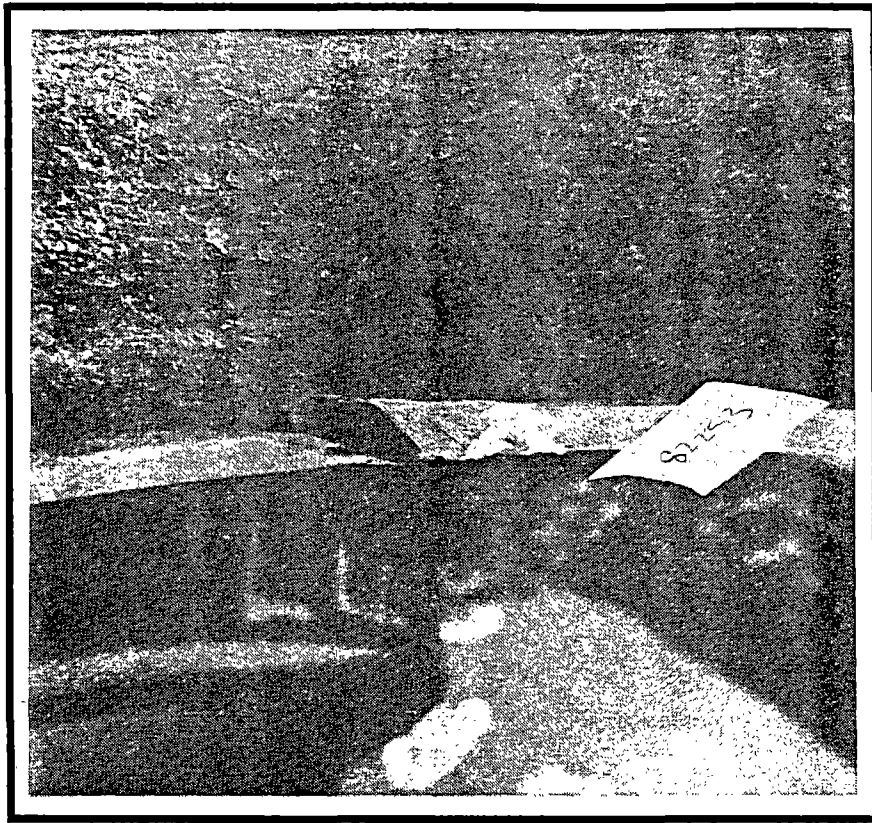
**Detector Response for Wheel No. 64796  
Stationary Test**



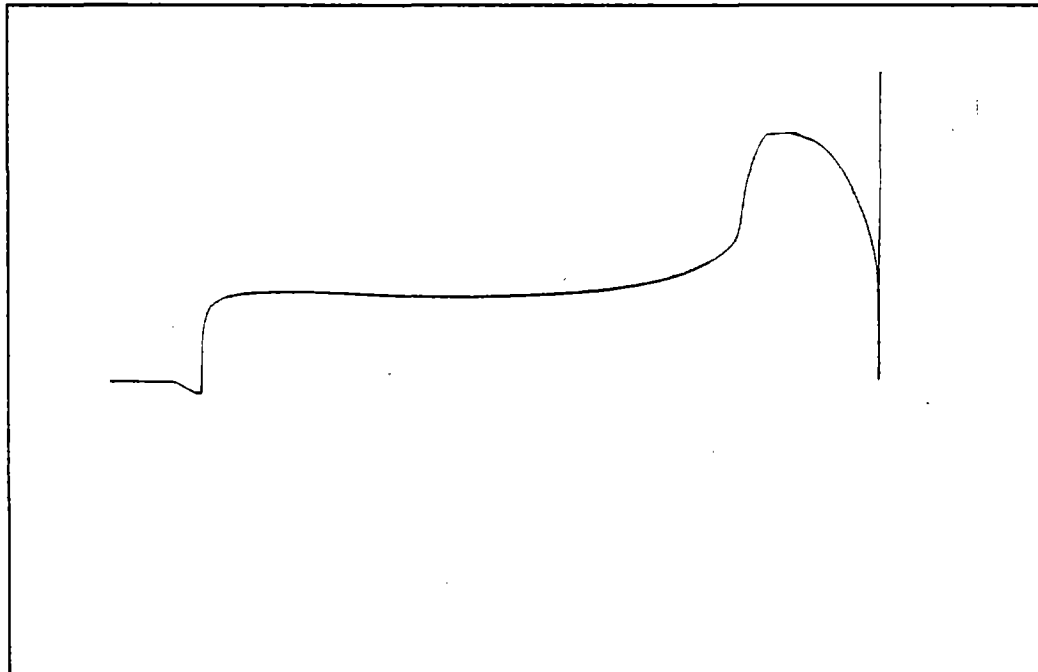
**Detector Response for Wheel No. 64796  
Roll-by Test -- 5 mph**



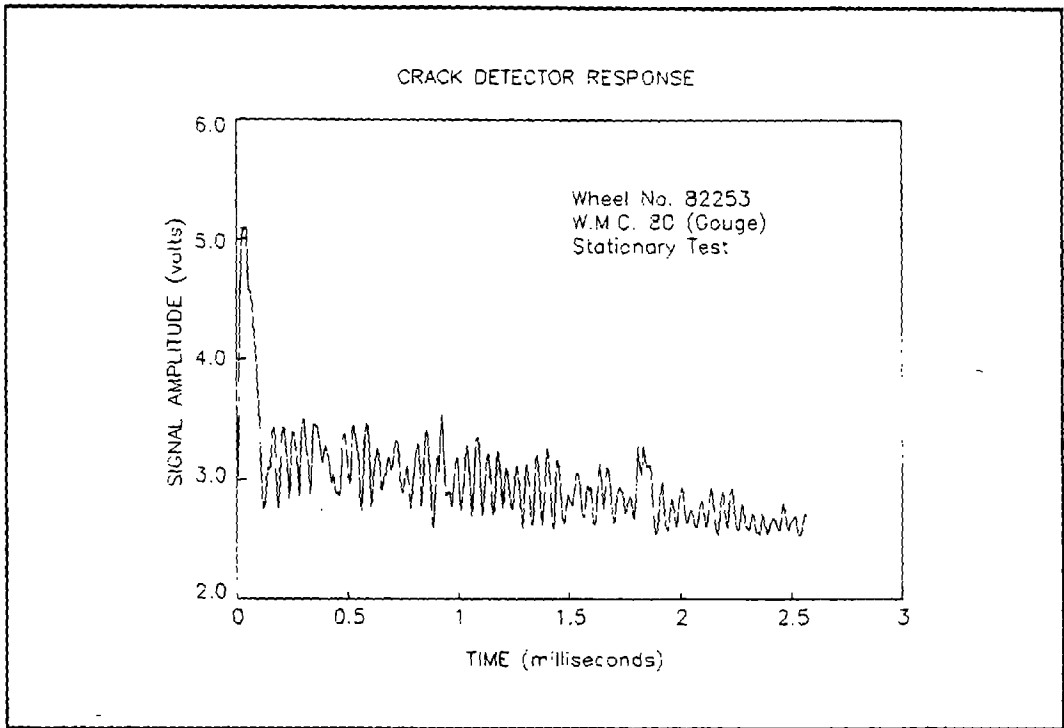
**Detector Response for Wheel No. 64796  
Roll-by Test -- 10 mph**



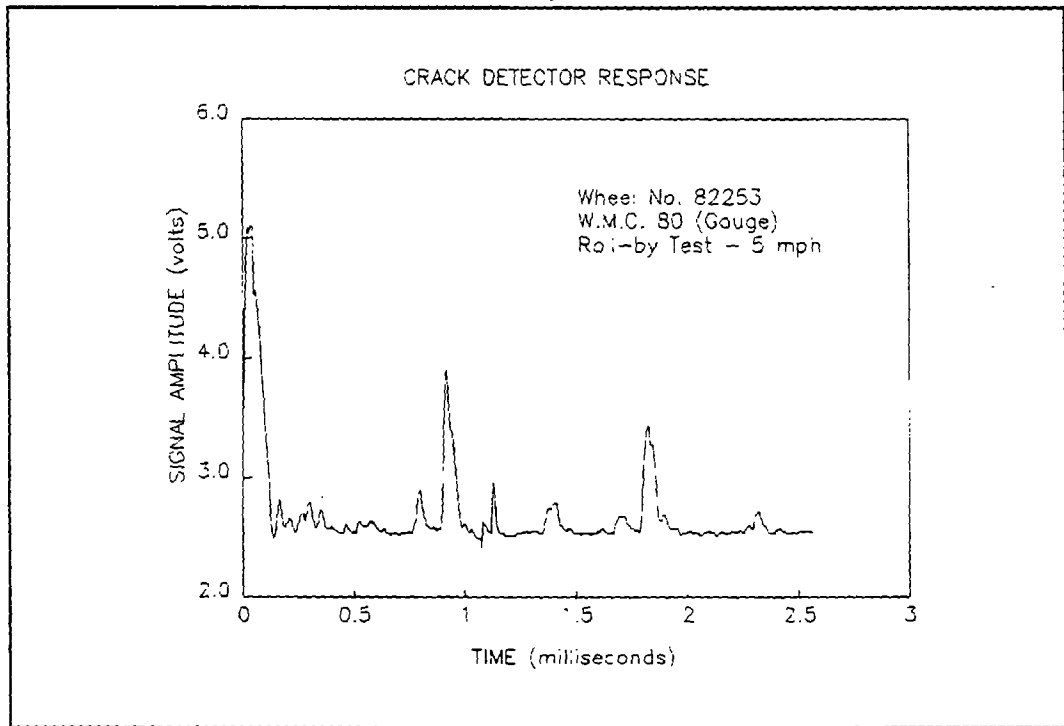
**View of Wheel No. 82253 Tread**



**Wheel No. 82253 Tread Profile**

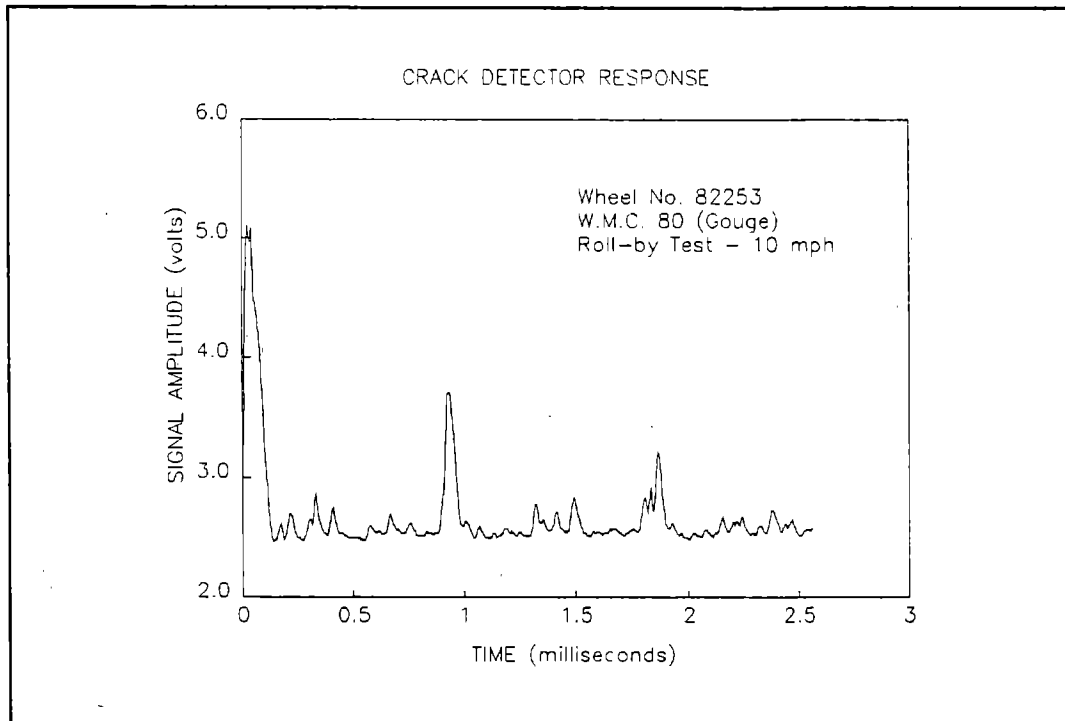


**Detector Response for Wheel No. 82253  
Stationary Test**



**Detector Response for Wheel No. 82253  
Roll-by Test -- 5 mph**

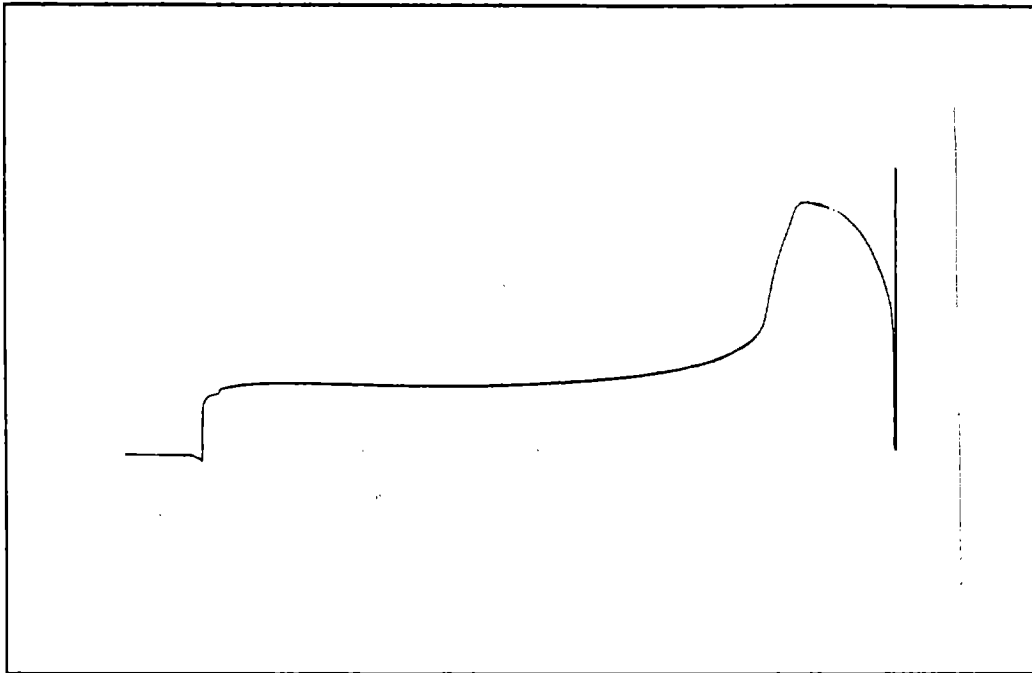




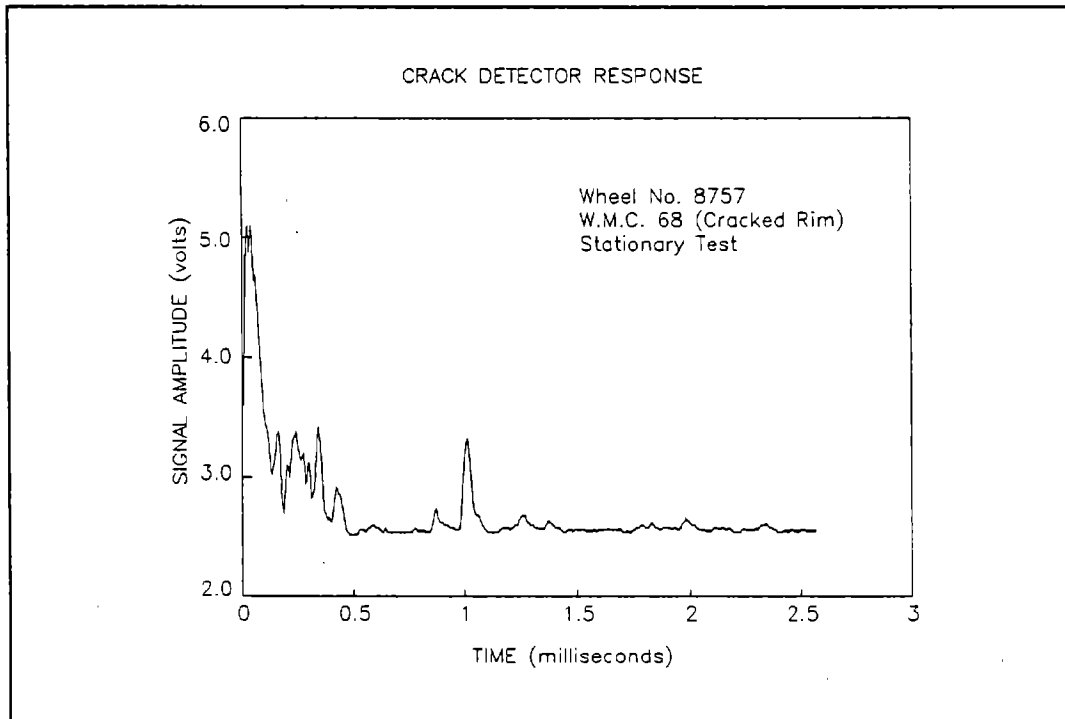
**Detector Response for Wheel No. 82253  
Roll-by Test -- 10 mph**



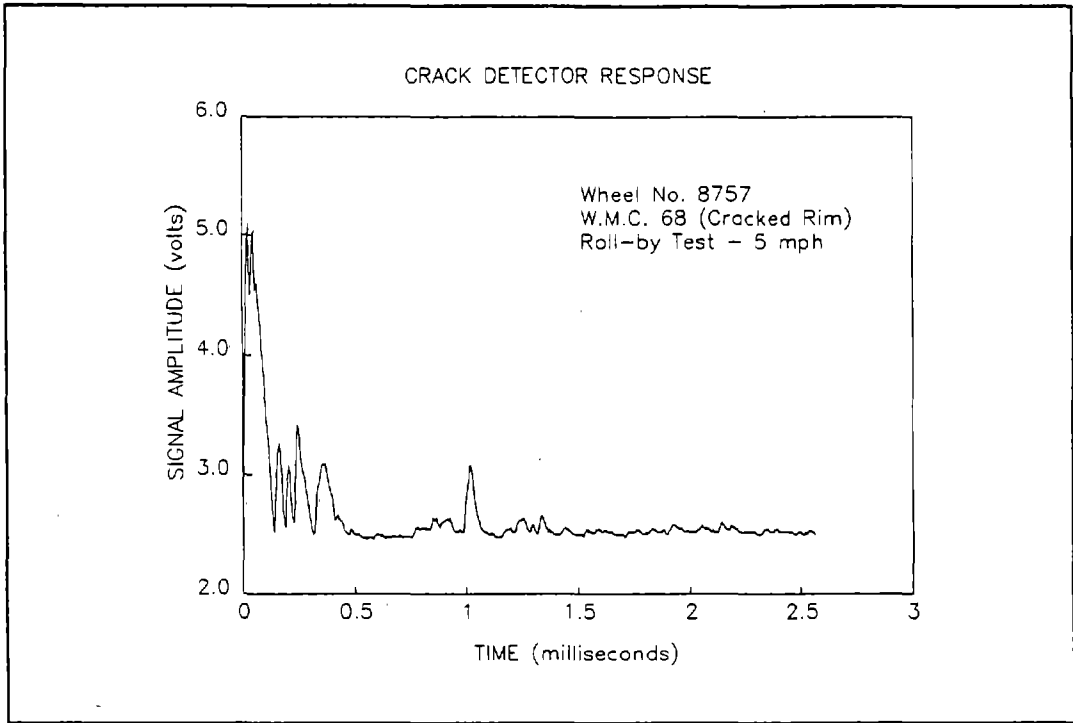
**View of Wheel No. 8757 Tread**



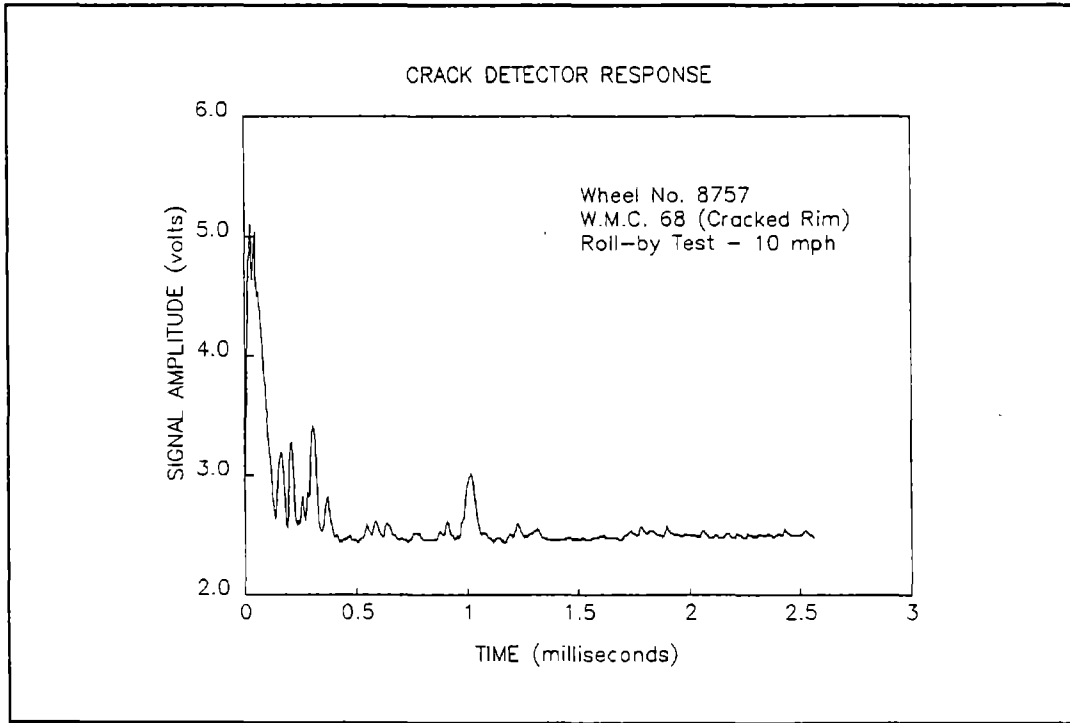
**Wheel No. 8757 Tread Profile**



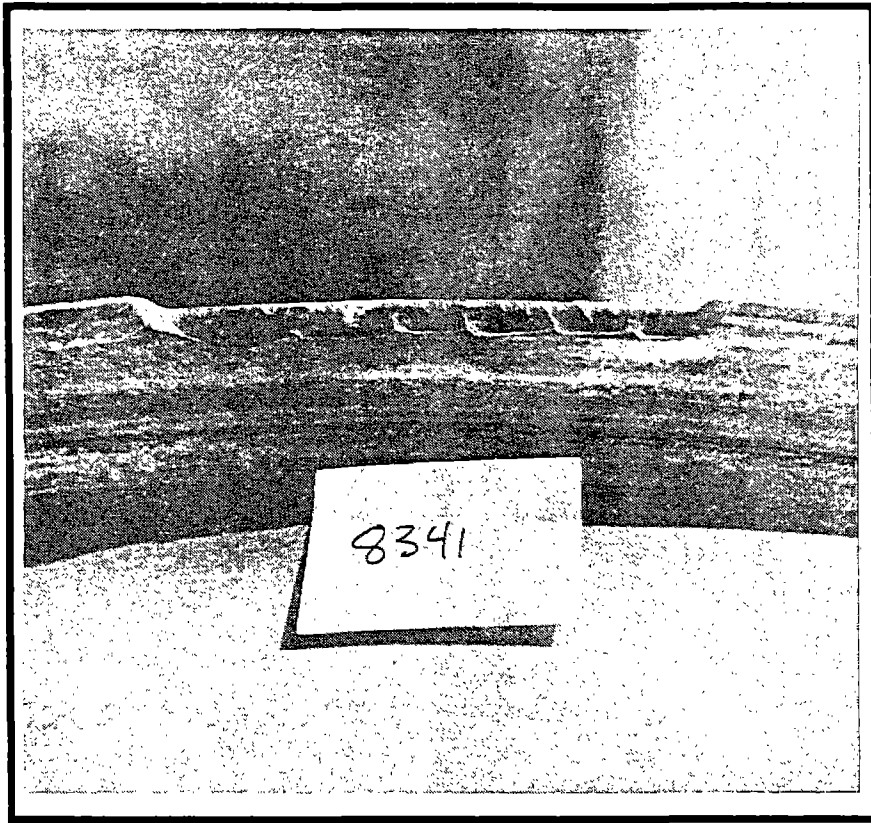
**Detector Response for Wheel No. 8757  
Stationary Test**



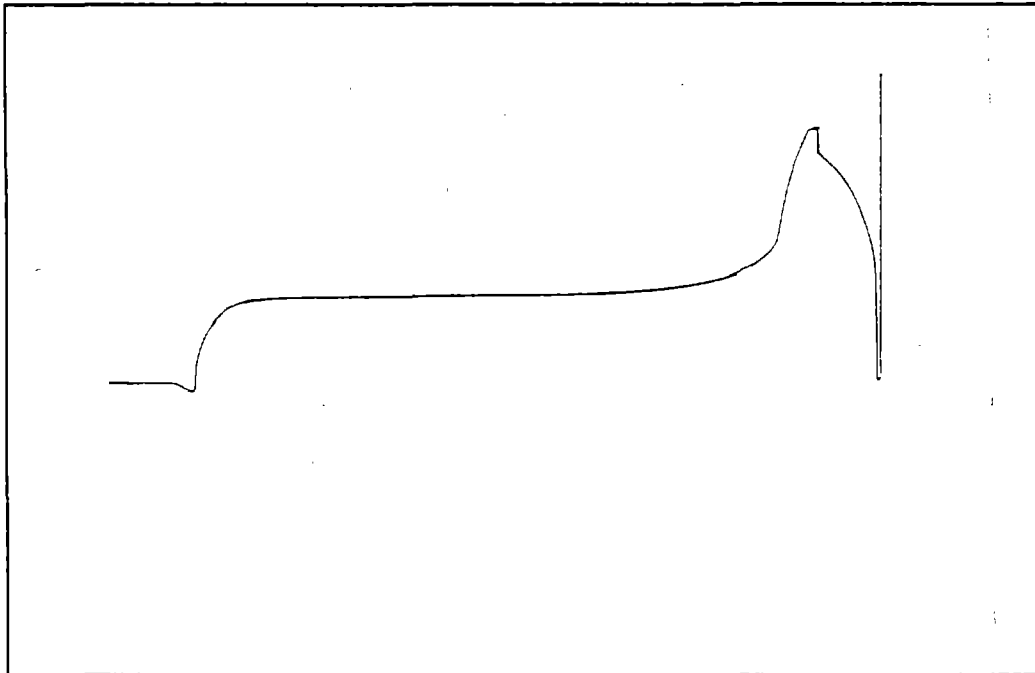
**Detector Response for Wheel No. 8757  
Roll-by Test - 5 mph**



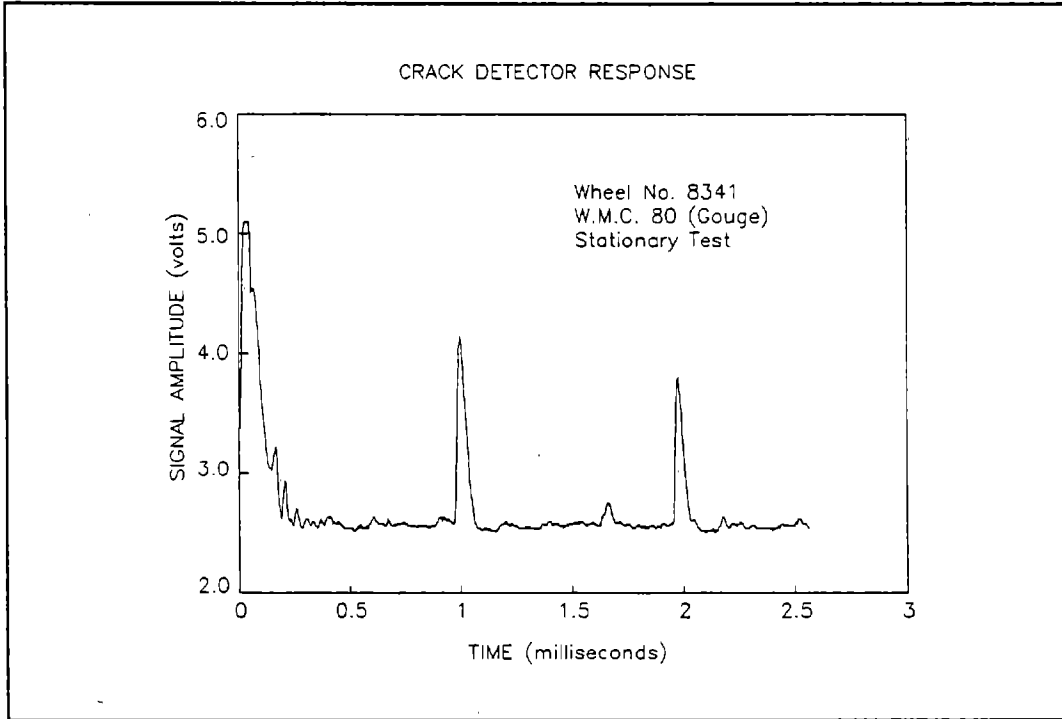
**Detector Response for Wheel No. 8757  
Roll-by Test -- 10 mph**



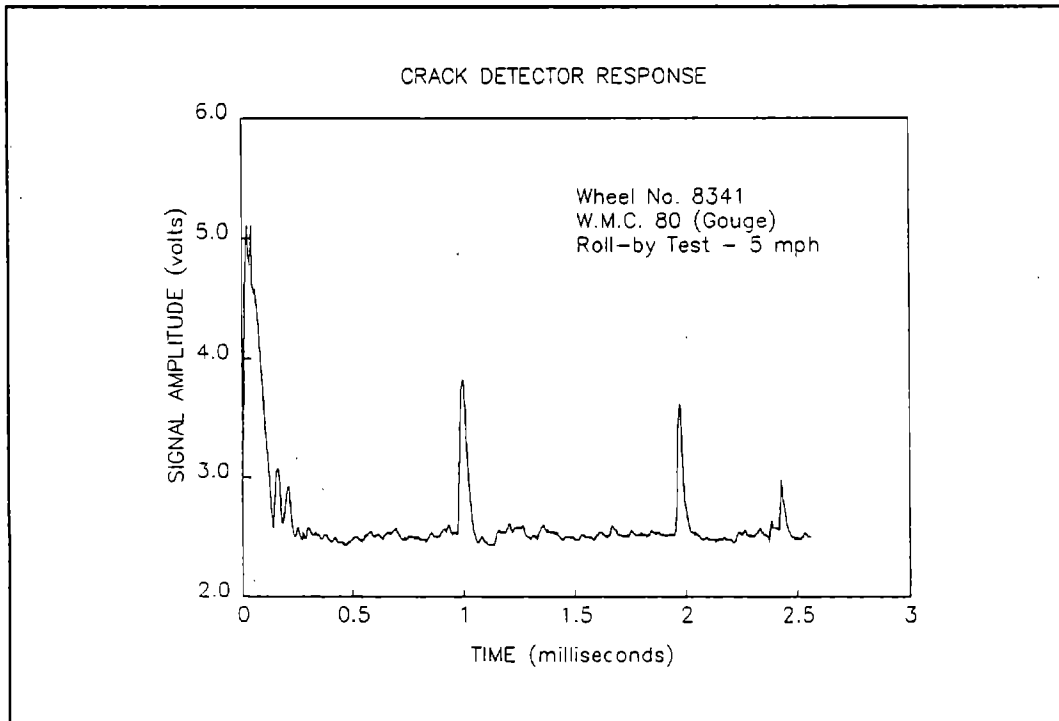
**View of Wheel No. 8341 Tread**



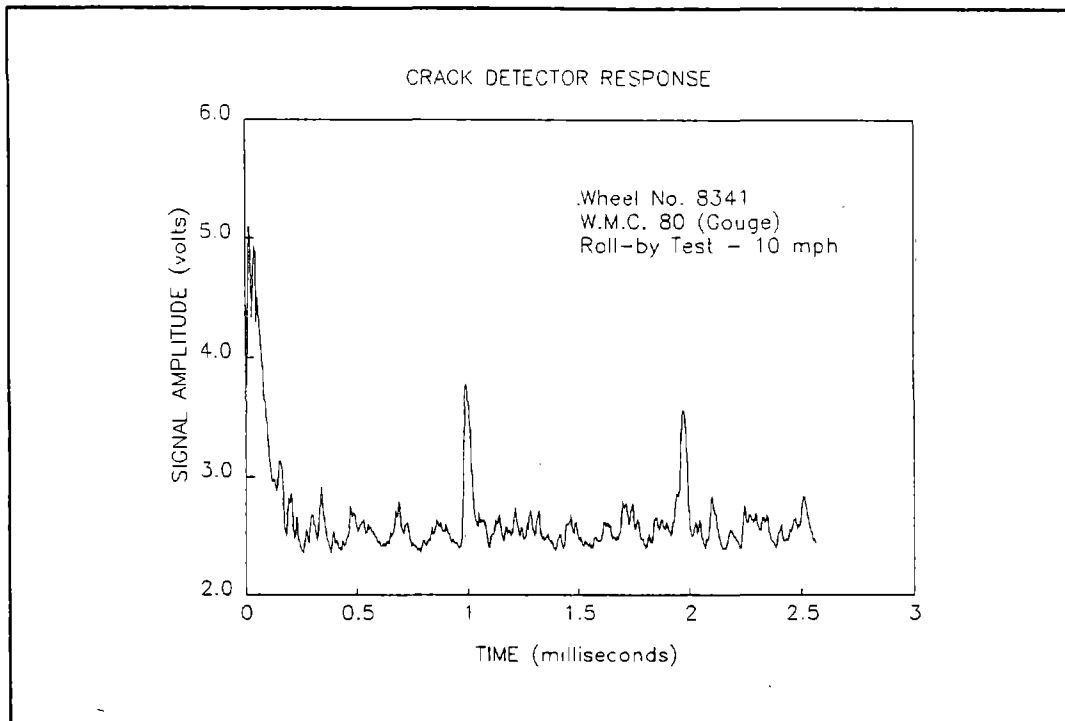
**Wheel No. 8341 Tread Profile**



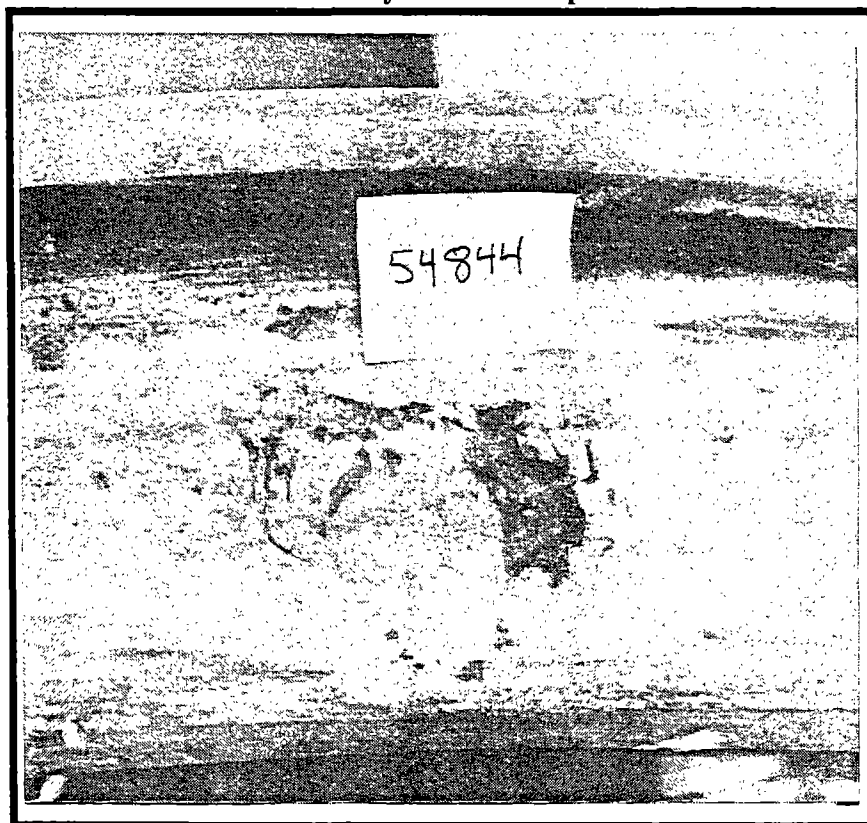
**Detector Response for Wheel No. 8341  
Stationary Test**



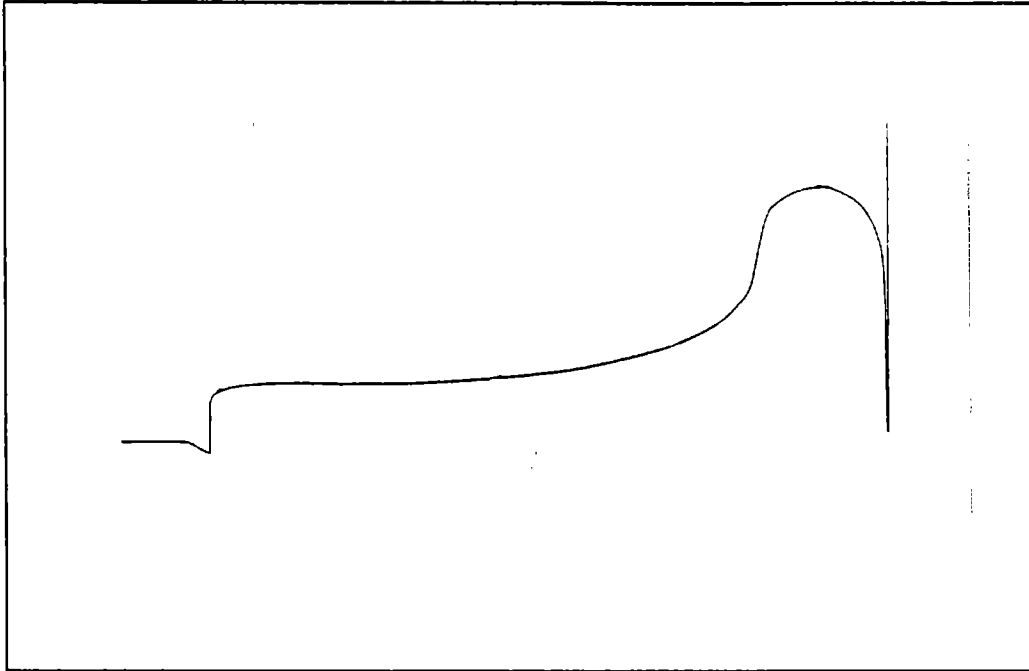
**Detector Response for Wheel No. 8341  
Roll-by Test - 5 mph**



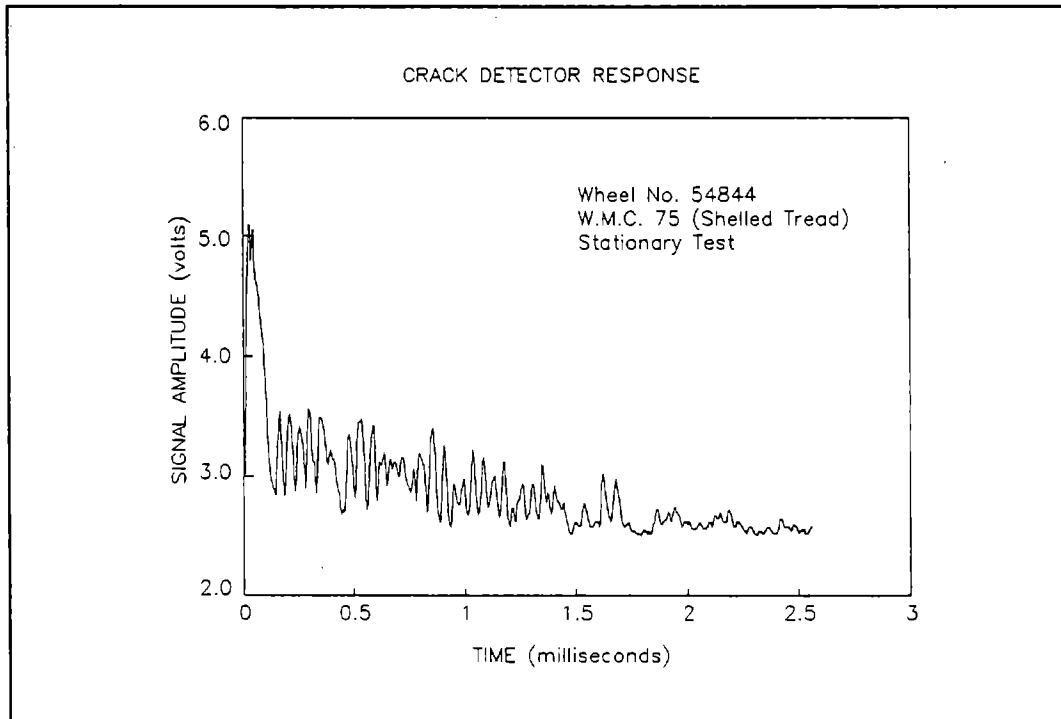
**Detector Response for Wheel No. 8341  
Roll-by Test -- 10 mph**



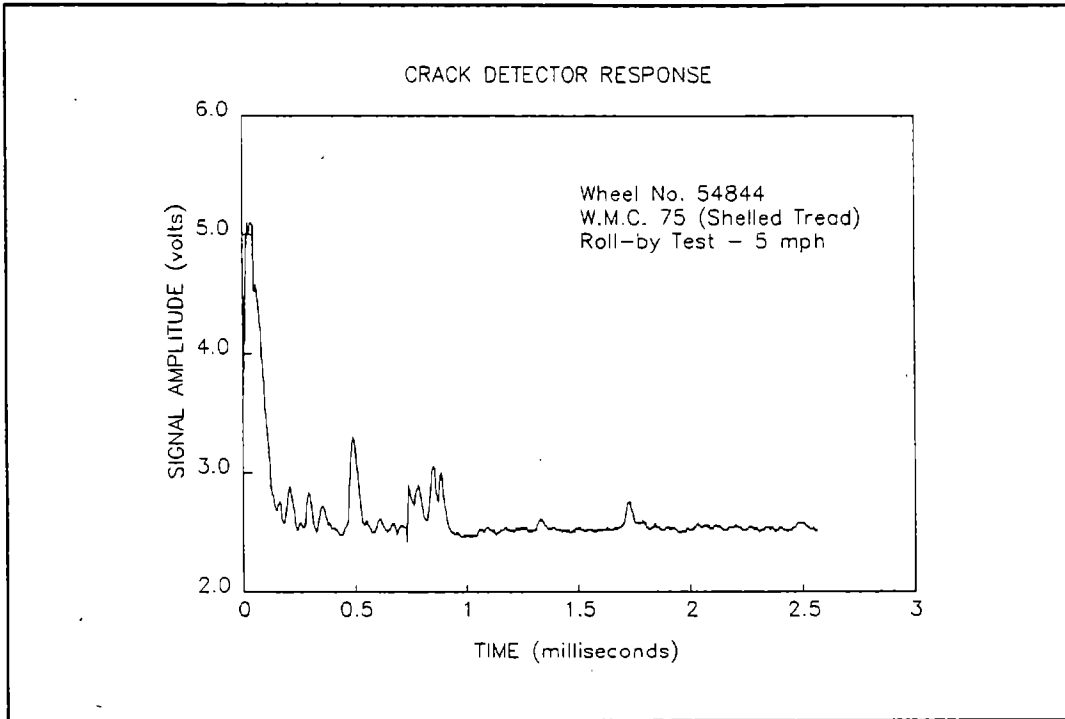
**View of Wheel No. 54844 Tread**



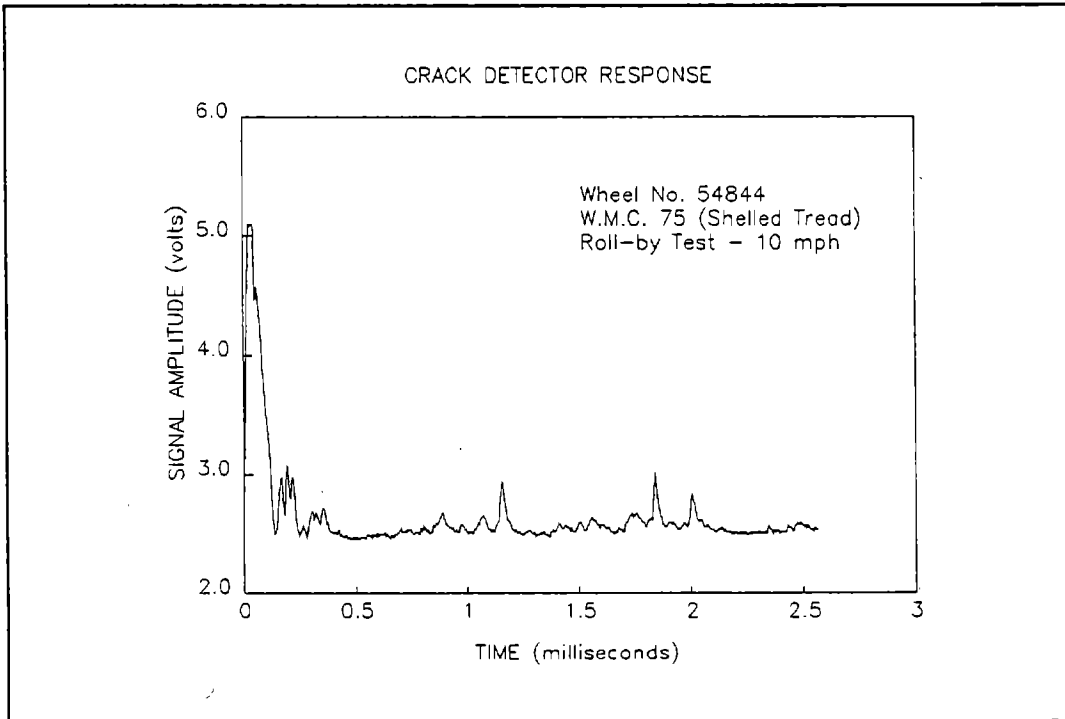
**Wheel No. 54844 Tread Profile**



**Detector Response for Wheel No. 54844  
Stationary Test**



**Detector Response for Wheel No. 54844  
Roll-by Test -- 5 mph**

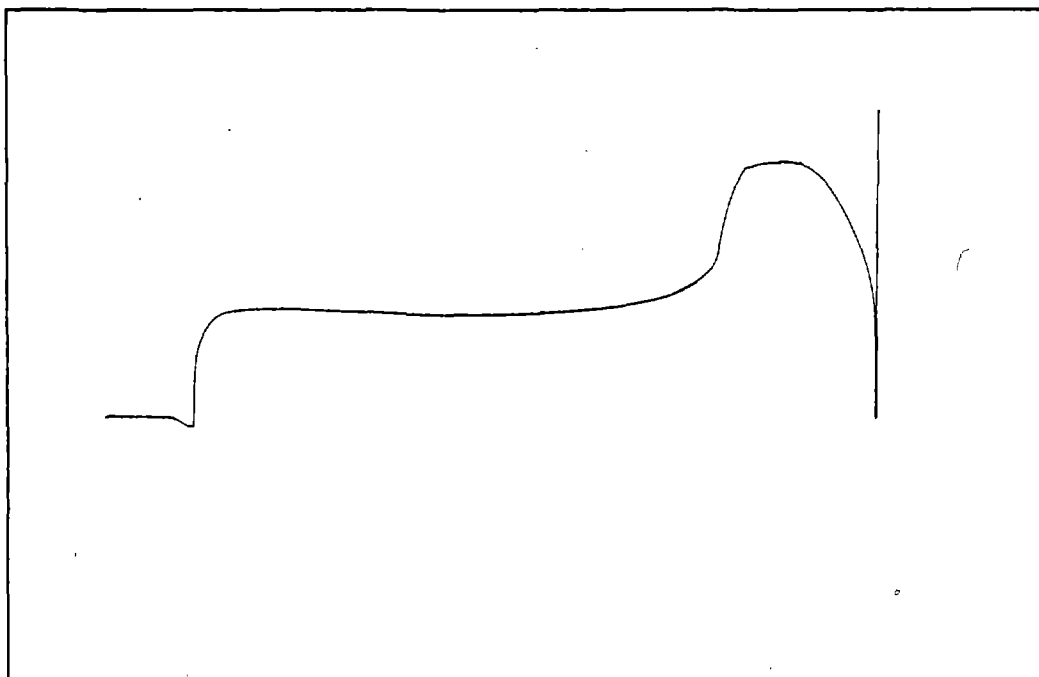


**Detector Response for Wheel No. 54844  
Roll-by Test -- 10 mph**

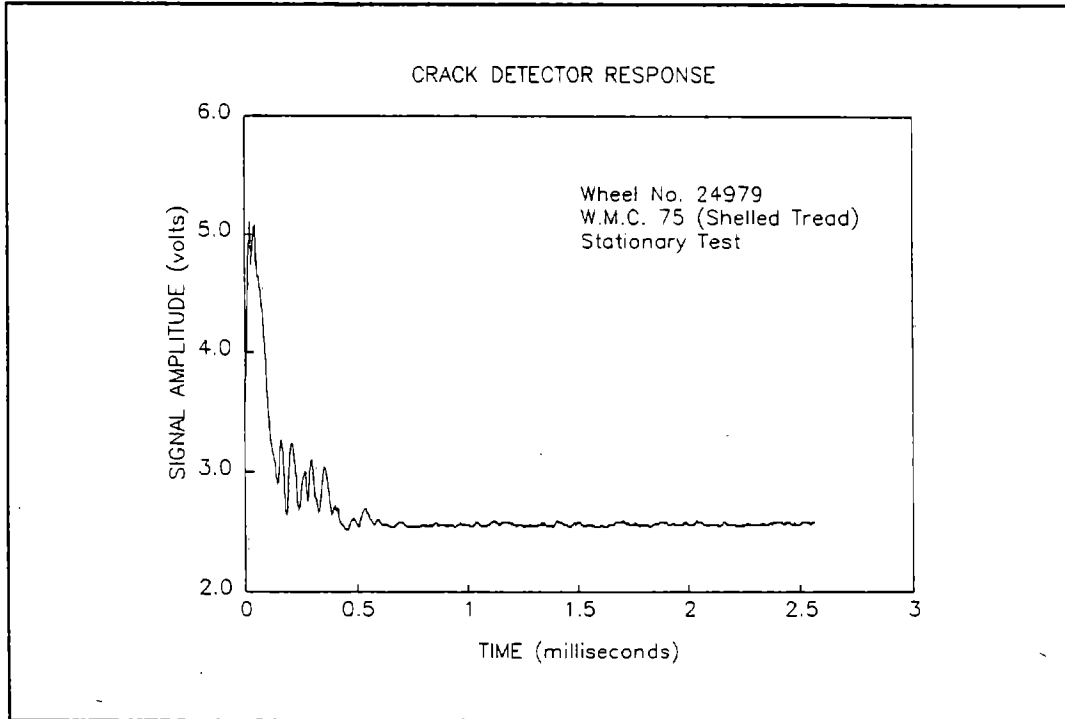




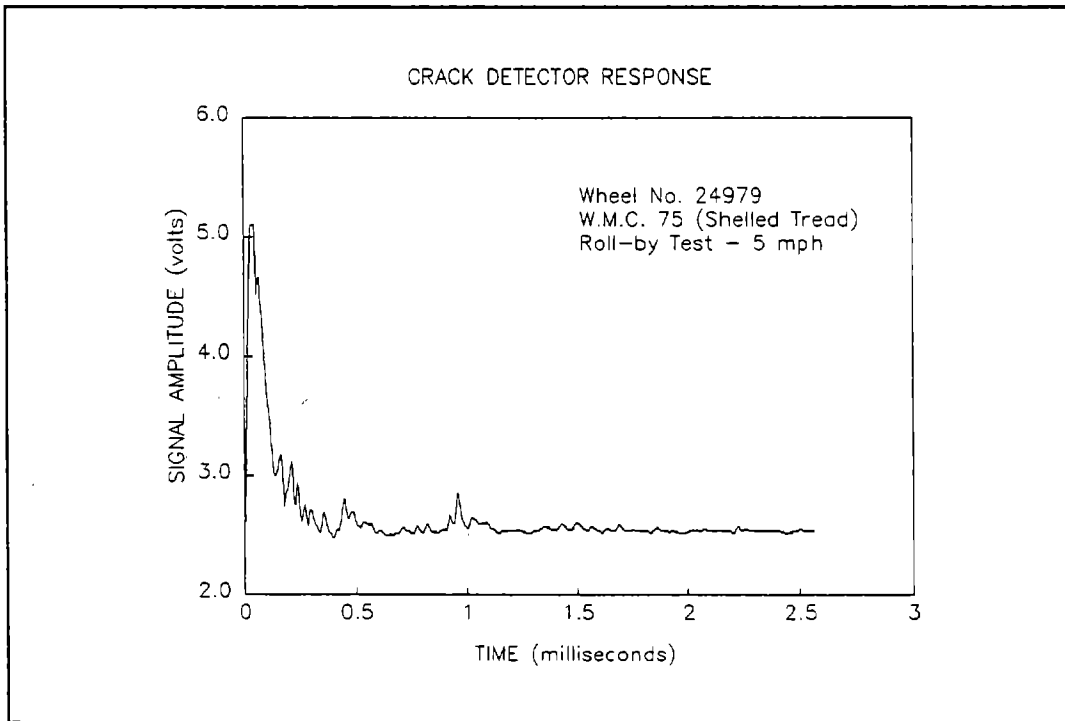
**View of Wheel No. 24979 Tread**



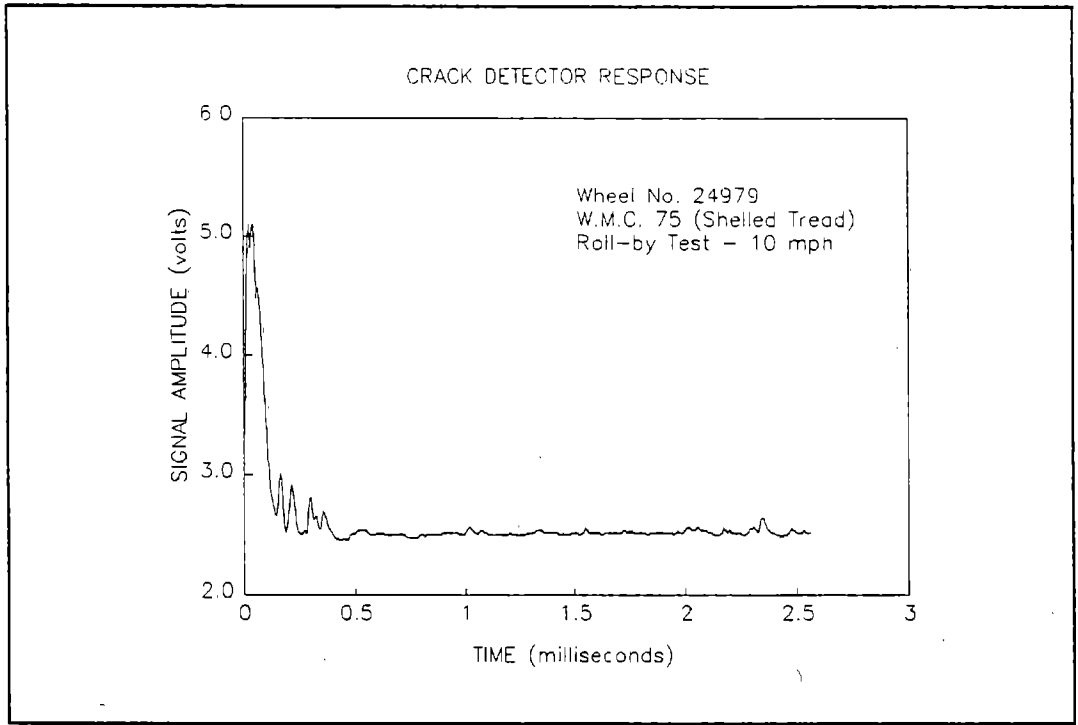
**Wheel No. 24979 Tread Profile**



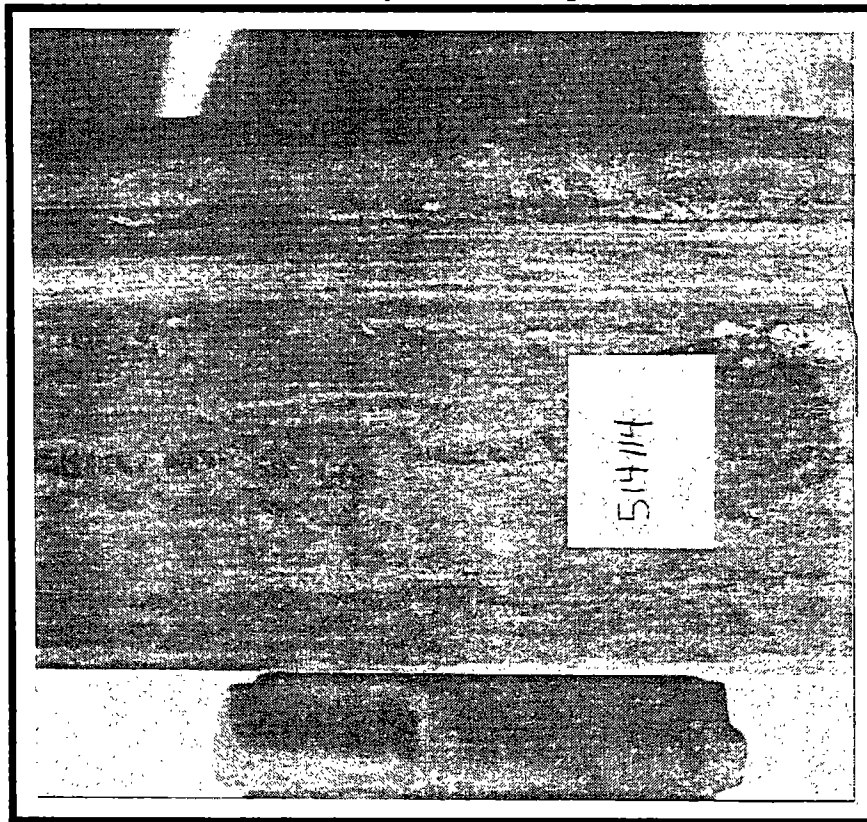
**Detector Response for Wheel No. 24979  
Stationary Test**



**Detector Response for Wheel No. 24979  
Roll-by Test -- 5 mph**

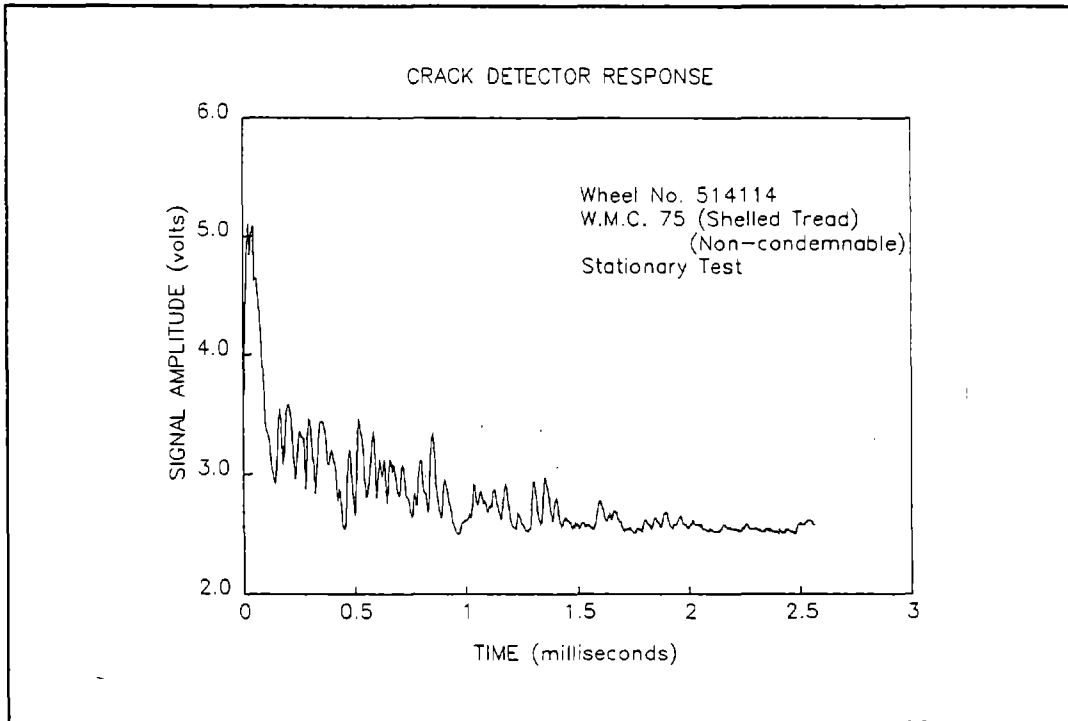


**Detector Response for Wheel No. 24979  
Roll-by Test -- 10 mph**

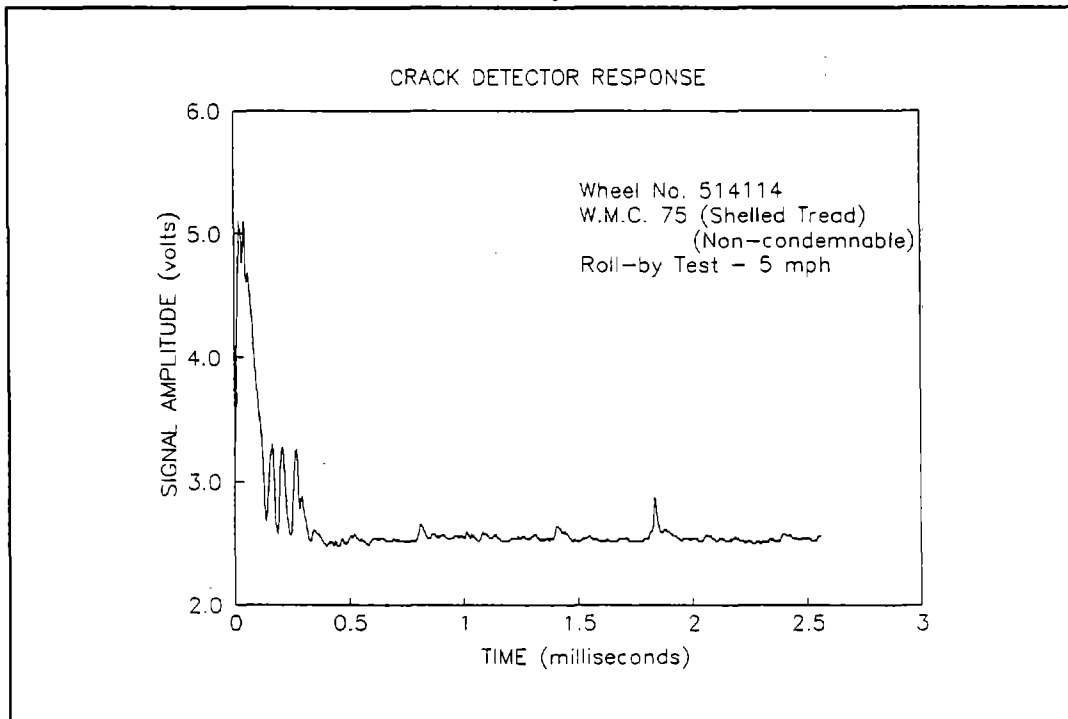


**View of Wheel No. 514114 Tread**

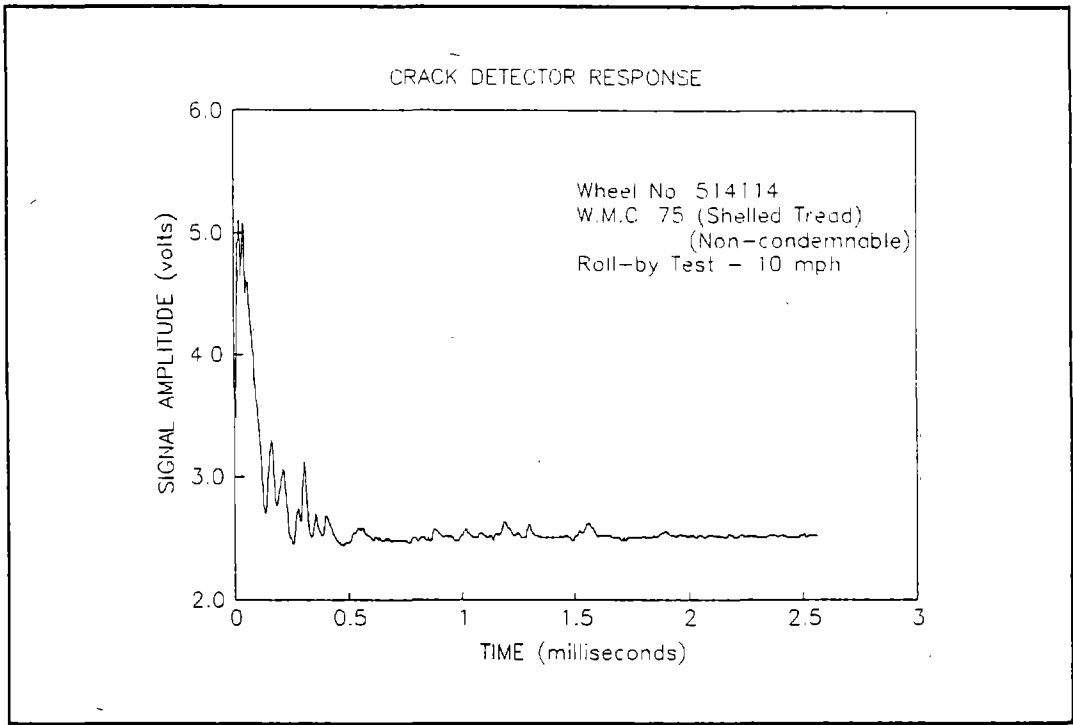
**(Tread profile not available for Wheel No. 514114)**



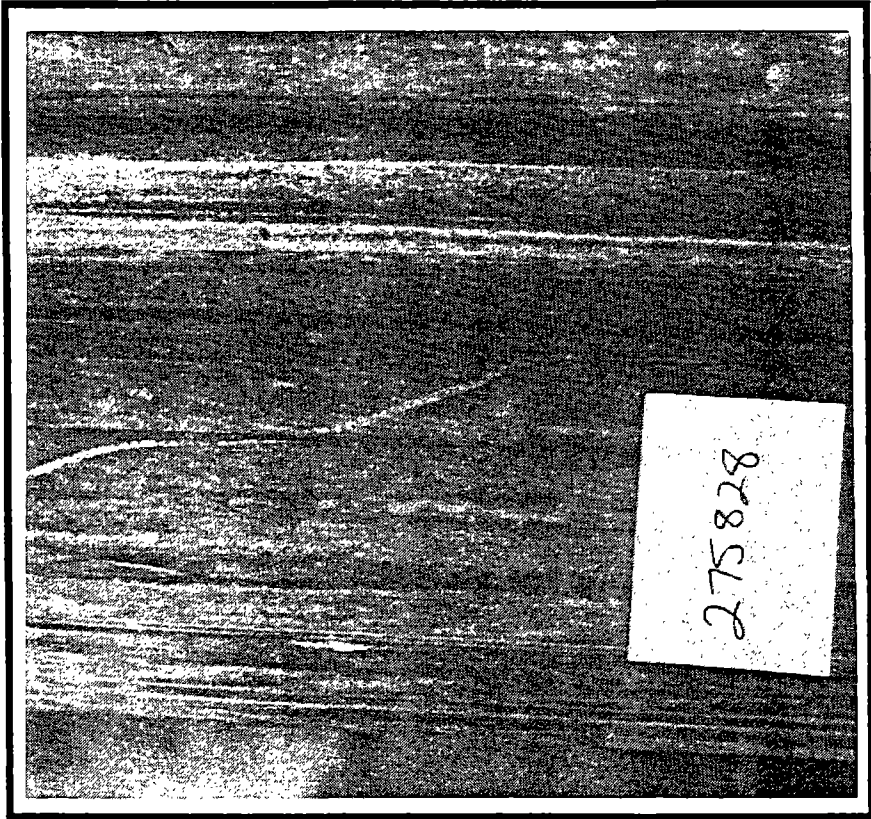
**Detector Response for Wheel No. 514114  
Stationary Test**



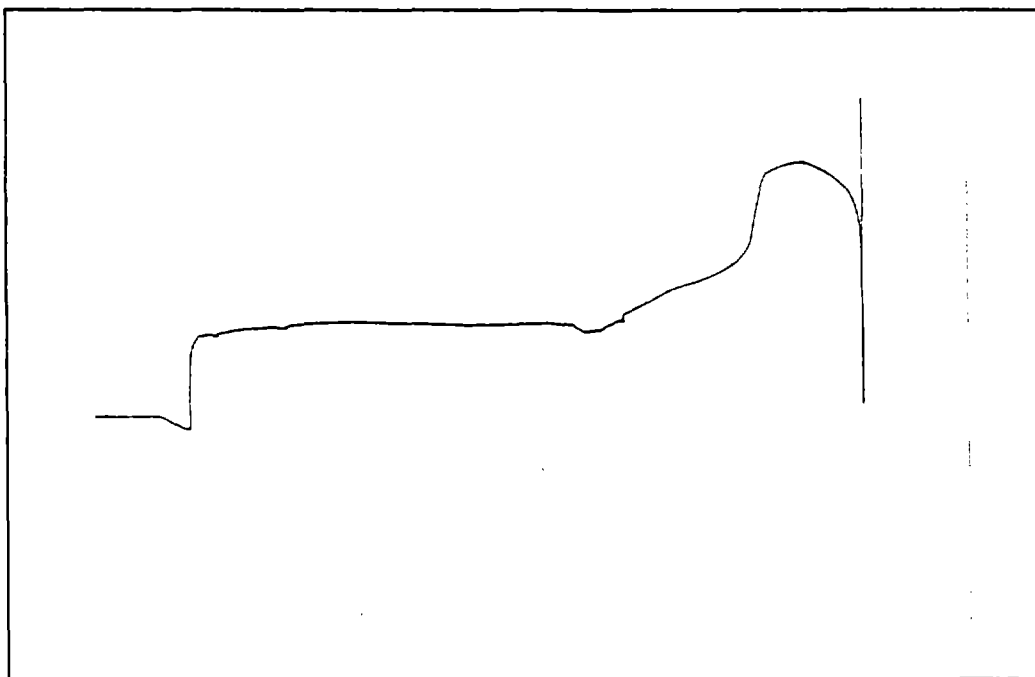
**Detector Response for Wheel No. 514114  
Roll-by Test -- 5 mph**



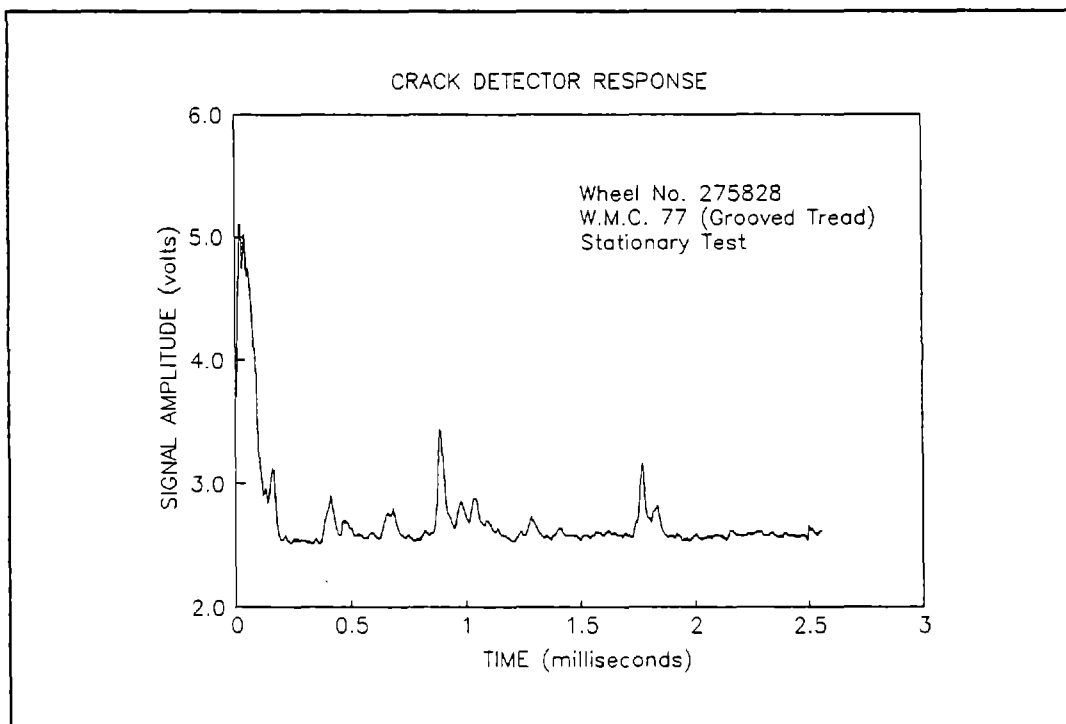
**Detector Response for Wheel No. 514114  
Roll-by Test -- 10 mph**



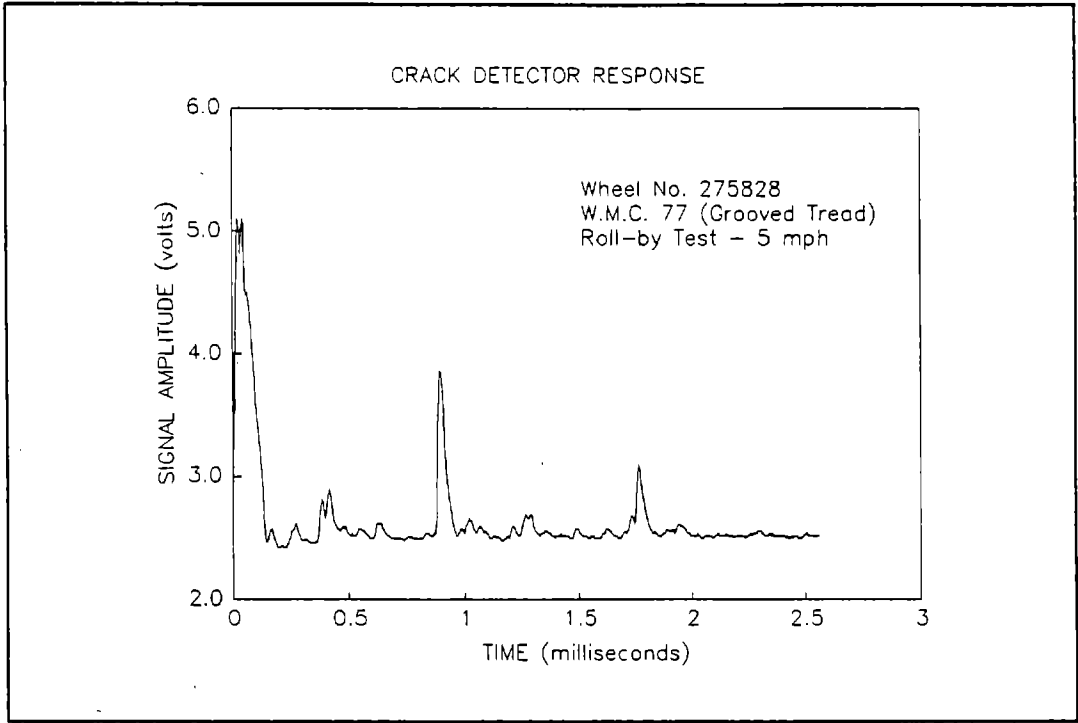
**View of Wheel No. 275828 Tread**



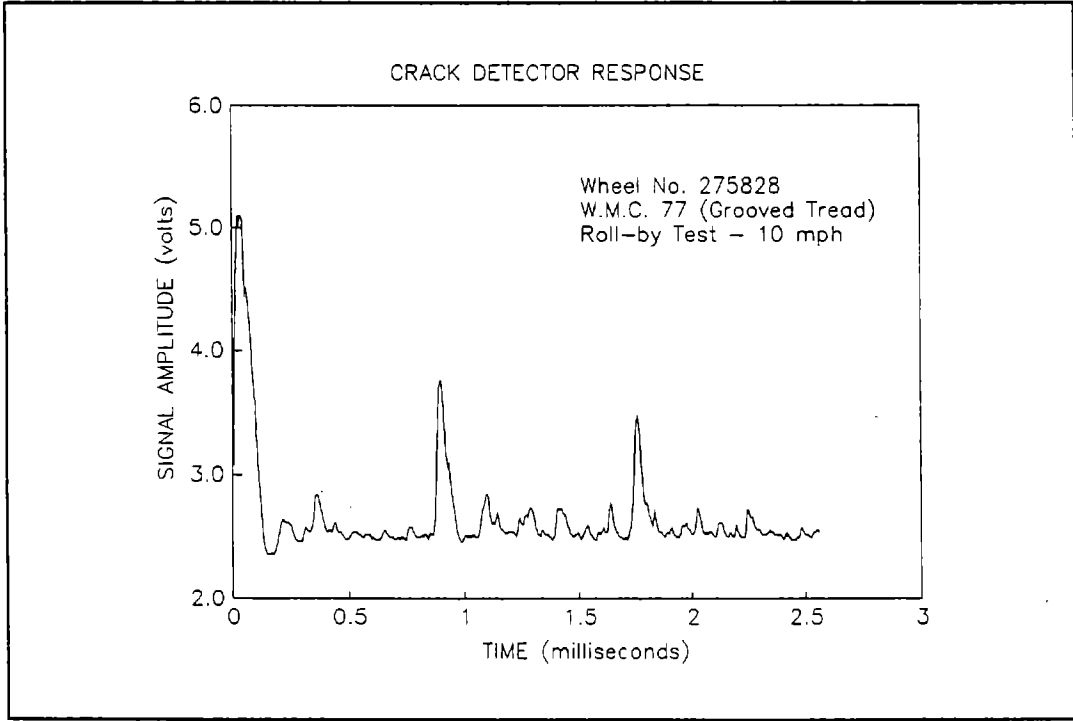
**Wheel No. 275828 Tread Profile**



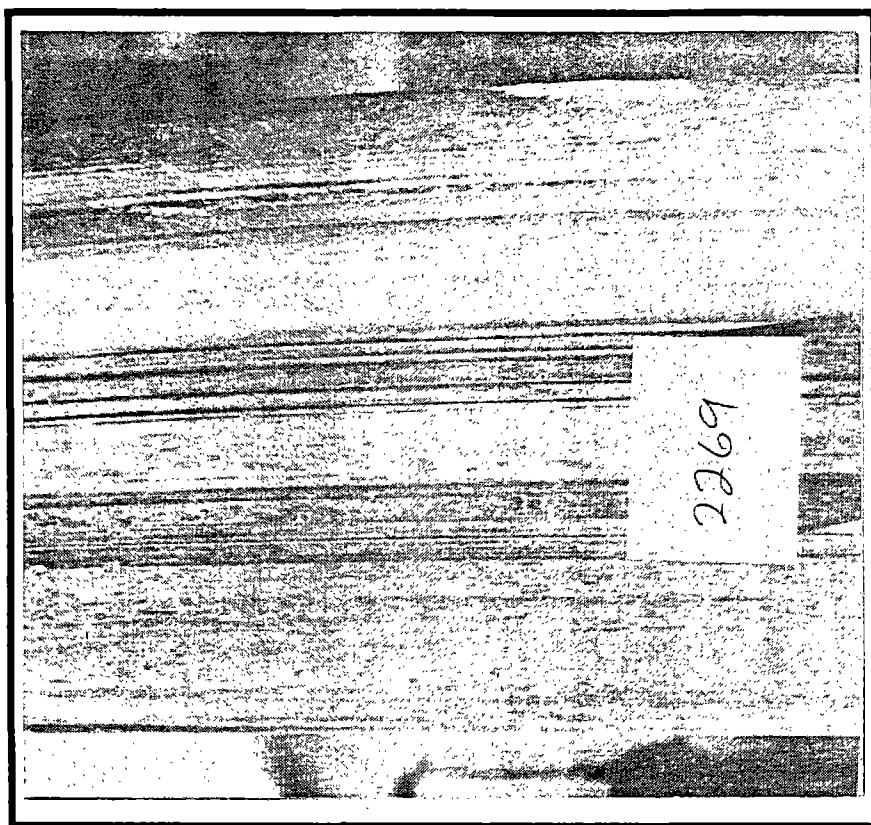
**Detector Response for Wheel No. 275828  
Stationary Test**



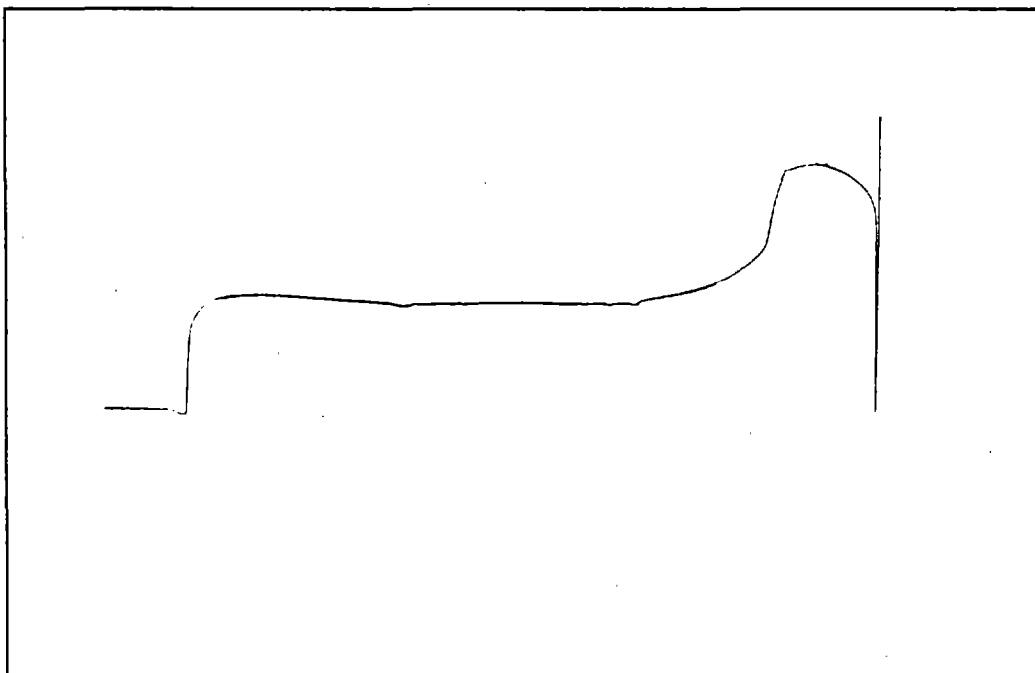
**Detector Response for Wheel No. 275828  
Roll-by Test -- 5 mph**



**Detector Response for Wheel No. 275828  
Roll-by Test -- 10 mph**

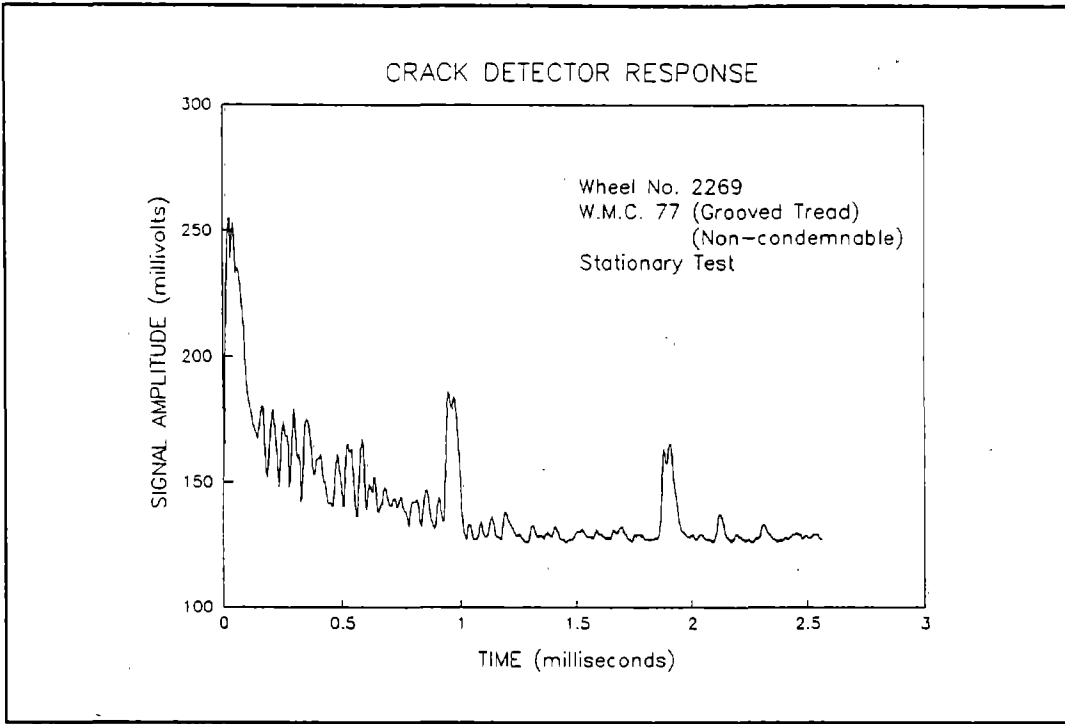


**View of Wheel No. 2269 Tread**

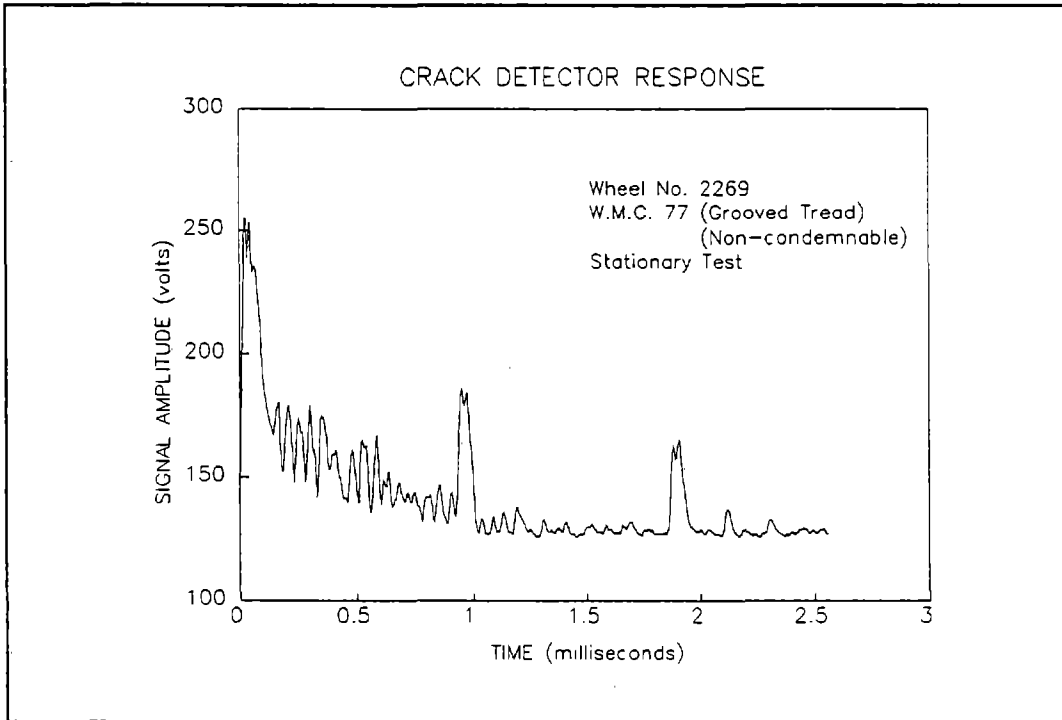


**Wheel No. 2269 Tread Profile**

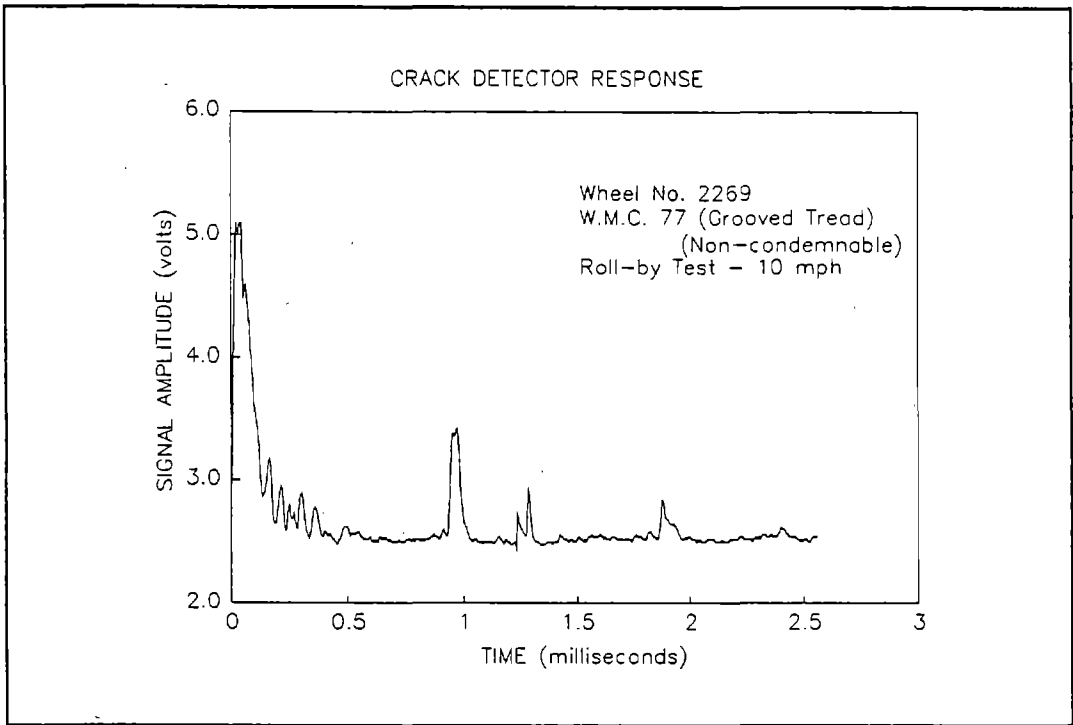




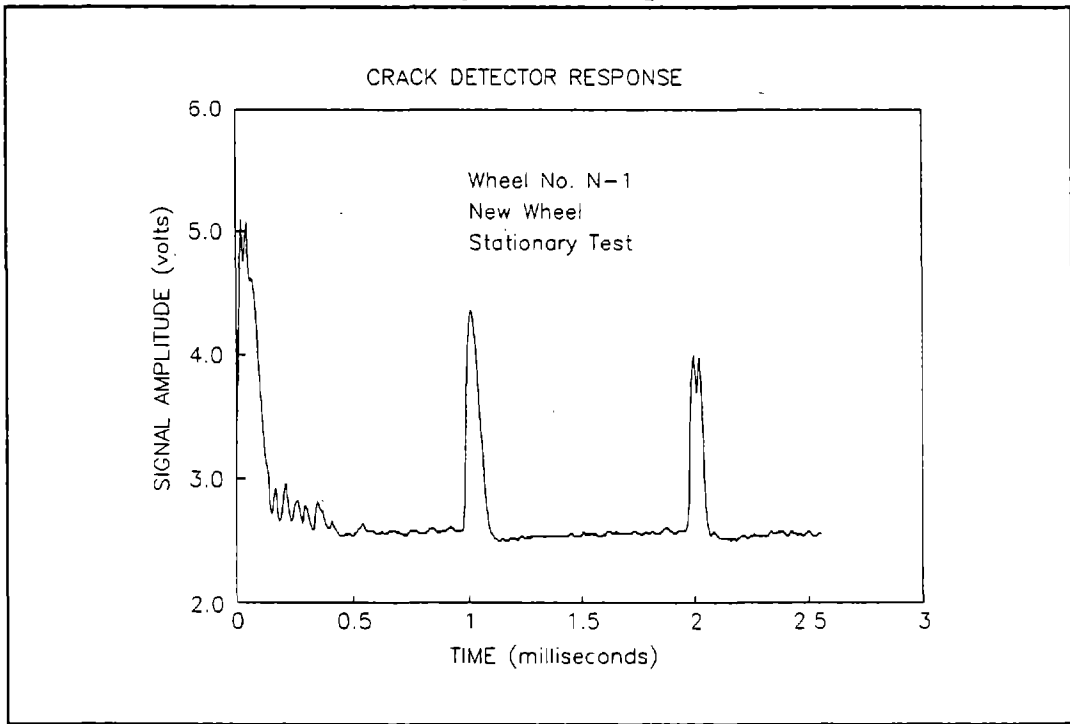
**Detector Response for Wheel No. 2269  
Stationary Test**



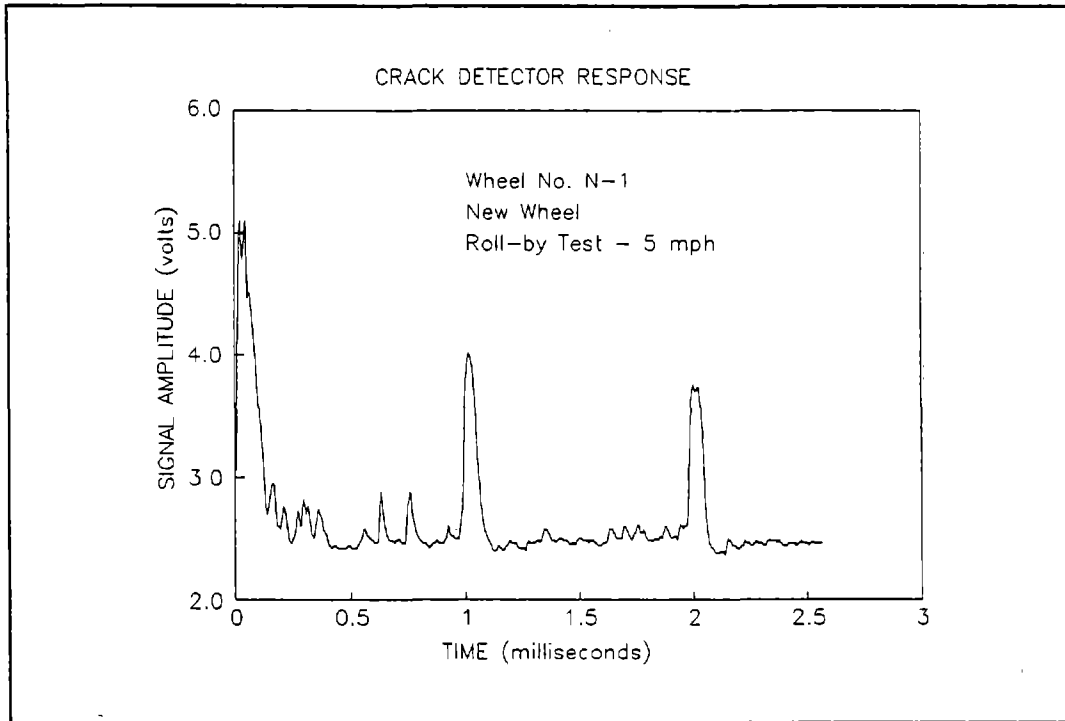
**Detector Response for Wheel No. 2269  
Roll-by Test -- 5 mph**



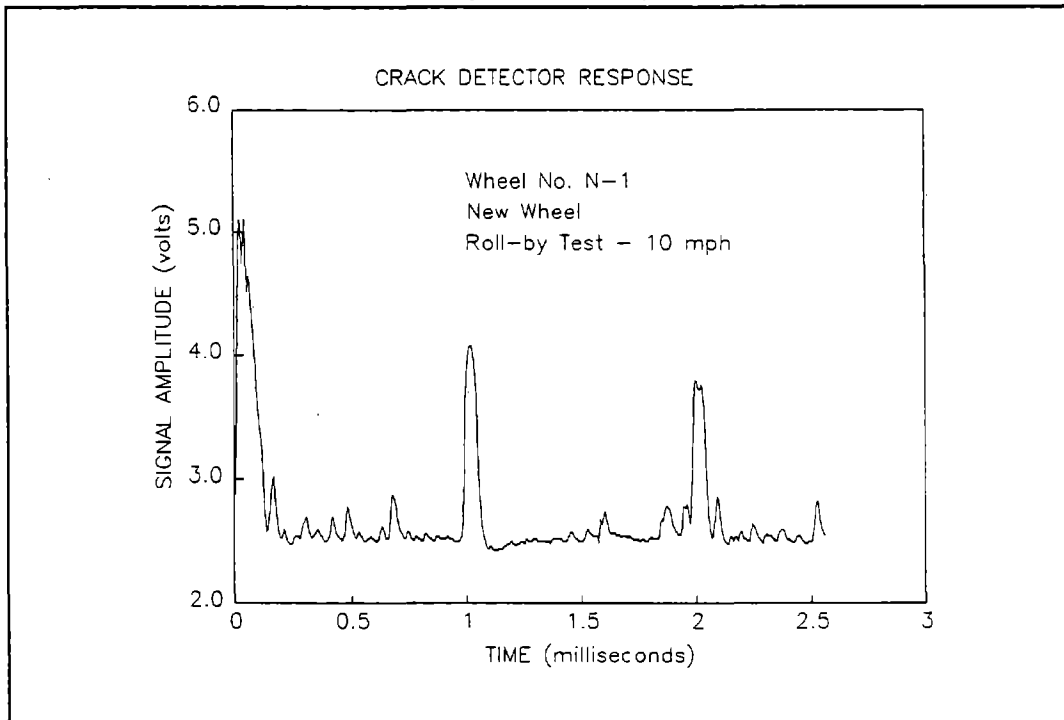
**Detector Response for Wheel No. 2269  
Roll-by Test -- 10 mph**



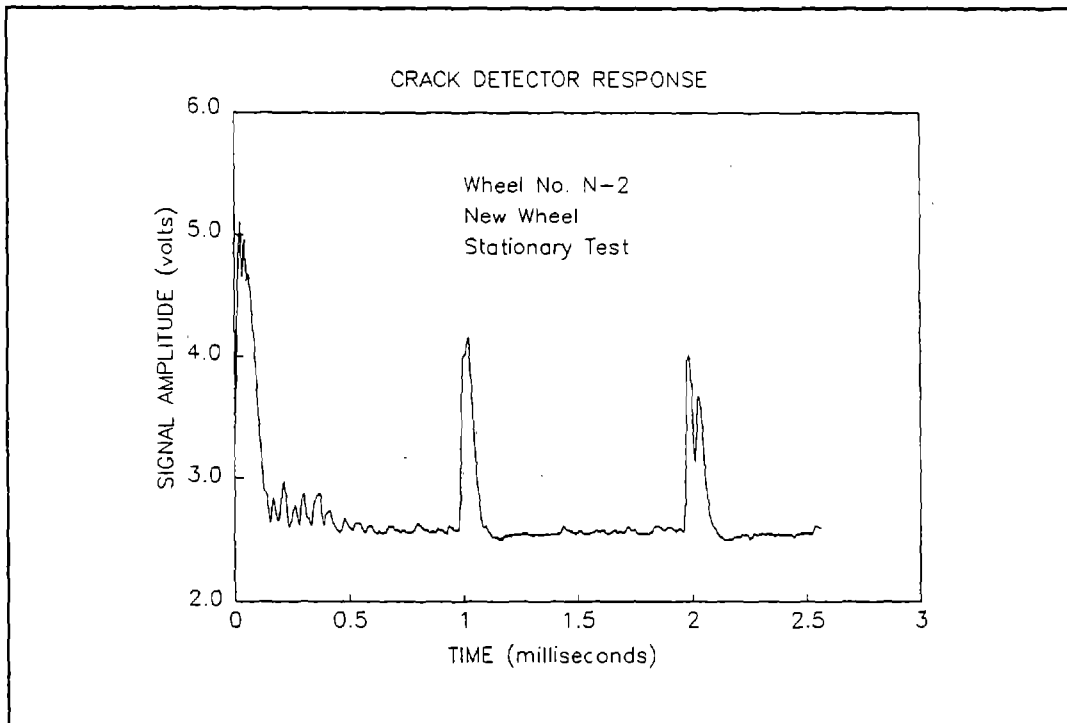
**Detector Response for Wheel No. N-1  
Stationary Test**



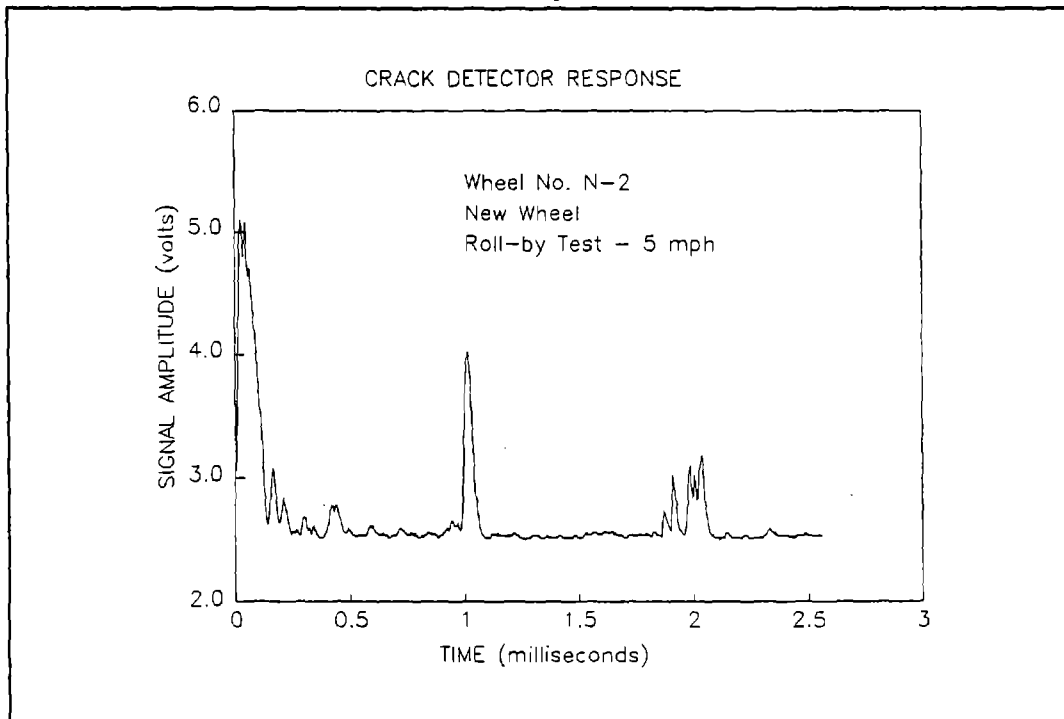
**Detector Response for Wheel No. N-1  
Roll-by Test -- 5 mph**



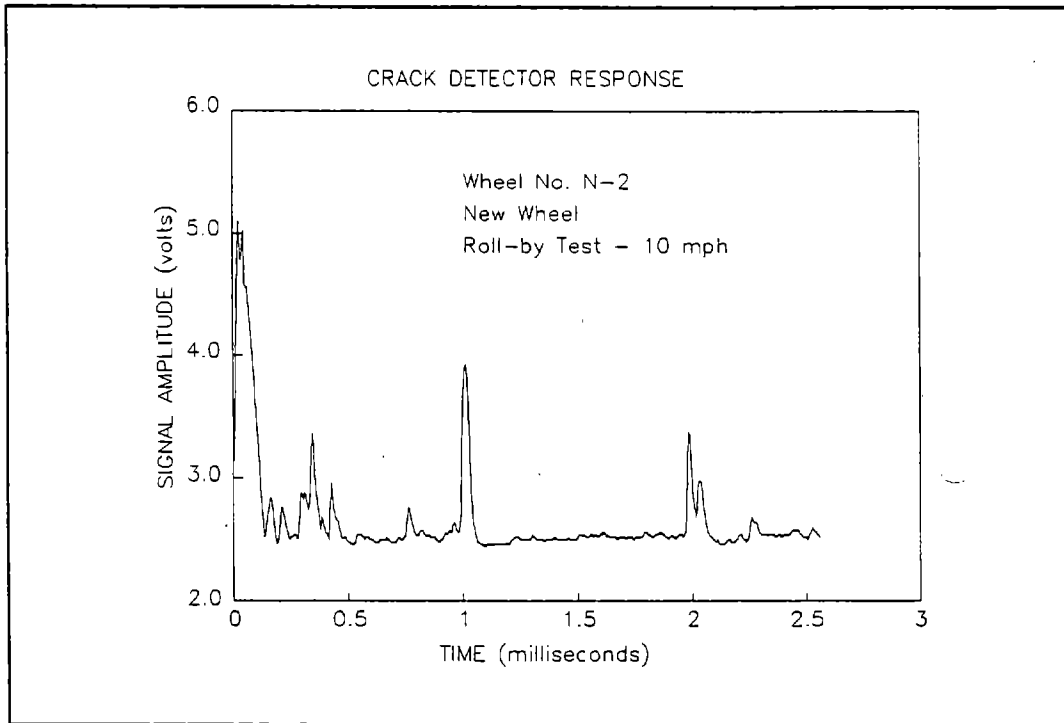
**Detector Response for Wheel No. N-1  
Roll-by Test -- 10 mph**



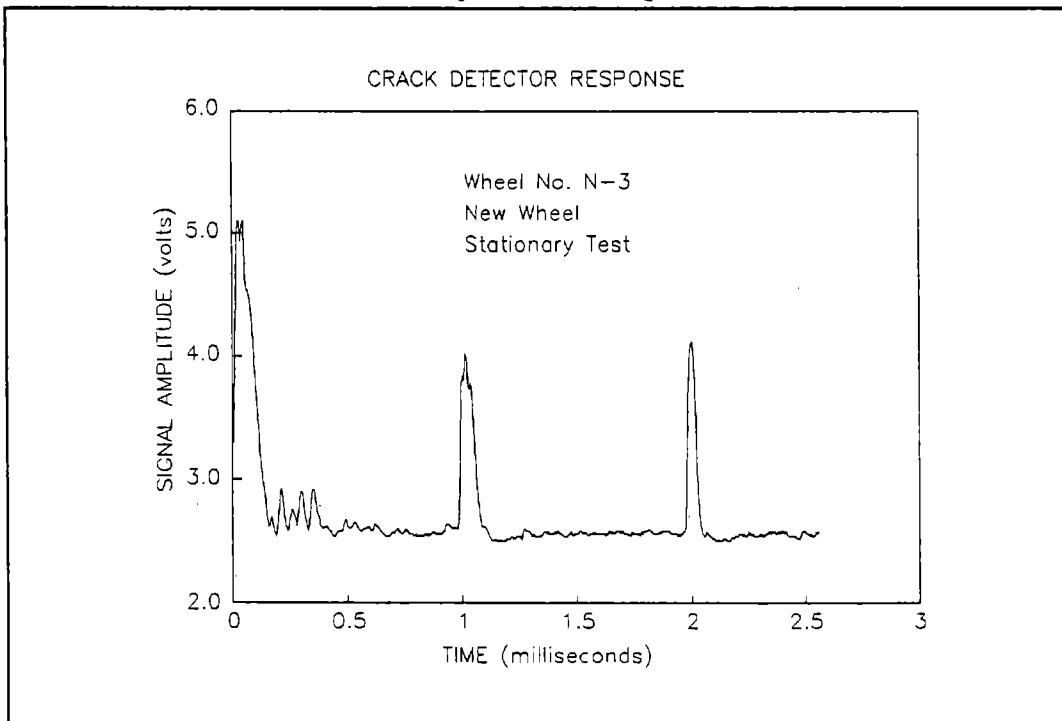
**Detector Response for Wheel No. N-2  
Stationary Test**



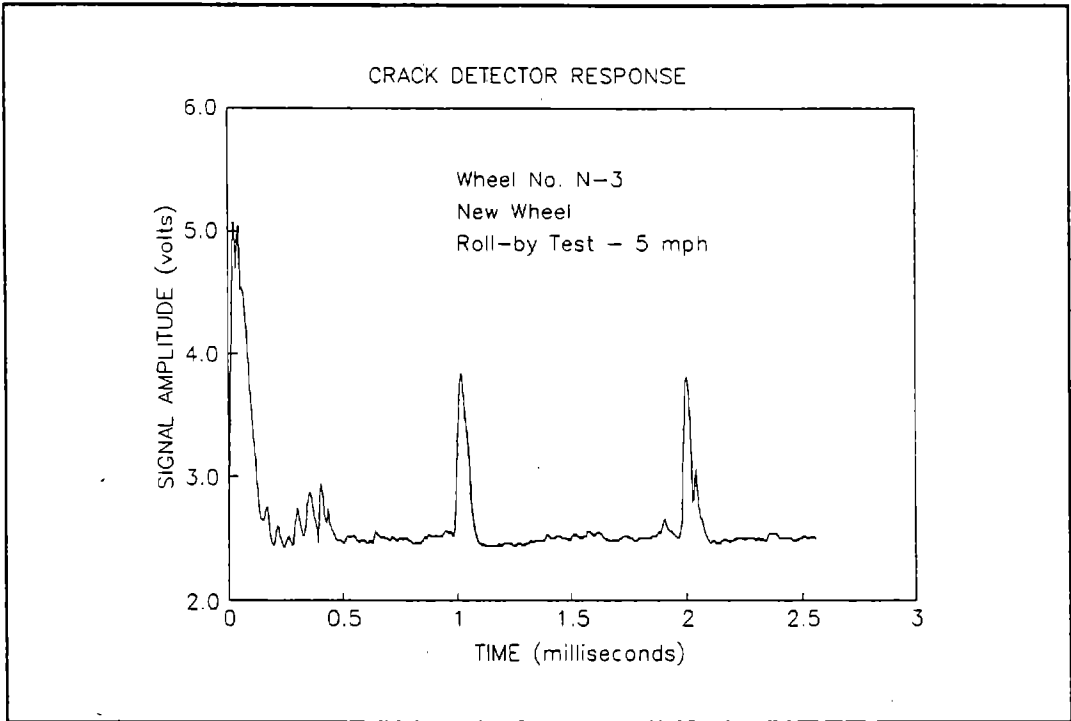
**Detector Response for Wheel No. N-2  
Roll-by Test -- 5 mph**



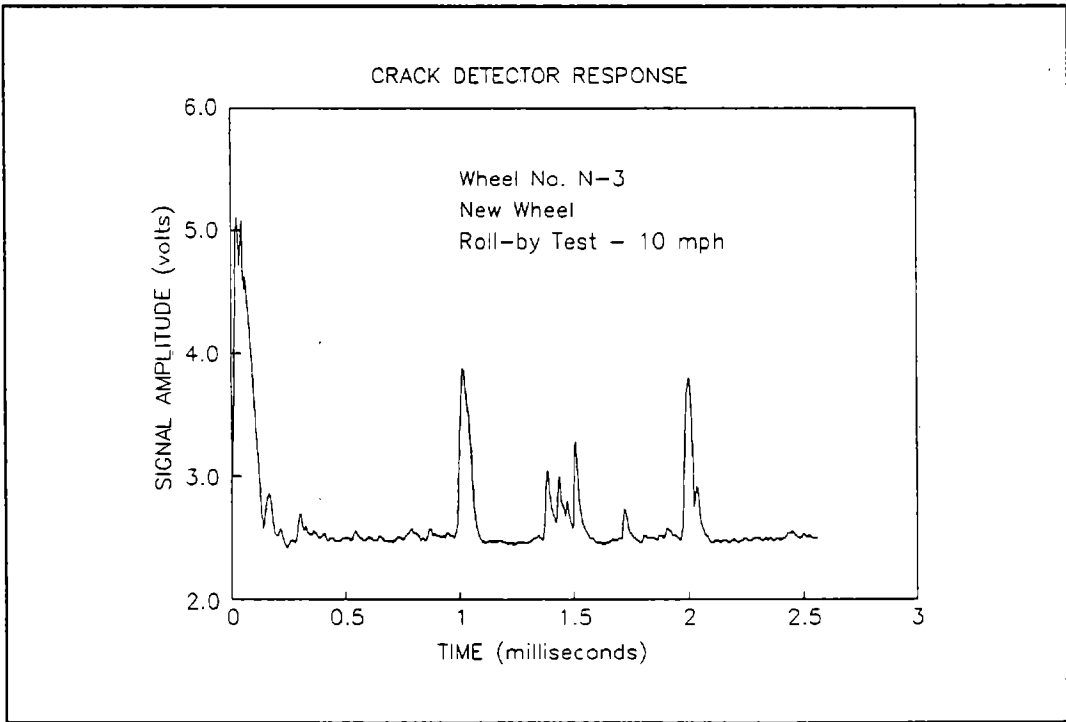
**Detector Response for Wheel No. N-2  
Roll-by Test -- 10 mph**



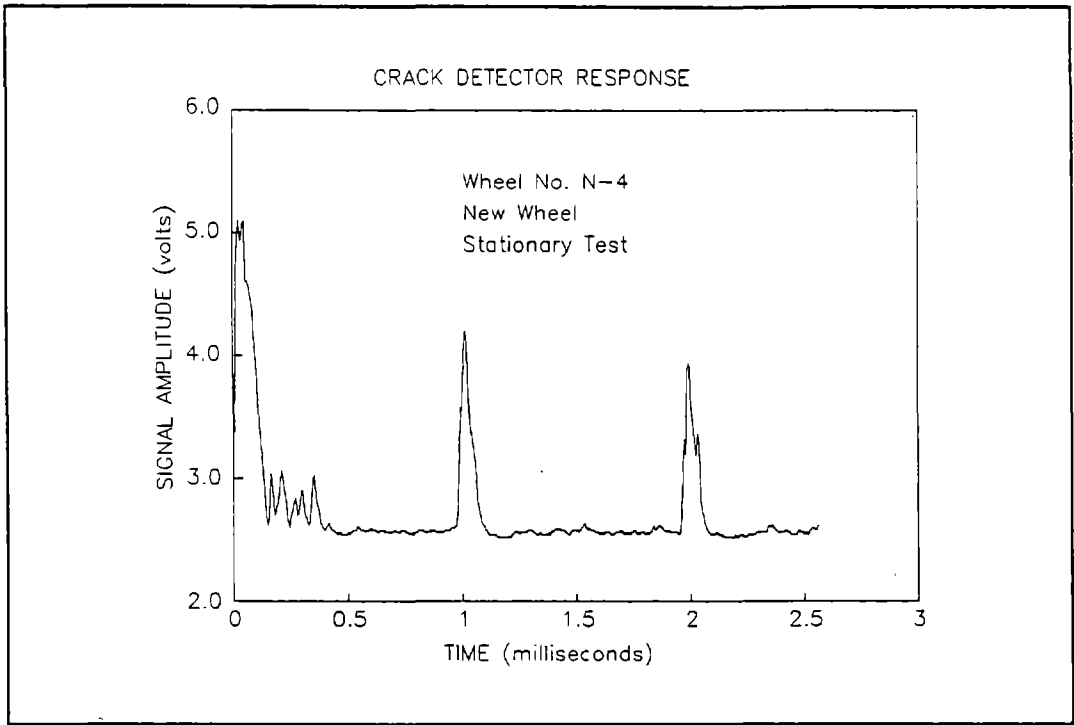
**Detector Response for Wheel No. N-3  
Stationary Test**



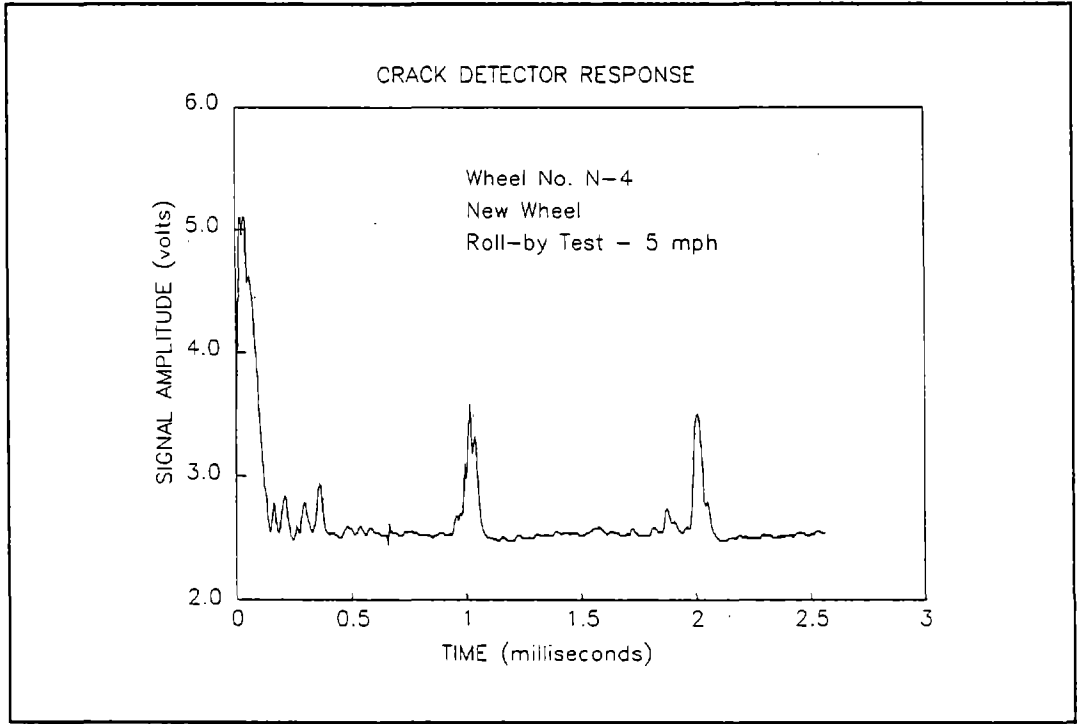
**Detector Response for Wheel No. N-3  
Roll-by Test -- 5 mph**



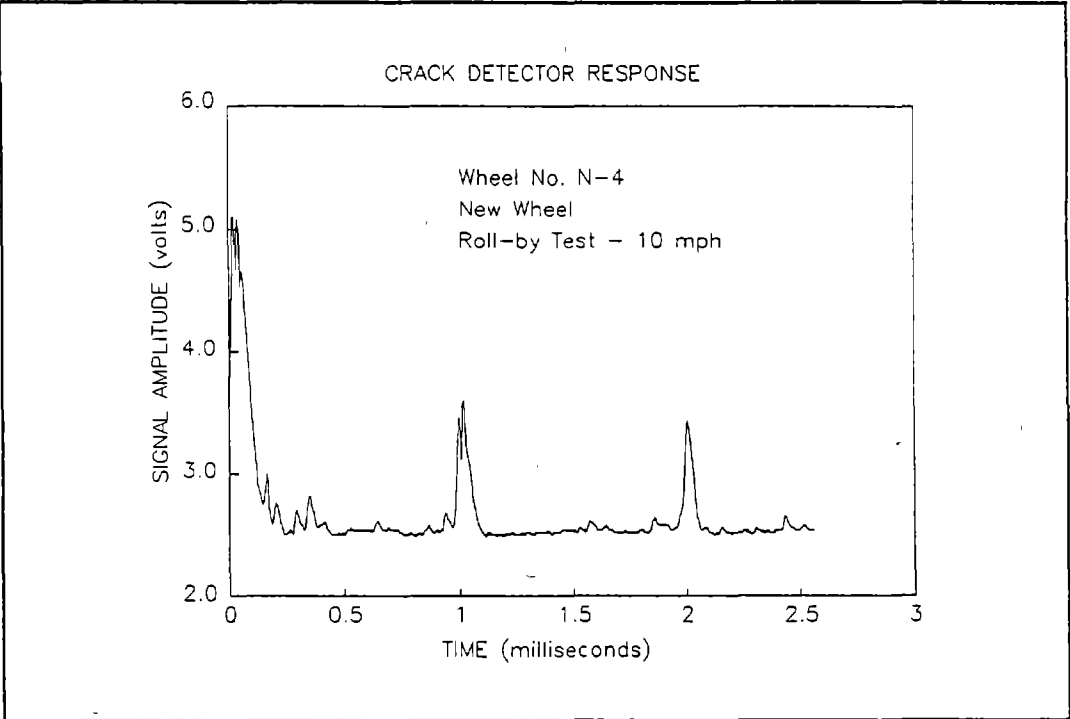
**Detector Response for Wheel No. N-3  
Roll-by Test -- 10 mph**



**Detector Response for Wheel No. N-4  
Stationary Test**



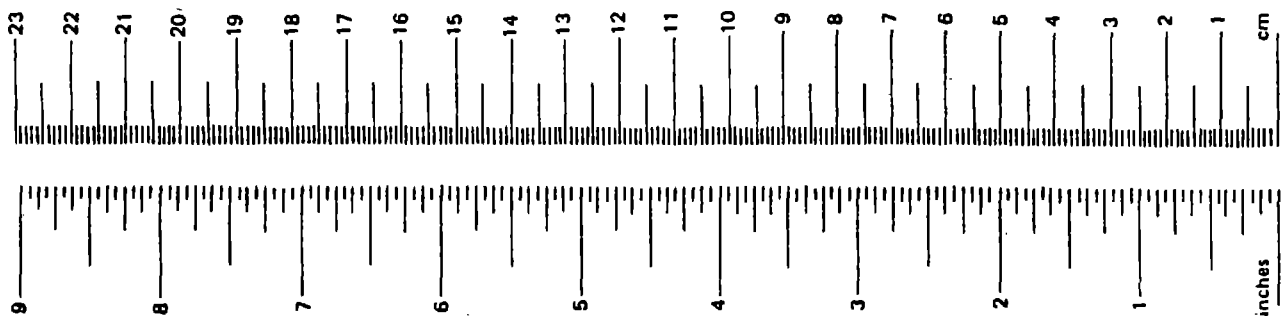
**Detector Response for Wheel No. N-4  
Roll-by Test -- 5 mph**



**Detector Response for Wheel No. N-4  
Roll-by Test -- 10 mph**



### METRIC CONVERSION FACTORS

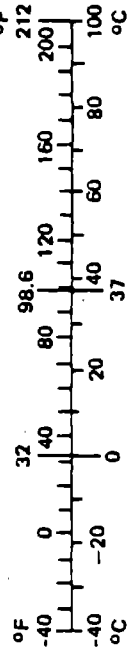


### Approximate Conversions to Metric Measures

Symbol	When You Know	Multiply by	To Find	Symbol
<b>LENGTH</b>				
in	inches	*2.50	centimeters	cm
ft	feet	30.00	centimeters	cm
yd	yards	0.90	meters	m
mi	miles	1.60	kilometers	km
<b>AREA</b>				
in <sup>2</sup>	square inches	6.50	square centimeters	cm <sup>2</sup>
ft <sup>2</sup>	square feet	0.09	square meters	m <sup>2</sup>
yd <sup>2</sup>	square yards	0.80	square meters	m <sup>2</sup>
mi <sup>2</sup>	square miles	2.60	square kilometers	km <sup>2</sup>
	acres	0.40	hectares	ha
<b>MASS (weight)</b>				
oz	ounces	28.00	grams	g
lb	pounds	0.45	kilograms	kg
	short tons (2000 lb)	0.90	tonnes	t
<b>VOLUME</b>				
Tsp	teaspoons	5.00	milliliters	ml
Tbsp	tablespoons	15.00	milliliters	ml
fl oz	fluid ounces	30.00	milliliters	ml
c	cups	0.24	liters	l
pt	pints	0.47	liters	l
qt	quarts	0.95	liters	l
gal	gallons	3.80	liters	l
ft <sup>3</sup>	cubic feet	0.03	cubic meters	m <sup>3</sup>
yd <sup>3</sup>	cubic yards	0.76	cubic meters	m <sup>3</sup>
<b>TEMPERATURE (exact)</b>				
°F	Fahrenheit temperature	5/9 (after subtracting 32)	Celsius temperature	°C

### Approximate Conversions from Metric Measures

Symbol	When You Know	Multiply by	To Find	Symbol
<b>LENGTH</b>				
mm	millimeters	0.04	inches	in
cm	centimeters	0.40	inches	in
m	meters	3.30	feet	ft
m	meters	1.10	yards	yd
km	kilometers	0.60	miles	mi
<b>AREA</b>				
cm <sup>2</sup>	square centim.	0.16	square inches	in <sup>2</sup>
m <sup>2</sup>	square meters	1.20	square yards	yd <sup>2</sup>
km <sup>2</sup>	square kilom.	0.40	square miles	mi <sup>2</sup>
ha	hectares (10,000 m <sup>2</sup> )	2.50	acres	
<b>MASS (weight)</b>				
g	grams	0.035	ounces	oz
kg	kilograms	2.2	pounds	lb
t	tonnes (1000 kg)	1.1	short tons	
<b>VOLUME</b>				
ml	milliliters	0.03	fluid ounces	fl oz
l	liters	2.10	pints	pt
l	liters	1.06	quarts	qt
l	liters	0.26	gallons	gal
m <sup>3</sup>	cubic meters	36.00	cubic feet	ft <sup>3</sup>
m <sup>3</sup>	cubic meters	1.30	cubic yards	yd <sup>3</sup>
<b>TEMPERATURE (exact)</b>				
°C	Celsius temperature	9/5 (then add 32)	Fahrenheit temperature	°F



\* 1 in. = 2.54 cm (exactly)

